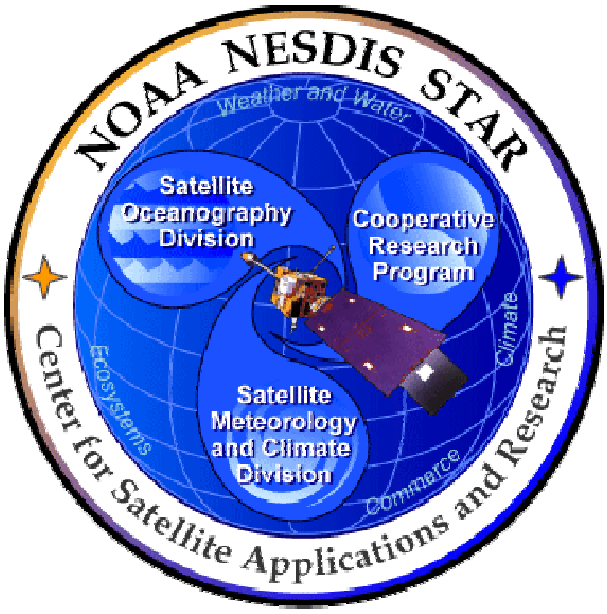


**NOAA NESDIS**
**CENTER for SATELLITE APPLICATIONS and RESEARCH**

# GOES-R Advanced Baseline Imager (ABI) Algorithm Theoretical Basis Document For Legacy Atmospheric Moisture Profile, Legacy Atmospheric Temperature Profile, Total Precipitable Water, and Derived Atmospheric Stability Indices

*Jun Li, CIMSS/University of Wisconsin-Madison*
*Timothy J. Schmit, STAR/NESDIS/NOAA*
*Xin Jin, CIMSS/University of Wisconsin-Madison*
*Graeme Martin, CIMSS/University of Wisconsin-Madison*
*CIMSS sounding team*
*Algorithm Integration Team*

Version 2.0
September 2010

# TABLE OF CONTENTS

## LIST OF FIGURES

Fig A1: The sketch map of all ancillary files and external functions/subroutines applied in the LAP sounding algorithm

**LIST OF TABLES**

Table A12: Meta-data

## LIST OF ACRONIMS

| | |
|---|---|
| ABI | Advanced Baseline Imager |
| ABS | Advanced Baseline Sounder |
| AEROSE | AERosol and Ocean Science Expedition |
| AIRS | Atmospheric InfraRed Sounder |
| AIT | Algorithm Integration Team |
| AMSR-E | Advanced Microwave Scanning Radiometer - EOS |
| ARM | Atmospheric Radiation Measurement |
| ATBD | Algorithm Theoretical Basis Document |
| BT | Brightness Temperature |
| CAPE | Convective available potential energy |
| CIMSS | Cooperative Institute for Meteorological Satellite Studies |
| CM | Cloud Mask |
| CrIS | Cross-track Infrared Sounder |
| cRTM | Community Radiative Transfer Model |
| CONUS | Continental United States |
| DP | Derived Product |
| ECMWF | European Centre for Medium-Range Weather Forecast |
| EOF | Empirical Orthogonal Functions |
| EOS | Earth Observing System |
| EUMETSAT | European Meteorological Satellite Agency |
| F&PS | Functional and Performance Specification |
| FOR | Field of Regard |
| FOV | Field of View |
| GEO | Geostationary Orbit |
| GFS | Global Forecast System |
| GOES | Geostationary Operational Environmental Satellite |
| HITRAN | High Resolution Transmission |
| HES | Hyperspectral Environmental Suite |
| IASI | Infrared Atmospheric Sounding Interferometer |
| IR | Infrared |
| KI | K-Index |
| LAP | Legacy Atmospheric Profile |
| LBLRTM | Line-by-line radiative transfer model |
| LEO | Low Earth Orbit |
| LI | Lifted Index |
| LPW | Layer Precipitable Water |
| LUT | Look-up Table |
| LZA | Local Zenith Angle |
| MODIS | Moderate Resolution Imaging Spectroradiometer |
| MRD | Mission Requirement Document |
| MSG | Meteosat Second Generation |
| NAM | North American Mesoscale |
| NASA | National Aeronautics and Space Administration |

| | |
|---|---|
| NCEP | National Centers for Environmental Prediction |
| NeDR | Noise Equivalent Difference of Radiance |
| NeDT | Noise Equivalent Difference of Temperature |
| NIR | Near Infrared |
| NOAA | National Oceanic and Atmospheric Administration |
| NWP | Numerical Weather Prediction |
| NWS | National Weather Service |
| PCA | Principle Component Analysis |
| PFAAST | Pressure-Layer Fast Algorithm for Atmospheric Transmittances |
| PSGS | Perot Systems Government Services, Inc. |
| RAOB | Radiosonde Observation |
| RH | Relative Humidity |
| RMSE | Root Mean Square Error |
| RTM | Radiative Transfer Model |
| RTTOV | Rapid Transmissions for TOVs |
| SE | Surface Emissivity |
| SEVIRI | Spinning Enhanced Visible & Infrared Imager |
| SI | Showalter index |
| SGP-CART | Southern Great Plains Cloud and Radiation Testbed |
| SSEC | Space Science and Engineering Center |
| SST | Sea Surface Temperature |
| TBC | To Be Confirmed |
| TBD | To Be Determined |
| TBR | To Be Reviewed |
| TIGR | TOVS Initial Guess Retrieval |
| TPW | Total Precipitable Water |
| PW | Precipitable Water |
| TOA | Top of Atmosphere |
| TOVS | TIROS Operational Vertical Sounder |
| TT | Total Totals Index |
| UW | University of Wisconsin |
| VAS | VISSR Atmospheric Sounder |
| VIS | Visible |
| VISSR | Visible/Infrared Spin Scan-Radiometer (VISSR) |

# ABSTRACT

This document is the Algorithm Theoretical Basis Document (ATBD) for the next generation of Geostationary Operational Environmental Satellite (GOES-R) Legacy Atmospheric Profile (LAP) and derived products generation. It is a high level description and the physical basis for the physical retrieval of atmospheric temperature and moisture profiles with infrared (IR) radiances measured by the Advanced Baseline Imager (ABI) to be flown on the GOES-R). The algorithm retrieves temperature and moisture profiles and the derived products including total precipitable water (TPW), layer precipitable water (LPW), lifted index (LI), convective available potential energy (CAPE), total totals index (TT), Showalter index (SI), and K-index (KI) from clear sky radiances within *M* by *M* ABI field-of-view (FOV) box area. This document contains a description of the algorithm, including scientific aspects and practical considerations. It is divided in the following main sections.

- Overview
- Algorithm detailed description
- Algorithm inputs and files description
- Practical considerations
- Initial validation

# 1 INTRODUCTION

## 1.1 Purpose of This Document

The legacy atmospheric profile (LAP) algorithm theoretical basis document (ATBD) provides a high level description and the physical basis for the retrieval of legacy atmospheric temperature and moisture profiles with infrared (IR) radiances taken by the Advanced Baseline Imager (ABI) flown on the next generation of Geostationary Operational Environmental Satellite (GOES-R) series of NOAA geostationary meteorological/environmental satellites. The legacy atmospheric profile (LAP) product provides temperature and moisture profiles, along with derived total precipitable water (TPW) and atmospheric instability indices from clear sky radiances within $M \times M$ ABI field-of-view (FOV) box area, here one FOV means one pixel. One field-of-regard (FOR) is defined as $M \times M$ FOVs. The derived instability indices include lifted index (LI), convective available potential energy (CAPE), total totals index (TT), Showalter index (SI), and K-index (KI). The ABI LAP product is a continuation of the current GOES Sounder product before it is presumably succeeded by an advanced hyperspectral IR sounding instrument in the post-GOES-R era (Schmit et al. 2008).

## 1.2 Who Should Use This Document

The intended user of this document are those interested in understanding the physical basis of the algorithms and how to use the output of this algorithm to optimize the LAP product for a particular application. This document also provides information useful to anyone maintaining, modifying, or improving the original algorithm.

## 1.3 Inside Each Section

This document is broken down into the following main sections.

- **Observing System Overview**: Provides relevant details of the ABI and provides a brief description of the products generated by the algorithm.

- **Algorithm Description**: Provides a detailed description of the LAP algorithm including its physical basis, its input and its output.

- **Test Data Sets and Outputs**: Provides a description of the test data set used to characterize the performance of the algorithm and quality of the data products. It also describes the results from algorithm processing using SEVIRI data.

- **Practical Considerations**: Provides an overview of the issues involving numerical computation, programming and procedures, quality assessment and diagnostics and exception handling.

- **Assumptions and Limitations**: All the assumptions and limitations concerning the algorithm theoretic basis have been described and discussed.

## 1.4 Related Documents

This document currently does not relate to any other document outside of the specifications of the GOES-R Ground Segment Functional and Performance Specification (F&PS) and to the references given throughout.

## 1.5 Revision History

Version 0.1 of this document was created by Dr. Jun Li of Cooperative Institute for Meteorological Satellite Studies (CIMSS) at the UW-Madison and Timothy J. Schmit of Center for Satellite Applications and Research (STAR) of NOAA/NESDIS, with the intent to accompany the delivery of the version 1.0 algorithms to the GOES-R AWG Algorithm Integration Team (AIT). (July 2008)

Version 0.1 comments/suggestions from N. Nalli (STAR/PSGS) (September 2008)

Version 1.0 was developed to meet 80% ATBD requirement. (May 2009)

Version 1.0 comments/suggestions from Mitch Goldberg (STAR/NESDIS) (June 2009)

Version 1.0 updates from Jun Li (CIMSS) (July 2009)

Version 1.1 updates from AIT and Jun (September 2009)

Version 2.0 updates from Xin Jin, Jun Li and Tim Schmit (June 2010)

Version 2.0 updates from AIT (September 2010)

## 1.6 Products Generated

The GOES-R ABI LAP algorithm is responsible for the retrieval of atmospheric temperature and moisture profiles for a FOR consisting of $M \times M$ ABI FOVs, in this document FOR specifically refers to the pixel group for one profile retrieval. At the time of this writing, $M = 5$ is assumed, although because current requirements call for 4 km mesoscale stability parameters, a smaller value for $M$ may be necessary. From the temperature and moisture profiles, the associated TPW and atmospheric stability indices such as LI, TT, KI, SI and CAPE are also derived. The product generation needs IR BTs from all ABI channels along with NWP output. The LAP output includes temperature and moisture profiles at all 101-levels but only the 54 level temperatures from 100 hPa to 1050 hPa and 35 level moistures from 300 hPa to 1050 hPa are useful. The surface skin temperature, TPW, PW at three atmospheric layers in sigma ordinate (PW_low: 0.9 – SFC, PW_mid: 0.7 – 0.9, PW_high: 0.3 – 0.7), LI, CAPE, TT, KI and SI are also products included in the output. Table 1 shows the requirements for LAP products. More requirement information can be found in the GOES-R MRD and the F&PS.

Note: In the LAP code, M = 3 is the default setting

Table 1. Requirements for GOES-R LAP products.

Table 1.1. Requirement on LAP temperature profile

| **Legacy Temperature Profile: CONUS** | **Requirement** |
|---|---|
| Product Geographic Coverage/Conditions | CONUS,<br>Full Disk,<br>Mesoscale |
| Product Vertical Resolution (km) | Reflects layering of NWP Models (TBR); inherent vertical resolution is only 3 to 5 km |
| Product Horizontal Resolution (km) | 10 |
| Product Mapping Accuracy (km) | 5 |
| Product Measurement Range (K) | 180 – 320 K |
| Product Measurement Accuracy (K) | 1K below 400 hPa and above boundary layer |
| Product Refresh Rate/Coverage Time | CONUS: 30 min<br>Full Disk : 60 min<br>Mesoscale: 5 min |
| Mission Product Data Latency | CONUS: 266 sec<br>Full Disk: 266 sec |

| | |
|---|---|
| | Mesoscale: 266 sec |
| Product Measurement Precision<br>Temporal Coverage Qualifier (K) | 2 K below 400 hPa and above boundary layer<br>Day and Night |
| Product Extent Qualifier | Quantitative out to at least 67º LZA |
| Cloud Cover Conditions Qualifier<br>Product Statistics Qualifier | Clear conditions associated with threshold accuracy over specified geographic coverage |

Table 1.2. Requirement on LAP moisture profile

| **Legacy Moisture Profile: CONUS** | **Requirement** |
|---|---|
| Product Geographic Coverage/Conditions | CONUS,<br>Full Disk,<br>Mesoscale |
| Product Vertical Resolution (km) | Reflects layering of NWP Models (TBR); inherent vertical resolution is only 3 to 5 km |
| Product Horizontal Resolution (km) | 10 |
| Product Mapping Accuracy (km) | 5 |
| Product Measurement Range (%) | 0 – 100 |
| Product Measurement Accuracy (%) | Sfc-500 mb: 18% 500-300 mb: 18%<br>300-100 mb: 20% |
| Product Refresh Rate/Coverage Time | CONUS: 30 min<br>Full Disk : 60 min<br>Mesoscale: 5 min |
| Mission Product Data Latency | CONUS: 266 sec<br>Full Disk: 266 sec<br>Mesoscale: 266 sec |
| Product Measurement Precision (%) | Scf-500mb: 18%<br>500-300 mb: 18%<br>300-100mb: 20% |
| Temporal Coverage Qualifier | Day and Night |
| Product Extent Qualifier | Quantitative out to at least 67º LZA |

| | |
|---|---|
| Cloud Cover Conditions Qualifier | associated with threshold accuracy |
| Product Statistics Qualifier | Over specified geographic coverage |

Table 1.3. Requirement on LAP Derived Stability Indices (5 indices: CAPE, Lifted Index, K-index, Showalter Index, Total Totals)

| **Legacy Moisture Profile: CONUS** | **Requirement** |
|---|---|
| Product Geographic Coverage/Conditions | CONUS,<br>Full Disk,<br>Mesoscale |
| Product Vertical Resolution | Not Applicable |
| Product Horizontal Resolution (km) | 10 |
| Product Mapping Accuracy (km) | 2 |
| Product Measurement Range | Lifted Index: --10 to 40 K<br>CAPE: 0 to 5000 J/kg<br>Showalter index: >4 to -10 K<br>Total totals Index: -43 to > 56<br>K index: 0 to 40 |
| Product Measurement Accuracy | Lifted Index: 2.0 K<br>CAPE: 1000 J/ kg<br>Showalter index: 2 K<br>Total totals Index: 1<br>K index: 2 |
| Product Refresh Rate/Coverage Time | CONUS: 30 min<br>Full Disk : 60 min<br>Mesoscale: 5 min |
| Mission Product Data Latency | CONUS: **159 sec** (under review)<br>Full Disk: **159 sec** (under review)<br>Mesoscale: 266 sec |
| Product Measurement Precision (%) | Scf-500mb: 18%<br>500-300 mb: 18%<br>300-100mb: 20% |
| Temporal Coverage Qualifier | Day and Night |
| Product Extent Qualifier | Quantitative out to at least 67º LZA |

| | |
|---|---|
| Cloud Cover Conditions Qualifier | associated with threshold accuracy |
| Product Statistics Qualifier | Over specified geographic coverage |

Table 1.4. Requirement on LAP Total Precipitable Water

| **Legacy Moisture Profile: CONUS** | **Requirement** |
|---|---|
| Product Geographic Coverage/Conditions | CONUS,<br>Full Disk,<br>Mesoscale |
| Product Vertical Resolution | Not Applicable |
| Product Horizontal Resolution (km) | 10 |
| Product Mapping Accuracy (km) | 2 |
| Product Measurement Range | 0 – 100 mm |
| Product Measurement Accuracy | Lifted Index: 2.0 K<br>CAPE: 1000 J/ kg<br>Showalter index: 2 K<br>Total totals Index: 1<br>K index: 2 |
| Product Refresh Rate/Coverage Time | CONUS: 30 min<br>Full Disk : 60 min<br>Mesoscale: 5 min |
| Mission Product Data Latency | CONUS: 266 sec<br>Full Disk: 806 sec<br>Mesoscale: 266 sec |
| Product Measurement Precision | 3 mm |
| Temporal Coverage Qualifier | Day and Night |
| Product Extent Qualifier | Quantitative out to at least 67º LZA |
| Cloud Cover Conditions Qualifier | associated with threshold accuracy |
| Product Statistics Qualifier | Over specified geographic coverage |

**TPW** (total precipitable water) is the amount of liquid water (in cm) if all the atmospheric water vapor in the column was condensed. The following equation is used to derive TPW:

$$TPW = \frac{1}{\rho_w g} \int_{p_s}^{0} q(p) \cdot dp \tag{1}$$

where $\rho_w$ equals to 1000 which means the water density in kg/m$^3$; $g$ equals to 9.8 which means the gravity acceleration in m/s$^2$; q(p) is the mixing ratio (g/kg) of water vapor profile at pressure level p; $p_s$ is the surface air pressure in hPa. Since the water vapor content is very rare above 300 hPa, only water vapor content between surface and 300 hPa is accumulated to derive TPW.

Layer precipitable water (PW) provides information on the water vapour contained in a vertical column of unit cross-section area in three layers in the troposphere:

Boundary Layer (BL, PW_low): [Surface - 900 hPa]
Middle Layer (ML, PW_mid): [900 hPa - 700 hPa]
High Layer (HL, PW_high): [700 hPa – 300 hPa]

In some cases, such as the center of a low pressure system the surface air pressure could be lower than 900 hPa. In other cases such as over the high altitude areas, the surface pressure can get lower than 700 hPa. The sigma pressure ordinate is applied to circumvent such cases. The boundaries for PW calculation are converted into sigma indices with the values of 1.0, 0.9, 0.7, and 0.3 respectively. The conversion between sigma pressure and normal air pressure ordinate is through the following equation:

$$P_{sig} = 0.005 + sig\_idx \cdot (P_s - 0.005) \tag{2}$$

where $P_{sig}$ is the pressure corresponding to a specific sigma level index; $sig\_idx$ is the sigma index; $P_s$ is the surface air pressure. Since the retrieved moisture profile doesn't necessary contain values at these levels for different surface pressures, a linear interpolation is conducted to find mixing ratio values at these levels.

$$q(p_{sig}) = q(p_{below}) + [q(p_{above}) - q(p_{below})] \cdot [\frac{\ln q(p_{sig}) - \ln q(p_{below})}{\ln q(p_{above}) - \ln q(p_{below})}] \tag{3}$$

where $q$ is the mixing ratio profile; $p_{above}$ is the pressure level just above $p_{sig}$ and $p_{below}$ is the pressure level just below $p_{sig}$.

**LI** (lifted index) in units of degrees Celsius (°C) provides estimations of the atmospheric stability in cloud-free areas. Among all the potential indices, the LI has been implemented and coded. The LI index (Galway, 1956) expresses the temperature difference between a lifted parcel and the surrounding air at 500 hPa. The parcel is lifted dry adiabatically from the mean lowest 100 hPa level to the condensation level, and then wet adiabatically to 500 hPa. In the LAP algorithm the same routine will be implemented for the GOES sounder. Negative values of LI indicate that the parcel is warmer than its environment and unstable.

In the GOES-R LAP code, it takes the following form to calculate LI in the code:

$$LI = T_{76} - (WLIFT5(T_{wb}) + 273.16 \quad (4)$$

where $T_{76}$ is the air temperature at the 76th level (500 hPa); *WLIFT5* is a function to calculate temperature at 500 hPa for the given wet-bulb potential temperature ($T_{wb}$), lifted along wet adiabatic process. The following equation is used to derive WLIFT5:

$$WLIFT5 = A0 + T_{wb} \cdot (A1 + T_{wb} \cdot (A2 + T_{wb} \cdot (A3 + T_{wb} \cdot (A4 + T_{wb} \cdot (A5 + T_{wb} \cdot A6))))) \quad (5)$$

here A0 to A6 are coefficients listed in Table A4. $T_{wb}$ is derived from the following equation:

$$T_{wb} = PT - WOBF(PT) + WOBF(T_c) \quad (6)$$

where $PT = (T + 273.16) \cdot (1000/P)^{0.28541} - 273.16$, the potential temperature (°C);

T: the air temperature in °C;

$P = P_s - 0.5 * P_{lid}$, the parcel pressure from surface ($P_s$) to 100 hPa ($P_{lid}$);

$T_C = T - (T - T_d) \cdot (A1 + A2 \cdot T + (T - T_d) \cdot (A3 + A4 \cdot (T - T_d) - A5 \cdot T))$, temperature at lifting condensation level, where T and $T_d$ are air and dew point temperature in °C, respectively; A1 to A5 are coefficients listed in Table A6. $T_d$ is widely used in the calculation of stability indices. In GOES-R LAP code it is derived depending on the air temperature T. If T is higher than -20 °C, the function *TEMSAT* is called to calculate temperature (K) at specified saturation vapor pressure $P_{sat}$ over water:

$$TEMSAT = A1 + V \cdot (A2 + V \cdot (A3 + V \cdot (A4 + A5 \cdot V))) + 273.16,$$

where $V = Log10(P_{sat})$, A1 to A5 are coefficients listed in Table A7. If $P_{sat}$ is lower than 0.0636 or higher than 123.3972, TEMSAT is set to 0. If T is lower than -20 °C, the function *TVPICE* is called to calculate temperature (K) at $P_{sat}$ over ice. It takes the same form as *TEMSAT* but with different coefficients:

$$TVPICE = A1 + V \cdot (A2 + V \cdot (A3 + V \cdot (A4 + A5 \cdot V))) + 273.16,$$

where $V = Log10(P_{sat})$, A1 to A5 are coefficients listed in Table A8. If $P_{sat}$ is lower than 1.403D-5 or higher than 6.108D0, *TVPICE* is set to 0. $T_d$ is the smaller value between *TEMSAT/TVPICE* and T. If *TEMSAT/TVPICE* equals to 0, $T_d$ is set as (T - 40).

WOBF is the difference between the wet-bulb potential temperature (°C) for saturated air and that for completely dry air at given temperature. It is calculated with two methods:
If temperature (T) is above 20°C, it takes this form:

$$WOBF = A4/(1 + (T - 20) \cdot (A1 + (T - 20) \cdot (A2 + (T - 20) \cdot A3)))^4 + A5 \cdot (T - 20) - A6$$

If temperature (T) is below 20°C, it takes this form:

$$WOBF = B4/(1 + (T - 20) \cdot (B1 + (T - 20) \cdot (B2 + (T - 20) \cdot B3)))^4$$

Here A1 to A6 and B1 to B4 are coefficients listed in Table A5.

The LI indicates the atmospheric thermodynamic instability, its value indicates that

0< LI, stable
-3< LI <0, marginally unstable
-6< LI <-3, moderately unstable
-9< LI <-6, very unstable

LI <-9, extreme unstable

The LI value itself cannot predict whether storms will occur. It gives the forecaster a general idea of the convective forcing if thunderstorms do develop. Unstable LI values (negative values) combined with high TPW values indicate that the troposphere is near saturation and has instability. The LI is less useful in winter when the bottom layer of the troposphere tends to be dry (low dew points) and cold (stable). Precipitation can be produced with stable LI due to other ingredients, which are not correlated with the LI like elevated convection, dynamic forcing without thermodynamic forcing and isentropic lifting. Therefore the LAP products must be used in conjunction with other data sources (forecast profiles, radio-sounding, and satellite imagery, Radar …) in order to alert the forecasters about the possibility of the occurrence of mesoscale events. The LAP is generated from the exploitation of ABI IR brightness temperatures (BTs). ABI provides one full resolution image (2 x 2 km at nadir) every 15 minutes at the satellite nadir for every IR channel. Thus, these products are useful in the prediction of severe weather due to their ability to measure high resolution temporal and spatial variations of atmospheric stability and moisture. A time sequence of the images is the best way to monitor drying and moistening trends as well as stability trends.

**CAPE** (convective available potential energy) in units of Joules per kilogram (J/kg) is a measure of the cumulative buoyancy of a parcel as it rises. Its definition is:

$$CAPE = g\int_{z_f}^{z_e}\frac{1}{T_{ve}}(T_{va}-T_{ve})dz \tag{7}$$

where $Z_f$ is the level of free convection, $Z_e$ is the equilibrium level, $T_{ve}$ and $T_{va}$ are wet-bulb potential temperature for the environment and the air parcel, respectively. $g$ equals to 9.806 which means the gravity acceleration in m/s$^2$. In the GOES-R LAP code, the integration is performed from the surface level to the 57$^{th}$ level corresponding to 100 hPa. $T_{ve}$ and $T_{va}$ at difference levels are calculated with these equations respectively:

$$T_{ve} = (T + 273.16)\cdot(1000/\mathrm{P})^{0.28541} - 273.16 \tag{8a}$$

$$T_{va} = (SATLFT + 273.16)\cdot(1000/\mathrm{P})^{0.28541} - 273.16 \tag{8b}$$

In the above two equations, $P$ is the air pressure at a specific level; $T$ is the air temperature (°C) and *SATLFT* is the temperature (°C) where moist adiabatically crosses $P$. The original algorithm to derive *SATLFT* in the sounding code was developed by Herman Wobus, a mathematician formerly at the navy weather research facility but now retired. The value returned by function *SATLFT* can be checked by referring to Table 78, pp. 319-322, Smithsonian meteorological tables, by Roland List (6$^{th}$ revised edition).

CAPE values larger than 1000 J/kg represent moderate amounts of atmospheric potential energy. Values exceeding 3000 J/kg are indicative of very large amounts of potential energy, and are often associated with strong/severe weather.

**TT** (Total Totals) Index in units of degrees Celsius (°C) is indicative of severe weather potential. And is computed using discrete pressure level information. It is a sum of two

separate indices: vertical totals (VT: measure of static instability) and cross totals (CT: measure of moist instability):

$$TT = VT + CT = (T850 - T500) + (T_d 850 - T500) \quad (9)$$

where $T$ and $T_d$ are air and dew point temperature in °C, respectively, for example, T500 represents atmospheric temperature at 500 hPa. In the GOES-R LAP code, the values of $T$ and $T_d$ at these specific pressure levels are linear interpolated from the original 101-level pressure ordinate.

Generally, TT values below 40 - 45 are indicators of little or no thunderstorm activity, while values exceeding 55 in the Eastern and Central United States or 65 in the Western United States are indicators of considerable severe weather.

**SI** (Showalter index) in units of degrees Celsius (°C) is a parcel-based index, calculated in the same manner as the LI, using a parcel at 850 hPa. That is, the 850-hPa parcel is lifted to saturation, then moist adiabatically to 500 hPa. The difference between the parcel and environment at 500 hPa is the SI. A SI value smaller than -3 indicates the possible condition for a severe weather.

**KI** (K-index) in units of degrees Celsius (°C) is a simple index using data from discrete pressure levels instead of a lifted parcel. It is based on vertical temperature changes, moisture content of the lower atmosphere, and the vertical extent of the moist layer. The higher the KI the more conducive the atmosphere is to convection. The formula for KI is:

$$KI = (T850 + T_d 850) - (T700 - T_d 700) - T500 \quad (10)$$

In the GOES-R LAP code, the values of $T$ and $T_d$ at these specific pressure levels (500/700/850 hPa) are linear interpolated from the original 101-level pressure ordinate. Severe weathers are very likely to occur if the value of KI exceeds 30.

Only clear ABI IR BTs within each Field-of-Regard (FOR) are processed for LAP and derived products. Usually there are multiple clear sky FOVs in each FOR. Two methods are available in the algorithm to select the representing value for the specific FOR: one is the simple average of all clear sky FOVs for each channel; another method is to determine the warmest FOV with largest value of the IR 10.8 channel and use the values of all IR channels at this FOV as representatives of this FOR. A subroutine named *Find_Good_BT* is presented for the BT manipulation in the main sounding retrieval module and called right after the determination of clear pixels within the FOR. The simple average method is better to reduce the instrumental noise. However, since there are always some cloudy pixels misidentified as clear pixels, which in general have lower value at IR 10.8 channel, the second method is better than the simple average in mitigating cloud impact. According to several cases with SEVIRI as used as proxy, it is found that the cold bias is much stronger than the instrumental noise (for details see 3.4.2.1); therefore the warmest FOV method is set as the default method in LAP sounding algorithm.

Temperature and moisture forecast information is used together with ABI IR clear BT for generation of LAP and derived products; two steps are used in the algorithm: regression followed by the variational iterative physical retrieval.

### 1.7 Instrument characteristics

The next-generation geostationary satellite series will enable many improvements and new capabilities for imager-based products. Given that GOES-R will not host a sounding instrument, the question becomes whether the products based on the ABI will provide an adequate substitute for legacy sounder-based products. The ABI (Schmit et al. 2005) on the next-generation GOES-R will certainly improve upon the current GOES imager with more spectral bands, faster imaging, higher spatial resolution, better navigation, and more accurate calibration. The ABI expands from five spectral bands on the current GOES imagers to a total of 16 spectral bands in the visible (VIS), near-infrared (NIR), and IR spectral regions. The coverage rate for full disk scans will increase to at least every 15 min, and the continental U.S. region will be scanned every 5 min. ABI spatial resolution will be 2 km at the subpoint for 10 IR spectral bands, 1 km for select NIR bands, and 0.5 km for the 0.64-µm VIS band (Schmit et al. 2005). However, the ABI was designed assuming a companion high-spectral-resolution IR sounder, originally called the Advanced Baseline Sounder (ABS), and more recently the Hyperspectral Environmental Suite (HES). Consequently, the ABI only has one carbon dioxide (CO2)-sensitive spectral band. It was envisioned that information from the ABI would improve select products from the HES, such as an improved sub-pixel characterization through the higher-spatial-resolution information of the ABI (Li et al. 2004a). Also, it was envisioned that information from the HES would improve ABI-based products, including cloud height (through the many spectral bands on the HES) and surface temperature through a better surface emissivity estimate. However, retrieval of atmospheric temperature and moisture profiles were to be computed solely with HES radiances.

Both the current GOES Sounder and ABI have three water vapor absorption channels although the spectral coverage is different. Studies have shown that the ABI, with numerical model forecast information used as the background, will be slightly inferior to the GOES-13/O/P sounder performance, yet both are substantially less capable than a high-spectral-resolution sounder with respect to information content and retrieval accuracy. The ABI will provide some continuity of the current sounder products to bridge the gap until the advent of the GOES advanced infrared sounder. Both theoretical analysis and retrieval simulations show that data from the ABI can be combined with temperature and moisture information from forecast models to produce derived products that will be adequate substitutes for the legacy products from the current GOES sounders (Schmit et al. 2008).

# 2 ALGORITHM DESCRIPTION

The LAP product is a continuation of the current GOES Sounder product. As we prepare for the next generation of geostationary satellites, it is important to ensure the continuity and quality of products that users depend on from the current satellite series. The GOES Sounders (Menzel and Purdom 1994) have provided quality hourly radiances and derived products over the continental United States (CONUS) and adjacent oceans for over a decade (Menzel et al. 1998). The derived products include: clear-sky radiances; temperature and moisture profiles; TPW and layer PW; atmospheric stability indices such as CAPE and LI. These products are used for a number of numerical weather prediction (NWP) and forecasting applications (Menzel and Purdom 1994; Bayler et al. 2001; Dostalek et al. 2001; Schmit et al. 2002). The GOES-13/14/15 Sounders will continue the mission of nowcasting (short-term forecasts) and NWP support. GOES-14 is the current on-orbit spare, while GOES-15 is under-going on-orbit testing.

The next generation GOES series will enable many improvements and new capabilities for imager-based products. Given that GOES-R will not host a sounding instrument, the question arises whether the ABI-based products will provide an adequate substitute for legacy sounder-based products.

The current GOES Sounders have 18 IR spectral bands to profile the atmosphere; while the current GOES Imagers have only 4 IR spectral bands, most of them provide surface and cloud information. With the advent of advanced imagers, like the ABI, producing 'legacy atmospheric profile type' products is possible (Schmit et al. 2008). However, the narrowband imager spectral coverage cannot match the performance of high spectral resolution advanced sounders (Schmit et al. 2009). The imagers have spectral resolution on the order of 50 – 200 $cm^{-1}$ for a single band, while advanced hyperspectral sounders have spectral coverage on the order of 0.5 $cm^{-1}$ for a single channel. The finer resolutions enable measurements of important spectral changes that result from vertical structures and other phenomena. Nevertheless, with the current four IR spectral band imager, certain products like TPW, LI and skin temperature have been produced (Hayden and Schmit 1991), evolving from experience with GOES VISSR and VAS data (Smith et al. 1985).

Although the advanced sounding products that were originally envisioned for GOES-R cannot be realized without the HES, legacy sounder products that are used by the NWS and others agencies must be provided. Schmit et al. (2008) showed that adequate substitute products can be generated from ABI data, in conjunction with information from short-term numerical model forecasts. The 'continuity' products produced from today's low-spectral resolution sounder include TPW, LI and surface skin temperature. Their study also showed that the ABI, combined with numerical model forecast information as the background, would be slightly inferior to the GOES-13/O/P Sounder performance, and substantially less capable than a high-spectral resolution sounder with respect to information content and retrieval accuracy. Current GOES sounder clear-sky radiances in bands 1-15 (14.7- to 4.4-µm) are assimilated in the NWP models. They will be replaced by ABI bands 7-16 (3.9- to 13.3-µm) which include only one $CO_2$ sounding band. Information from the future NPP/JPSS Cross-track Infrared Sounder (CrIS) and

other polar-orbiting high-spectral polar-orbiting IR sounders in conjunction with the finer spatial resolution ABI data may substitute for current sounder temperature information for radiance used within NWP, especially related to the large scale patterns. Research based on current polar orbiting systems has shown the benefits of combining high-spectral resolution IR sounder measurements with high spatial resolution imager data (Li et al. 2004; 2005). For NWP assimilation of GOES Sounder measurements, moisture is the key information. Regarding information content, both the ABI and current sounder have three narrow "water vapor" ($H_2O$ absorption) bands and longwave window bands. However, a HES-type sounder (Wang et al. 2007) with faster scanning and high spectral resolution remains essential for regional NWP, surface emissivity, better nowcasting products, moisture profiles, moisture flux, better cloud heights, and many additional environmental applications.

## 2.1 Algorithm Overview

This section describes the input needed to process the LAP and derived products. While the LAP products are derived for each FOR, the algorithm does require knowledge of the clear mask information for each FOV within the FOR. At the moment, the LAP algorithm can run on full disk (within the specified local zenith angle limitation), or CONUS, or mesoscale region. The LAP algorithm is also designed to run with information from only FOR.

## 2.2 Processing outline

The process initialization gives access to ABI IR radiances or BTs, ABI CM, local zenith angle and ancillary data (topographic data, land-sea mask, longitude, latitude). Only if the pixel or FOR is labelled as clear air (find 10 or more clear pixels within the FOR) and the local zenith angle of this pixel or FOR is below the configurable maximum zenith threshold (67 degree), the LAP TPW, PW, LI, CAPE, TT, KI, TT, and SI parameters are calculated for this FOR.

BTs of all IR channels are read into the LAP algorithm although some of them are not used. NWP files are used as background. The 3.9-um channel is excluded in retrieval because it is difficult to simulate accurately by community Radiative Transfer Model (cRTM), or Pressure-Layer Fast Algorithm for Atmospheric Transmittances (PFAAST). The 8.5-um is selectable because the surface emissivity at this channel has large fluctuation over desert. This channel is excluded in the default setting. The 9.7-um channel is used only in regression and is excluded in the physical retrieval. Table 2 summarizes the current channels used by the LAP product, although most VIS, NIR and IR bands are used by the cloud mask (CM) product generation.

Table 2. Channel numbers and approximate central wavelengths for the ABI.

| *Channel Number* | *Wavelength (μm)* | *Used in LAP Sounding* | |
|---|---|---|---|
| | | *Regression* | *Physical* |
| 1 | 0.47 | | |
| 2 | 0.64 | | |
| 3 | 0.86 | | |
| 4 | 1.38 | | |
| 5 | 1.61 | | |
| 6 | 2.26 | | |
| 7 | 3.9 | | |
| 8 | 6.15 | ✓ | ✓ |
| 9 | 7.0 | ✓ | ✓ |
| 10 | 7.4 | ✓ | ✓ |
| 11 | 8.5 | | (✓)* |
| 12 | 9.7 | ✓ | |
| 13 | 10.35 | ✓ | ✓ |
| 14 | 11.2 | ✓ | ✓ |
| 15 | 12.3 | ✓ | ✓ |
| 16 | 13.3 | ✓ | ✓ |

*: This channel is selectable in physical retrieval. It is safe to use over ocean only and must be avoided over desert.

Note: There are two arrays holding channel index usage in the GOES-R LAP code: the one for regression is fixed and the one for physical retrieval is changeable. It is easy to turn on or turn off the channel in the physical retrieval based on the actual performance of this channel after launch.

The algorithm relies on spectral and spatial information. The performance of the LAP is therefore sensitive to any imagery artifacts or instrument noise. Calibrated measurements are also critical because the LAP compares the observed radiances to those calculated from a forward radiative transfer model (RTM). The channel specifications are given in the GOES-R mission requirement document (MRD. The land-sea mask and the surface emissivity (SE) maps for the month at the IR channels are also used as input during the processing step on land pixels. The software has been designed in a very modular way.

The whole process includes:

(1) Pre-processing:

- Initialization: reading of processing options from the configuration file, calculating the minimal number of clear pixels required for a retrieval based on the FOR size and the minimal fraction of clear sky determined in the configuration file, reading of all coefficient file names, get IR SE maps, initialisation of RTM, get calibrated ABI IR BTs and associated geographical ancillary data to process, read of ABI CM, etc.
- Determined by configuration file, optional ABI clear averaging or warmest BT to process on FOR of M x M pixels. Mean of clear pixels BTs on FOR or BTs of warmest clear pixel at IR10.8, are the two available methods to calculate BTs of the FOR

- Take collocated forecast temperature and moisture profiles and other 2-D forecast products such as surface skin temperature, surface air pressure, and surface wind speed: spatial, temporal and vertical interpolation of [6 - 18 hours] range forecast NWP model to the RTM pressure levels of temperature and moisture profiles at the center of FOR position. The forecast can be 6-hour, 12-hour, or 18-hour forecast but the forecast will be outputted at least every 6 hours. The forecasts from two time steps will be interpolated to match the satellite observations. Temporally and vertically in space, it is linear interpolation. Horizontally the bi-linear interpolation is applied, based on the relative distance of the center pixel to the four nearest NWP grids. (Please refer to profile_utils.c in /geocat/src for details). Ideally, the highest temporal resolution forecast information should be used.
- Read in the regression coefficient array for non-linear regression to generate the first guess.
- Read in the look-up table (LUT) array for oceanic surface emissivity.
- Bias adjustment of ABI BTs. The bias correction coefficients are read from the configuration file and BT correction is made.
- Performing of non-linear regression to build the first guess profiles of temperature and moisture using bias corrected BTs, NWP profiles, NWP surface pressure, month, latitude, and local zenith angle (LZA).
- If over ocean/lake, perform a LUT-based interpolation method to get surface emissivity over water based on the near surface wind speed.

(2) Processing:

- Performing of physical retrieval for temperature and moisture profiles in Physical Retrieval Module using the first guess.
- Checking that the retrieved profiles of temperature and moisture are between limits and they have physical sense.
- Performing direct calculation of FOR TPW, PW, LI, CAPE, KI, TT, and SI parameters from the retrieved profiles of temperature and moisture.

(3) Post-processing:

- The following quality flags are output for each FOR:
    - Overall quality;
    - Retrieval quality, including failure to converge;
    - Quality of surface temperature first guess in term of the difference between calculated BT and observed BT at 11-μm.
- The following quality information is output for each FOR:
    - Number of clear sky pixels within the FOR;
    - Residual of the profile;
    - Number of iterations done;
    - Quality information bit-field: contains a single bit indicating ocean or land.
- Writing of output file.

A flowchart (Fig A1) is presented in the Appendix Section to help readers understand the whole process.

Note: A linear regression mode is assumed for bias correction. So far it is not done because we don't have field data. However, there are two arrays are hardcoded in the sounding code and one is filled with 1.0 for slope and the other is filled with 0.0 for offset. These two arrays will be removed in the future and an ancillary data file will be introduced, containing the coefficients for bias correction.

## 2.3 Algorithm Input

### 3.3.1 Primary Sensor Data

The list below contains the primary sensor data used by the LAP algorithm. The primary sensor data means information that is derived solely from the ABI observations and navigation.

- Calibrated BTs (K) for IR bands 7-16 from *M* x *M* (where *M*=5) FOV array, or calibrated BTs (K) for IR bands 7-16 from *M* x *M* FOV array
- Sensor LZA at the center of each *M* x *M* FOV array
- Latitude at the center of each *M* x *M* FOV array
- Longitude at the center of each *M* x *M* FOV array
- ABI channel use index array
- NeDR (radiance detector noise) array
- ABI CM for each pixel in the *M* x *M* FOV array (developed by cloud team)

### 3.3.2 Ancillary Data

The following lists and briefly describes the ancillary data required to run the LAP algorithm. Ancillary data means information that is not included in the ABI observations or navigation data.

- **Non-ABI dynamic data**

  (1) Surface pressure from 6–18 hour forecast from NWP model.
  (2) Surface pressure level index from 6–18 hour forecast from NWP model.
  (3) Near surface wind speed vectors (zonal and meridional) from 6–18 hour forecast from NWP model.
  (4) Surface skin temperature from 6–18 hour forecast from NWP model.
  (5) Temperature profile from 6–18 hour forecast from NWP model.
  (6) Moisture profile from 6–18 hour forecast from NWP model.
  (7) Forecast error covariance matrix from comparisons between forecast and radiosondes (matchup files) (Li et al. 2008). Assume there is no correlation between temperature and moisture in the error covariance matrix.

It is suggested that for CONUS or mesoscale processing, regional NWP output will be used, while global NWP data will be used in full disk processing.

- **Non-ABI static data**

(1) Land Mask
(2) Surface Elevation
(3) Temperature profile EOF file derived from the matchup files (Li et al. 2008).
(4) Water vapor profile (in term of logarithm of mixing ratio) EOF file derived from the matchup files (Li et al. 2008).
(5) IR SEs for ABI bands from UW-Madison baseline fit database. A global database of monthly IR land SE derived from the MODIS operational land surface emissivity product (MOD11). Emissivity is available globally at ten wavelengths (3.6, 4.3, 5.0, 5.8, 7.6, 8.3, 9.3, 10.8, 12.1, and 14.3 μm) with 0.05 degree spatial resolution (Seemann et al. 2008). Monthly SEs have been integrated into the ABI spectral response functions to match the ABI bands.
(6) LUT for ABI IR SEs over ocean as a function of LZA and wind speed above ocean surface. (http://ams.confex.com/ams/pdfpapers/104810.pdf).
(7) Regression coefficient file. This coefficient file contains 81 regression coefficient datasets. Each coefficient dataset corresponds to one LZA ranging from 0 to 80 degrees. The regression coefficient file is an array of 81*110 * (3*L+1+9), where L(=101) is the atmospheric pressure levels used in RTM.

The names of all Non-ABI static data files are labeled in the green boxes in Fig A1 except the IR SE files which are loaded into GEOCAT automatically when the program starts. In addition, a clear-sky fast and accurate forward RTM is needed in the iterative physical retrieval process. Currently the cRTM is used as the forward RTM. To run cRTM for ABI, the Planck-function and band-correction coefficients must be loaded into memory at the beginning (this is done by calling a subroutine which reads in these coefficients from a static data file ). Other ancillary static files needed for the cRTM ABI cases are provided. These files contain regression coefficients and are called in a subroutine for the calculation of atmospheric transmittance. For a complete view of the RTM mechanism, please refer to the Fig A1.

## 2.4 Theoretical Description

### 2.4.1 Physics of the Problem

LAP retrieval is a process of iteratively adjusting a first guess profile based on the BT residuals between observed and calculated ABI IR bands. The first guess is used in the initial calculation. ABI spectral and spatial radiance signatures are used in the retrieval process.

Assuming $CO_2$ is a well-mixed gas, an IR band with $CO_2$ absorption contains temperature profile information (assuming a non-isothermal atmosphere), while IR bands with varying gas absorption (e.g., $H_2O$) contains both temperature and the gas concentration information. ABI has 10 IR bands within which three bands contain strong water vapor absorption, one has strong ozone absorption and one has $CO_2$ absorption. The other ABI IR bands are atmospheric "window" bands that contain information of the surface skin temperature, emissivity and low level moisture.

The LAP algorithm infers a temperature and moisture profile from the satellite observed radiances in a given set of spectral bands. The air mass parameters are then derived from this profile. The method is an optimal estimation using an inversion technique. The method thus tries to find an atmospheric profile which best reproduces the observations (Rodgers, 1976). In general, this is a multi-solution problem, and therefore a "background profile" is here used as a constraint. This background profile is often from a short range forecast model, which is fed to the iteration scheme as an initial proposal for a solution. The original background is then slowly modified in a controlled manner until its radiative properties fit the satellite observations. In addition to the background, a first guess which is the starting point in the iteration procedure is used. The first guess is important, for example, if the first guess contains structure similar to the real atmosphere, the final solution will be good. A typical first guess field is a short-term forecast; however, we found a regression is usually better than the forecast since the regression uses combined forecast and ABI IR radiances as predictors, so the regression is used here as the first guess. Major limitations of this method are the high computational effort and the fact that the retrieved profiles tend to retain features of the first guess due to low spectral resolution and few spectral bands.

## 2.4.2 Mathematical Description

### 3.4.2.1 Use of Field of Regards (FOR)

The LAP execution on FOR basis has been evaluated, instead of pixel by pixel basis. This has been done in order to speed up the processing and because the processing in FOR could reduce noise, and also the spatial resolution of ABI LAP products will be similar to that of the current GOES Sounder. A box of *M* x *M* FOVs has been considered as adequate (see Figure 1) for one FOR. The width of the FOR (*M* x *M* pixels) will be an adjustable parameter in the configuration file. This will allow adjusting *M* depending on the size of the region to process and the machine characteristics of the user.

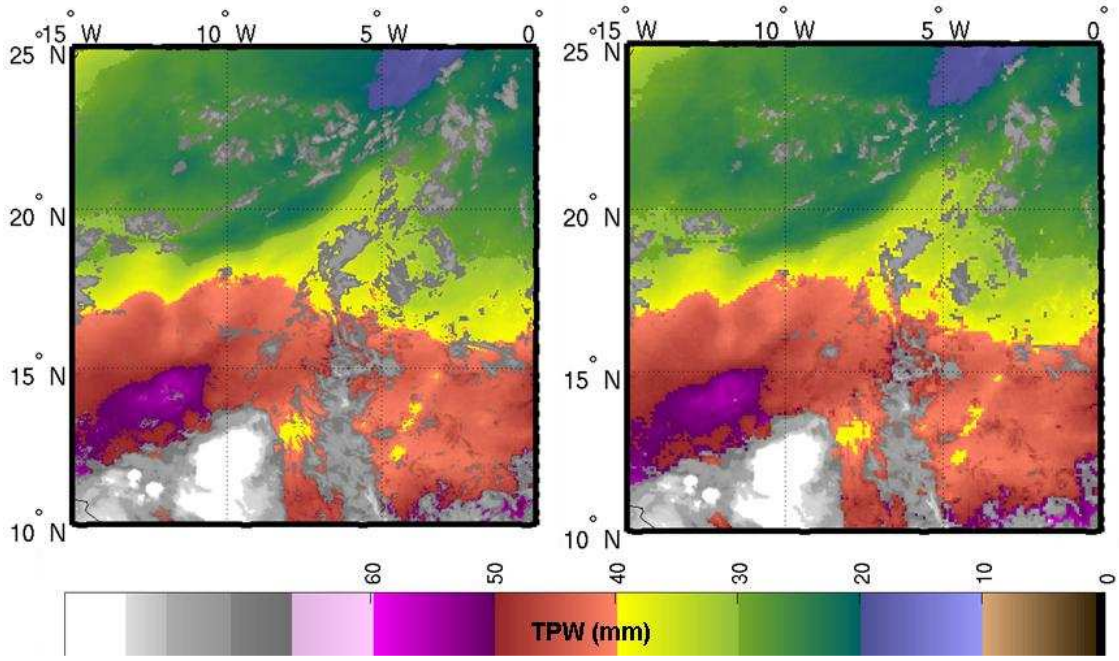


Figure 1. FOR – 1 x 1 FOV (left) versus FOR 3 x 3 (right) FOVs SEVIRI TPW at 00UTC on 18 August 2006.

Figure 2 shows the differences on the spread between RTTOV-9.2 simulated BT versus SEVIRI BT obtained with the mean of clear pixels and with the IR10.8 warmest clear pixel SEVIRI BT for grid boxes of 0.5ºx0.5º. ECMWF analysis 00 and 12 UTC has been used as input to RTTOV-9.2. Due to the different behaviour, two methods for calculating the FOR BTs will be implemented and checked in LAP:

(1) Mean BTs of all clear pixels within the FOR

(2) The BTs at the IR10.8 warmest clear pixel within the FOR

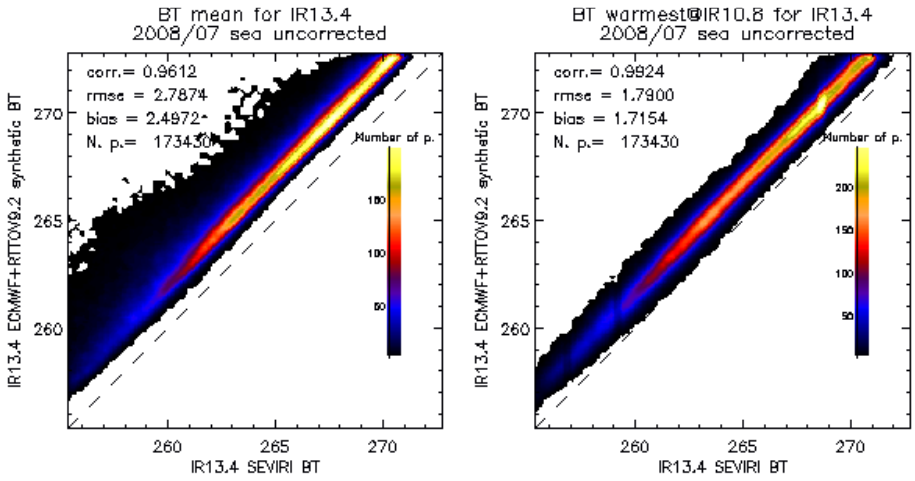


Figure 2. Scatter plots of IR13.4 SEVIRI BT versus ECMWF+RTTOV-9.2 synthetic BT. (Left) Mean of SEVIRI BT clear pixels in 0.5º x 0.5 º box. (Right) SEVIRI BT at IR10.8 warmest clear pixel in 0.5º x 0.5º box.

#### 3.4.2.2 NWP Profiles Interpolation to L Levels of RTM

As explained before, it is convenient to use a 6 – 18 hour range forecast NWP output from a model as background profile. The LAP software should be able to work with any NWP model and it should accept the set of levels available on the NWP files. Since it is not adequate to provide error matrices, EOFs, regression coefficients, etc for any number of pressure levels, it is necessary to perform the interpolation of different NWP model to RTM L pressure levels (e.g., 101 levels from 0.05 to 1100 hPa). Then, it is necessary to provide the functions and tools to manage NWP GRIB files and to apply spatial, temporal and vertical interpolation in order to get a collocated background profile of temperature and humidity at the FOR.

Temporal and vertical interpolations are made inside AIT mainframe processing. Temporal interpolation is made at NWP pressure levels between previous and following available NWP data close to the time of the image. In the case of vertical interpolation, it has been added a special function to make the vertical interpolation. A function has been developed to make the vertical interpolation that interpolates the temperature and humidity profiles from any set of pressure levels to RTM *L* pressure levels. This interpolation function interpolates linearly in logarithm of the pressure the NWP forecast temperature and humidity fields available on user-defined vertical pressure levels to the RTM *L* pressure levels.

Besides the profile interpolation, some NWP surface products including the surface pressure and surface skin temperature are also employed in the retrieval. They are interpolated into the satellite FOR resolution (each FOR contains *M* x *M* pixels) before regression. The surface pressure is required as a predictor for non-linear regression. The NWP surface skin temperature over ocean and lakes will be used as a fixed value in the physical retrieval and the regressed sea surface temperature will be discarded.

#### 3.4.2.3 Radiance Bias Adjustment

Radiance bias adjustment is very important for retrieval accuracy. The biases are caused by both measurement problems and errors in the radiative transfer model. The bias correction is based on finding the difference between the observed BTs and those simulated from the RTM (synthetic radiances). Usually there are two ways for radiance bias estimation

(1) using collocated NWP analysis and radiance measurements;
(2) using quality controlled radiosonde observations (RAOBs) and collocated radiance measurements

One issue in radiance bias calculation is the emissivity estimate. Due to the emissivity uncertainty, radiance bias estimation on window bands might not be reliable; especially on desert pixels. A possible solution is to conduct the bias adjustment using observations over ocean which requires a number of collocated RAOB and ABI observations over clear sky. BT bias correction for water vapor and $CO_2$ absorption bands should help the

retrievals. A small number of collocated SEVIRI BTs and RAOBs are applied in the GOES-R LAP algorithm to demonstrate the improvement after bias adjustment (Fig. 3) (Jin et al. 2008a). The coefficient of the bias adjustment's robust regression will be read from the configuration file. When GOES-R will be launched, initial bias configuration will be provided.

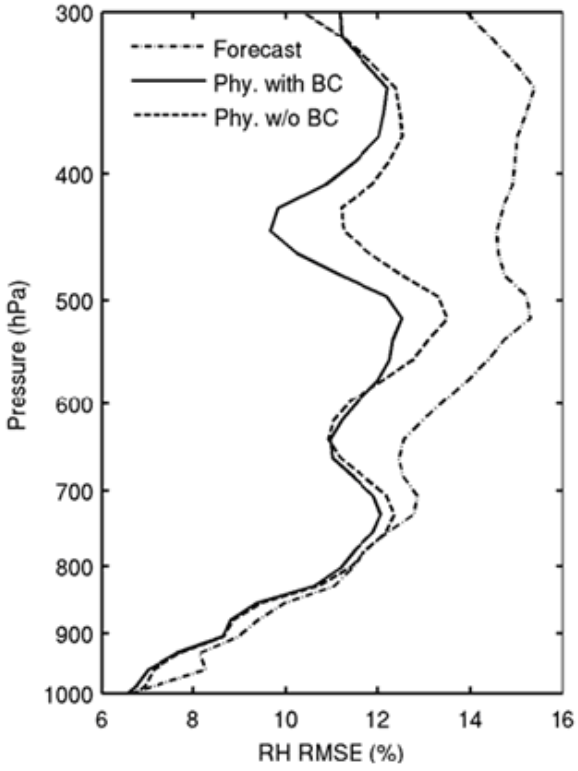


Figure 3. The retrieved RH RMSE profiles using SEVIRI BTs with (solid line) and without (dashed line) bias correction (BC) in physical retrieval. The dash-dotted line is the forecast RMSE for comparison.

#### 3.4.2.4 Use Generalized Least Squares Regression as First Guess

The LAP algorithm uses the general least squares (GLS) regression as the first guess; the regression uses ABI IR band radiances and forecast profile as predictors, Figure 4 shows the flowchart of the first step – deriving a regression first guess. A global radiosonde dataset with surface skin temperature and IR SEs physically assigned (Seemann et al. 2003; 2008) is used to generate the regression coefficients. The predictands include temperature/moisture/ozone profiles as well as surface skin temperature and SE; the basic predictors include ABI IR spectral band BTs, surface pressure, latitude, month, and land/ocean flag. Since ABI only has a few sounding spectral bands, the temperature/moisture profiles from NWP forecast model are used as additional predictors. Here we use temperature forecast between 100 and 1050 hPa and mixing ratio forecast between 300 and 1050 hPa as additional predictors. Given $Z$ (e.g., temperature or water vapor/ozone mixing ratio at a given pressure level) as a predictand, the regression equation is written in the following form:

$$Z = A_0 + \sum_{j=1}^{N} B_j T_{bj} + \sum_{j=1}^{N} C_j T_{bj}^2 + \sum_{l=1}^{n} b_{tl} T_l + \sum_{l=1}^{m} b_{wl} \log(w_l) + D_1 p_s + D_2(Lat) + D_3(mon) + D_4(Pland) \quad , \qquad (11)$$

here $T_{bj}$ is the channel $j$ BT; $T_l$ and $w_l$ are forecast temperature and water vapor mixing ratio at level $l$, respectively; $p_s$ is the surface pressure; *Lat* is the latitude between ± 70; *mon* is the month between 1 and 12; *Pland* is the land/ocean flag (1.0 for land and 0.0 for ocean). *A*, *B*, *b*, *C* and $D_1$ *to* $D_4$ are regression coefficients; *N*, *n* and *m* are the number of ABI IR spectral bands, profile temperatures and profile mixing ratios used as predictors, respectively. As of this writing, we have chosen 8 out of 10 ABI IR bands for baseline predictors (see Tab. 2). Considering the diurnal changes in Band 7 (3.9 µm) and the aerosol/dust contamination in Band 11 (8.5 µm) these two spectral bands are not used in the regression. 81 regression coefficient sets are generated; each coefficient set corresponds to one LZA ranging from 0° to 80°. Since the predictors have very different error levels, the GLS fit is applied. The error level for surface pressure is 10 hPa, land/ocean flag 0.01, latitude 0.1, month 0.0001. The error levels for temperature and moisture profiles are derived from the comparison of nearly 9000 collocated NOAA88 radiosonde measurements and the GFS forecast profiles at the ARM SGP site (Li et al. 2008).

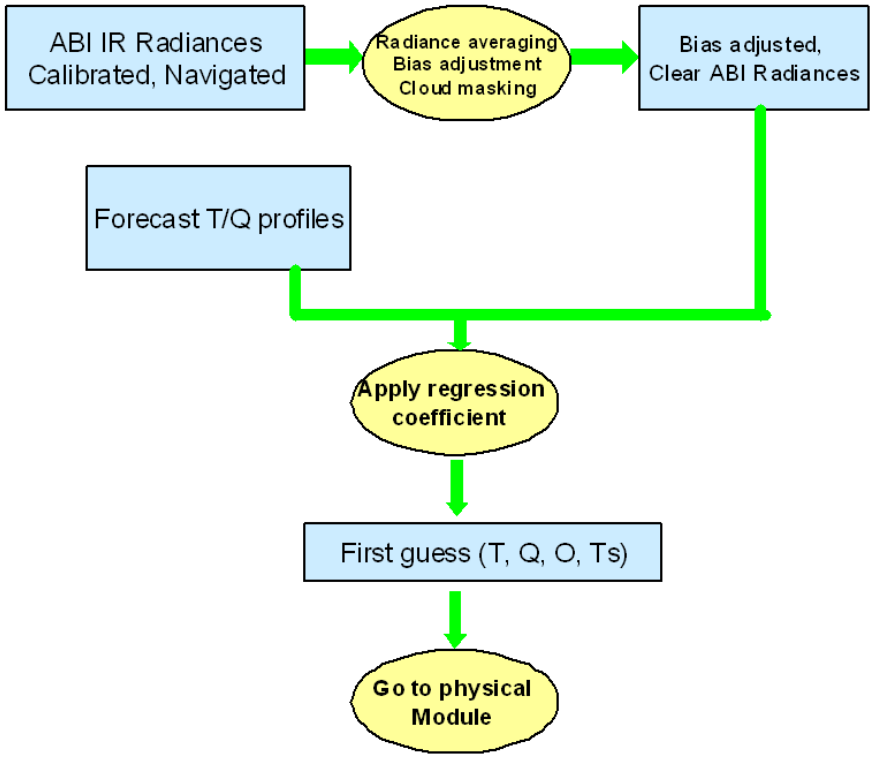


Figure 4. Regression flowchart for the LAP algorithm.

In order to generate the regression coefficients, the regression problem can be simplified by assuming a linear relationship between the atmospheric state vector **X** and the

measurements as well as additional predictors $\mathbf{Y}$ using $\mathbf{X} = \mathbf{C}\mathbf{Y}^{\mathbf{T}}$ , where $\mathbf{C}$ is the matrix of regression coefficients. $\mathbf{X}$ has the dimension of *nlevs* (number of levels) by *nsamps* (number of profiles/samples), while $\mathbf{Y}$ has the dimension of *nsamps* × *nchans* (number of channels) and $\mathbf{C}$ is *nlevs* × *nchans*. The superscript *T* refers to transposition. Since the elements in matrix $\mathbf{X}$ have non-constant variances, according to the method of GLS, a non-constant error covariance matrix must be introduced which is denoted as $\mathbf{\Omega}$. The best fitting solution is the one that minimizes the sum of the squared deviations from the data, i.e. $\mathbf{\Sigma}(\mathbf{X}-\mathbf{C}\mathbf{Y}^{\mathbf{T}})^2$, and minimization yields $\mathbf{C} = (\mathbf{Y}^{\mathbf{T}}\mathbf{\Omega}^{-1}\mathbf{X})^{-1}\mathbf{X}^{\mathbf{T}}\mathbf{\Omega}^{-1}\mathbf{Y}$.

To generate the regression coefficients, a global training data set, prepared at CIMSS to be used in clear-sky regression retrieval applications for various instruments, is utilized. The so-called SeeBor database (Borbas et al. 2005) comprises global temperature, humidity and ozone profiles from TIGR3, NOAA88, and ECMWF, supplemented by profiles from desert radiosondes and ozone sondes. The total number of training set profiles is approximately 15700. For each profile, some surface parameters critical for RTM calculation, such as surface skin temperature and SE at ABI IR bands are also accompanied. Other surface parameters such as surface pressure and surface type are provided as well.

The regression derived profile is used as the first guess for physical retrieval iterations. Since the forecast profile is used together with ABI IR BTs as predictors, the regression should be no worse than the forecast.

In summary, the following combination (in Table 3) is recommended for the first guess and background options, option 1 is recommend, and option 2 is acceptable if regression is not used.

Table 3. Options for first guess and background selection.

| Option | First guess option ($X_0$) | Background ($X^b$) | Background error covariance ($B$) |
|---|---|---|---|
| 1 | Regression | Regression | Forecast error covariance |
| 2 | Forecast | Forecast | Forecast error covariance |

Note that in the practice, the background can also come from the regression since the regression is close to the background; we find that using regression as both background and first guess provide the best results. This practical approach is not consistent with the theory of maximum likelihood since the radiances are used twice in both regression and physical retrieval, but it is consistent with the regularization inverse theory which is more mathematically solid. Therefore the regression is recommended for both first guess and background in the physical retrieval for practical purposes.

#### 3.4.2.5 Physical Retrieval Algorithm for LAP

The LAP retrieval approach uses an optimal method of combining ABI observations and a background in the form of short-term forecast from a NWP model which accounts for the assumed error characteristics of both. If we neglect scattering by the atmosphere, the

clear-sky radiance measured by the GOES-R ABI for a specific IR spectral band within a FOV is given by

$$R(\nu) = \varepsilon_s(\nu) B_s(\nu) \tau_s(\nu) - \int_0^{p_s} B(\nu) d\tau(0, p) + [1 - \varepsilon_s(\nu)] \int_0^{p_s} B(\nu) d\tau^*(\nu) \quad , \tag{12}$$

where $R(\nu)$ is the clear spectral radiance in the IR region as seen by the ABI IR band with central wavenumber $\nu$, $B$ is the Planck radiance which is a function of temperature at pressure ($p$), $\tau$ is the atmospheric transmittance function, subscript $s$ denotes surface, $\tau^* = \tau_s^2 / \tau$, and $\varepsilon_s$ is the SE. The BT $Tb(\nu)$ can be also calculated from $R(\nu)$. The measured BT for a given ABI IR band $k$ is

$$y_k^m = Tb_k + e_k \quad , \tag{13}$$

where $e_k$ is the measurement error plus other uncertainties such as calibration and radative transfer calculation errors.

The variational retrieval is performed by adjusting the atmospheric profile state, $X$, from the background, $X^b$, to minimize a cost function, $J(X)$ (Rodger 1990; Li and Huang 1999; Ma et al. 1999; Li et al. 2007). The regularization parameter (also called smoothing factor) is introduced for convergence and solution stability. The cost function is defined by

$$J(X) = [Y^m - F(X)]^T E^{-1} [Y^m - F(X)] + [X - X^b]^T \gamma B^{-1} [X - X^b] \quad , \tag{14}$$

where $\gamma$ is the regularization parameter, $\mathbf{B}$ and $\mathbf{E}$ are the error covariance matrices of background, $\mathbf{X}^b$, and the observation vector (channel radiances), $\mathbf{Y}^m$, respectively, $\mathbf{F}(\mathbf{X})$ is the forward RTM operator and superscripts $T$ and $-1$ are the matrix transpose and inverse, respectively. $\mathbf{Y}$ is vector of ABI IR BTs (10 IR channels for ABI), $\mathbf{X}$ is state vector containing temperature profile $T(p)$ and moisture profile $q(p)$ on L vertical pressure levels plus the surface skin temperature, $\mathbf{F}$ is fast RTM (operator) for radiances. That is

$$\begin{aligned} Y &= (y_1, y_2, \ldots, y_N) = (Tb_1, Tb_2, \ldots, Tb_N) \\ X &= (x_1, x_2, \ldots, x_{2L+1}) = (T_1, T_2, \ldots, T_L, \ln q_1, \ln q_2, \ldots, \ln q_L, T_s) \\ F &= (f_1, f_2, \ldots, f_N) \end{aligned}$$

By using the Newtonian iteration

$$X_{n+1} = X_n + J''(X_n)^{-1} \cdot J'(X_n) \quad , \tag{15}$$

the following quasi-nonlinear iterative form is obtained

$$\delta X_{n+1} = (F_n'^T \cdot E^{-1} \cdot F_n' + \gamma B^{-1})^{-1} \cdot F_n'^T \cdot E^{-1} \cdot (\delta Y_n + F_n' \cdot \delta X_n) \quad , \tag{16}$$

where $\mathbf{X}$ is the vector of atmospheric state to be solved, $n$ is the iteration step, $n = 0$ denotes first guess, $\delta X_n = X_n - X^b$, $\delta Y_n = Y^m - F(X_n)$. That is

$$\delta X = \delta \begin{pmatrix} T_1 \\ T_2 \\ . \\ . \\ . \\ T_L \\ \ln q_1 \\ \ln q_2 \\ . \\ . \\ . \\ \ln q_L \\ T_s \end{pmatrix} = \begin{pmatrix} T_1 - T_1^b \\ T_2 - T_2^b \\ . \\ . \\ . \\ T_L - T_L^b \\ \ln q_1 - \ln q_1^b \\ \ln q_2 - \ln q_2^b \\ . \\ . \\ . \\ \ln q_L - \ln q_L^b \\ T_s - T_s^b \end{pmatrix} \qquad \delta Y = \delta \begin{pmatrix} Tb_1 \\ Tb_2 \\ . \\ . \\ . \\ Tb_N \end{pmatrix} = \begin{pmatrix} Tb_1^m - Tb_1^c \\ Tb_2^m - Tb_2^c \\ . \\ . \\ . \\ Tb_N^m - Tb_N^c \end{pmatrix}$$

is the measured BT for ABI channel *k*, while is the calculated BT for ABI channel *k* through RTM **F.** F' is the tangent linear operative (Jacobian) of forward model **F**. The regularization parameter is adjusted in each iteration according to the discrepancy principal (Li and Huang 1999; Li et al. 2000).

The reason to introduce the regularization parameter is to balance the contributions from background and satellite observations in the solution. It is important when the background (e.g., forecast) error is not Gaussian, or the error exhibits only a locally Gaussian distribution. Since there are correlations among atmospheric variables, only a limited number of variables are needed to explain the vertical structure variation of an atmospheric profile (Smith, 1976). The number of independent structure functions can be obtained from a set of global atmospheric profile samples. Assume

$$X - X^b = \Phi A, \tag{17}$$

where $A = (\alpha_1, \alpha_2, \ldots, \alpha_M)$, and

$$\Phi = \begin{bmatrix} \Phi_T & 0 & 0 \\ 0 & \Phi_q & 0 \\ 0 & 0 & \Phi_{T_s} \end{bmatrix},$$

$\Phi_T$ is the $\tilde{N}_q$ matrix $\tilde{N}_T$ of the first EOFs of the temperature profile, $\Phi_q$ is the matrix of the first EOFs of the water vapor mixing ratio profiles, $\Phi_{Ts}$=1, and $M = \tilde{N}_T + \tilde{N}_q + 1$. In LAP processing, 1 temperature EOF and 3 water vapor mixing ratio EOFs are used. By definition, $\Phi^T\Phi$=1. Defining $\tilde{F}' = F' \cdot \Phi$, Eq. (13) becomes

$$A_{n+1} = (\tilde{F}_n'^T \cdot E^{-1} \cdot \tilde{F}_n' + \gamma B^{-1})^{-1} \cdot \tilde{F}_n'^T \cdot E^{-1} \cdot (\delta Y_n + \tilde{F}_n' \cdot A_n), \tag{18}$$

where $A_0 = 0$, and

$$\left\| F(A(\gamma)) - Y^m \right\|^2 = \sigma^2 , \tag{19}$$

where σ is the observation error of ABI, and define

$$\|X\|^2 = \frac{1}{N}\sum_{i=1}^{N} x_i^2 , \quad X = (x_1, x_2, ..., x_N) .$$

Eq. (17) and Eq. (18) are applied to derive the solution from ABI IR radiances.

In the LAP physical retrieval process, the water vapor profile is expressed as logarithm of mixing ratio given that the logarithm varies more linearly with the IR radiances than does the base mixing ratio. Figure 5 shows the practical flowchart of one dimensional variational (1DVAR) physical retrieval algorithm implemented in the LAP sounding code.

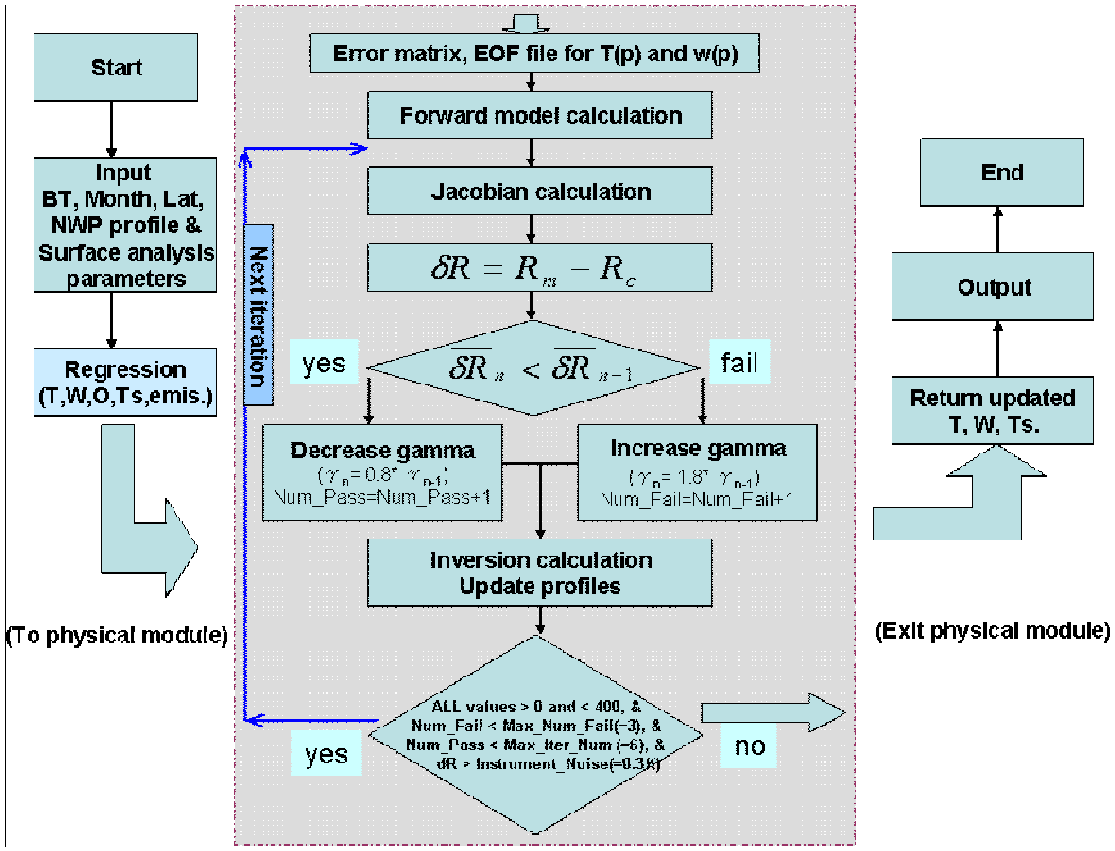


Figure 5. Variational iterative physical retrieval flowchart of the LAP retrieval algorithm.

2.4.2.5.1 **Atmospheric profiles (Xn)**

The atmospheric profiles of temperature and moisture are represented by the vector $\mathbf{X}_n$, where n=0 denotes the first guess profile. As of this writing, the LAP algorithm relies on the cRTM for the radiative transfer calculations, where the profile parameters are represented at a maximum of *L* prescribed pressure levels. The implementation of the physical retrieval uses 6-hour forecast or finer fields provided by NCEP (National Centers for Environmental Prediction) on half degree or finer latitude/longitude grid. Each profile is interpolated both in space and time to fit the time and location of the actual satellite observation. Since the forecast sea surface temperature (SST) is usually better than the regressed value as less impacted by the cloud contamination in clear pixels, it is also used in the retrieval as the temperature at the lowest layer and kept unchanged in the physical iteration. A total number of 121 clear sky radiosondes collected during the 2004 and 2006 AEROSE in the tropical North Atlantic Ocean are used for evaluation (Nalli et al. 2006). The comparison of ECMWF forecast SST, regressed SST and the measured SST is plotted in Figure 6. It is found that the forecast SST is much closer to the observation than the regressed that has an increased negative bias, showing the cloud contamination in the clear pixels. When over land, the regressed skin temperature is used in the retrieval and updated in each iteration. The observation vector thus has a length of $2L + 1$, that is, *L* temperatures, *L* humidity (mixing ratio) values and 1 surface skin temperature. Therefore, the NCEP Global Forecast System (GFS) forecast is used as the background profile $\mathbf{X}^b$.

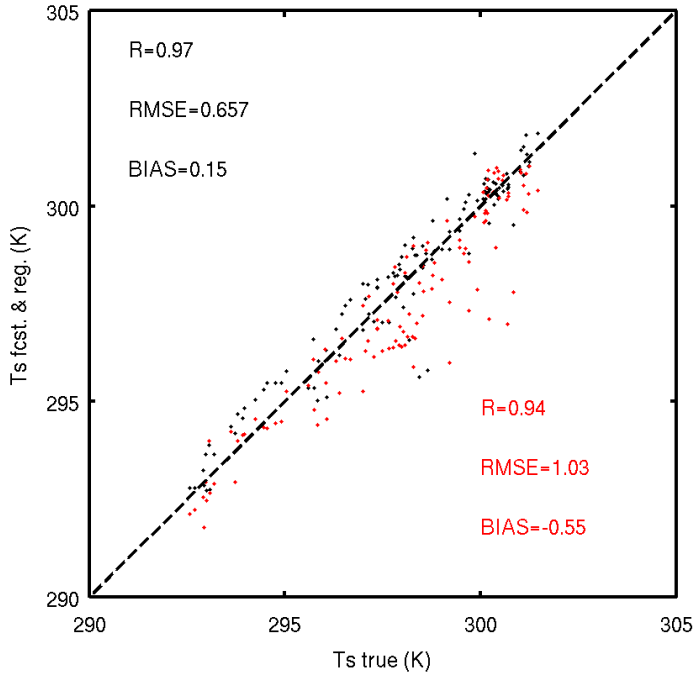


Figure 6. Forecast (black) and regressed (red) sea surface temperature against the measurement. The number of samples is 121.

#### 2.4.2.5.2 **The fast radiative transfer model and Jacobian matrix (*F* ′)**

The radiative transfer model employed in this version delivered to AIT is based on cRTM. Note that RTTOV and cRTM provide tangent linear Jacobian calculations, while

PFAAST does not provide Jacobian calculation and an approximate analytical form (Li 1994) is used.

The Jacobian matrix $F_n^{'}$ (the subscript **n** denotes the *n*th iteration in the physical retrieval procedure) describes the change of the radiance at the TOA with a changed atmospheric parameter:

$$F_n^{'}(i,j) = \frac{\partial Y_n(i)}{\partial X_n(j)} \tag{20}$$

Where *i* is the spectral band index in the radiance vector (**Y**), *j* is the parameter index in the profile vector (**X).**

If there are a total of *N* spectral bands used for physical retrieval, the matrix has thus *N* columns and 2*L*+1 rows. It is indeed the computation of these Jacobians that is a substantial factor of the computational load of the retrieval algorithm.

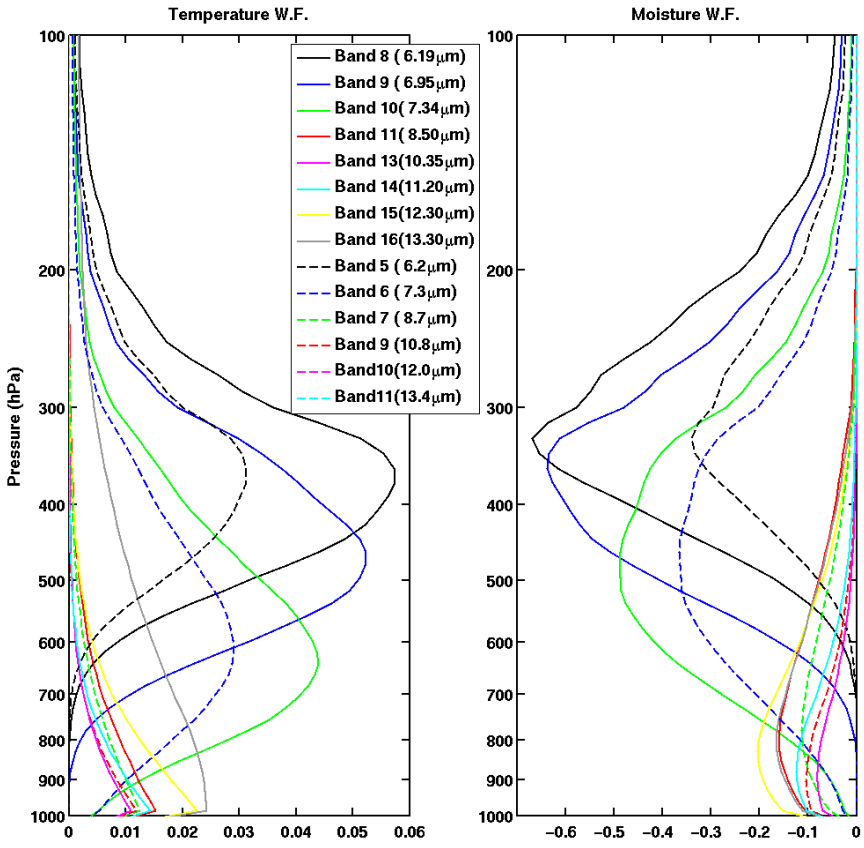


Figure 7. SEVIRI (dashed line) and ABI (solid lines) Jacobian calculations for temperature (left panel) and water vapour mixing ratio (right panel) with U.S. standard atmosphere and a LZA of zero.

Figure 7 shows the temperature (left panel) and water vapour mixing ratio (right panel) Jacobian calculations for some SEVIRI (dash lines) and ABI (solid line) IR spectral

bands from U.S. standard atmosphere with a LZA of zero. PFAAST is used in the calculations.

From the Jacobian calculations, it can be seen that SEVIRI 13.4 µm band provides temperature profile information; SEVIRI 6.2 and 7.3 µm spectral bands provide water vapour information. The information from forecast temperature profile along with the 13.4 µm provides temperature profile. Temperature profile is needed for moisture retrieval in order to derive the moisture information since these water vapour absorption bands also contain temperature information. The 12 µm and 13.4 µm bands also contain weak water vapour absorption, hence providing useful boundary layer moisture information. ABI has one more water vapour absorption band than SEVIRI.

Some comparisons among PFAAST, cRTM and RTTOV are done.

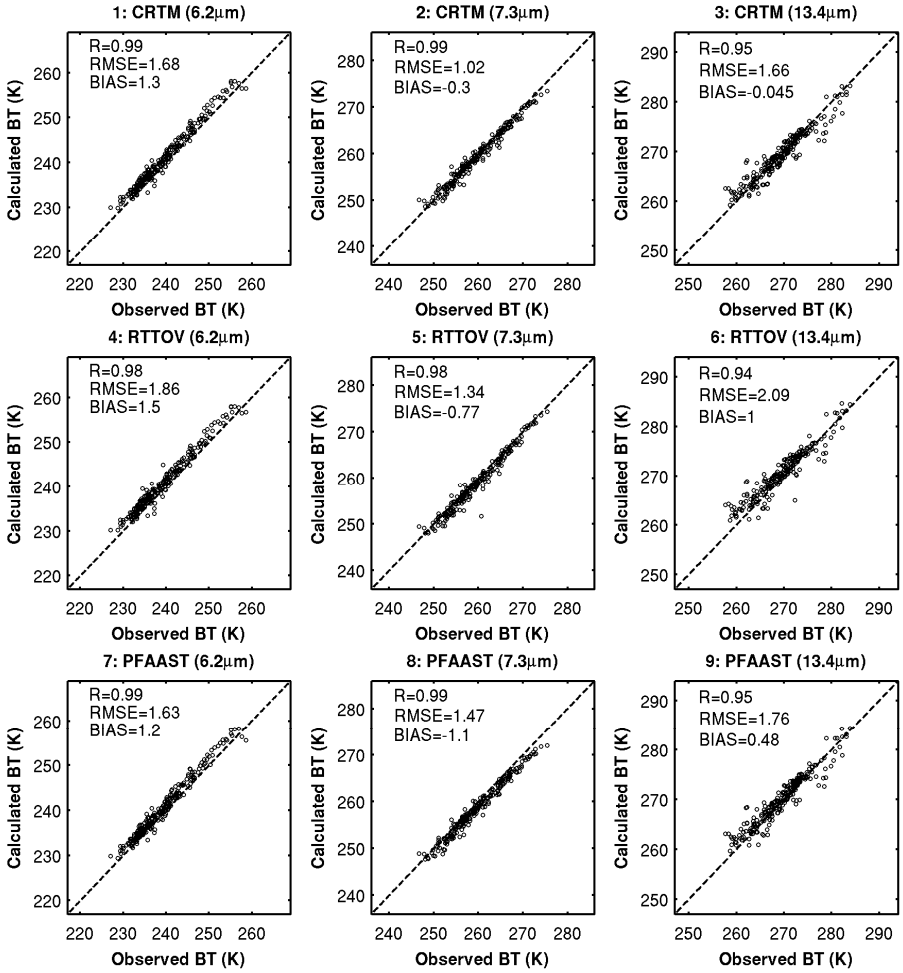


Figure 8. The scatterplot of BT from CRTM, RTTOV and PFAAST for band 6.2-, 7.3- and 13.4-µm against SEVIRI observations over land. 457 samples for August 2006 are included in calculations.

Figure 8 shows the comparison of BTs between RTM simulations and SEVIRI measurements for the three absorption bands. We found these models have similar

performances at the 6.2-µm, but cRTM has better agreement with observations at both 7.3 and 13.4-µm bands.

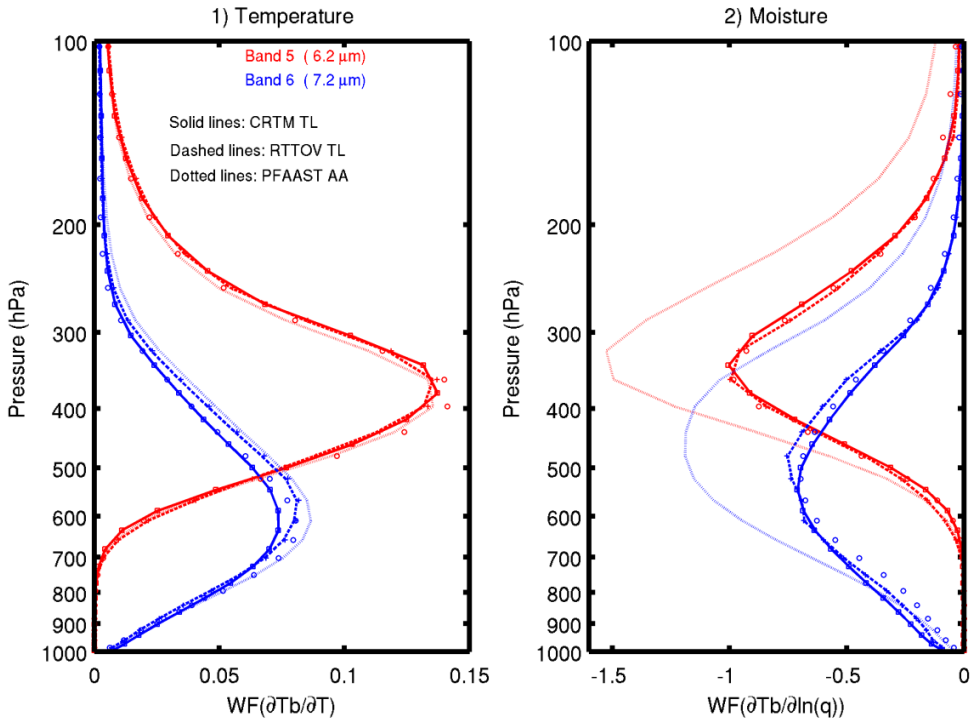


Figure 9. Comparison of Jacobians approaches in cRTM, RTTOV and PFAAST for the SEVIRI 6.2- and 7.3-um bands using US76 standard atmospheric model, given LZA of zero. Also plotted are results of perturbation method, using squares (□) for CRTM, pluses (+) for RTTOV and circles (○) for PFAAST.

Jacobian accuracy is also very important for LAP retrieval. Figure 9 shows the temperature (left) and water vapor mixing ratio (right) Jacobian calculations for SEVIRI water vapour absorption bands from cRTM, RTTOV and PFAAST based on the U.S. standard atmosphere with LZA of zero. The water vapor is expressed as a logarithm of mixing ratio in the Jacobian calculations. It is found that these approaches have very similar performances in extracting temperature profile information, but have quite large differences in extracting moisture profile information. The Jacobian approaches in cRTM and RTTOV are very close to the perturbation method, i.e. the true value.

#### 2.4.2.5.3 **Observed brightness temperatures (Ym)**

The observed BT vector $\mathbf{Y}^{\mathbf{m}}$ represents the satellite measured BTs in the *N* spectral bands. The original satellite measurements must be bias-adjusted to account for the (possible) bias between the satellite observation and the RTM. Such biases must be assessed in an independent step, (see section 3.2.4 for detail), for example, by comparing the clear sky radiances with the calculated radiances using the same RTM and collocated forecast/analysis atmospheric profiles.

#### 2.4.2.5.4 **Calculated brightness temperature (Yn)**

The calculated BTs $\mathbf{Y_n = F\ (X_n)}$ are computed from the atmospheric profile vector for iteration step *n* with the RTM. $\mathbf{Y_n}$ must be computed as a vector for all *N* IR spectral bands.

#### 2.4.2.5.5 **Discrepancy principle for regularization parameter**

The reason to introduce the regularization parameter γ (also called smoothing factor) is to (1) speed up the convergence, and (2) stabilize the solution in case the background error is not a Gaussian distribution, or only locally Gaussian distribution. The factor γ is to weight the contribution of background and satellite observations for the solution. If γ is too large, more weight is given to background and the solution tends to not deviate far from background. However, if γ is too small, more weight is given to satellite observations, but since the inverse problem is ill-posed and there are only a few spectral bands (equations), the solution could be unstable. Objective selection of γ is therefore very important for accurate and stable solution. The discrepancy principal is used to select this regularization parameter (Li and Huang 1999) which is reflected by Eq. (19), where

$$\sigma^2 = \sum_{k=1}^{N} e_k^2 , \tag{21}$$

$e_k$ is the square root of the diagonal of **E** or the observation error of spectral band *k*, which includes instrument error and forward model error, that is,

$$e_k^2 = \eta_k^2 + f_k^2 , \tag{22}$$

where $\eta_k$ is the instrument noise of spectral band *k*, whereas $f_k$ is the forward RTM error that is assumed to be 0.15 K or less for the same spectral band. Usually $\sigma^2$ can be estimated from the instrument noise and estimated RTM error.
Since Eq. (19) has a unique solution for γ, the atmospheric parameters and the regularization factor can be determined simultaneously. For simplicity, a numerical approach (Li et al. 2000) is adopted for solving Eq. (19); γ is changed in each iteration according to

$$\gamma_{n+1} = q_n \gamma_n , \tag{23}$$

where *q* is a factor for γ to increase or decrease. Based on Eq. (23), *q* is obtained within each iteration by satisfying the following conditions:

$q$ = 1.0;

If $\left\| F(X_n)\text{-}Y^{\mathrm{m}} \right\|^2 < \sigma^2$, then $q_n = 1.8$;
If $\left\| F(X_n)\text{-}Y^{\mathrm{m}} \right\|^2 = \sigma^2$, then stop the iteration;
If $\left\| F(X_n)\text{-}Y^{\mathrm{m}} \right\|^2 > \sigma^2$, then $q_n = 0.8$.

The $q$ factor has been found from empirical experiments to ensure that the solution is stable between iterations. Thus, $\gamma$ continues to change until the iterations stop.

#### 2.4.2.5.6 **Iteration checking and residual estimation**

In the retrieval processing, several checks are made for retrieval quality control. The quantity $Rs_{\mathrm{n}} = \left\| F(X_n)\text{-}Y^{\mathrm{m}} \right\|^2$ is computed to check the convergence or divergence as follows:

If any element of $X_n > 400$ *or* $<0$, the profiles are not reasonably reconstructed from eigenvector space to normal space, stop iteration, use first guess as final retrieval.
If $\delta^2 < Rs_{\mathrm{n+1}} < Rs_{\mathrm{n}}$, iteration is convergent, set $q_n = 0.8$, continue to next iteration and accumulate the count of passed iteration;
If $Rs_{\mathrm{n+1}} > Rs_n$, iteration is divergent, $q_n = 1.8$, continue to next iteration and accumulate the count of failed iteration;
If $Rs_{\mathrm{n+1}} < 0.3$ stop iteration.
If the count of passed iteration > 6 stop iteration.
If the count of failed iteration >= 3 stop iteration.

The degree of convergence for each iteration depends on the accuracy of the previous atmospheric and surface state. In addition, in each iteration, each level of water vapor profile is checked for super-saturation. A unity magnitude of RH (=99%) is assumed at any supersaturated level. Moreover a unity magnitude of RH (=2%) is assumed at any level in case of dry bias.

#### 2.4.2.5.7 **Other considerations**

The algorithm testing is conducted on a Dell workstation running Linux using code written in FORTRAN. For computation efficiency, the following transform can be performed for Eq. (18):

$$\hat{\bar{F}}_n^{'} = E^{-\frac{1}{2}} \cdot \tilde{\bar{F}}_n^{'}, \tag{24a}$$

$$\delta\bar{Y}_n = E^{-\frac{1}{2}} \cdot \delta Y_n, \tag{24b}$$

Then Eq. (18) becomes

$$A_{n+1} = (\bar{F}_n^{'T} \cdot \bar{F}_n^{'} + \gamma B^{-1})^{-1} \cdot \bar{F}_n^{'T} \cdot (\delta\bar{Y}_n + \bar{F}_n^{'} \cdot A_n). \tag{25}$$

Using Eq. (25) instead of Eq. (18) will avoid some matrix multiplications and reduce computation time.

In addition,

(1) For the regression, all the ABI IR bands will be used except the 3.9- and 8.5-µm bands
(2) For the physical retrieval, all ABI IR bands are used except the 8.5-, 9.7- and 3.9-µm bands
(3) Forecast profiles (temperature/moisture) and surface skin temperature should be spatially and temporally interpolated into ABI FORs
(4) Surface temperature and moisture, if available, can be used to improve the boundary layer temperature and moisture retrievals
    a. The science codes contain the option of including surface temperature and moisture observations
    b. The surface temperature and moisture observations are treated as two additional spectral bands in the physical retrieval.

### 2.4.3 Algorithm Output

The Product Refresh Rate for the algorithm consists of a 30 minute CONUS refresh and a 60 minute full disk refresh. Under these instances, the algorithm will only be run every half hour and every hour, respectively. No temporal aggregation is required.

The output of the algorithm for each FOR includes:

Product:(1) LAP products: 101-level atmospheric temperature profile in K, 101-level atmospheric moisture profile in g/kg.
(2) Derived products: TPW, PW_low, PW_mid, PW_high, LI, CAPE, KI, SI, and TT.
(3) Surface skin temperatures in K: updated if over land; unchanged from NWP forecast if over ocean/lake

Detailed description of the product can be found in Table A1.

Quality Flags:

(4) General Quality Flag: including some general information of each pixel such as space background, latitude range, local zenith angle range, missing NWP data, or number of clear pixel, and etc. Please see Table A2 for the detail;
(5) Retrieval Quality Flags: non-convergent iterations, large residual, bad or missing radiance data, etc. The definition of the value assigned to each condition is listed in Tab A2.
(6) First Guess Quality Flags: the 11-µm BT difference between observation and calculation using first guess to drive the RTM. This is critical as the uncertainty of surface skin temperature is the largest error source in the physical iteration. The definition of each value assigned can also be retrieved from Table A2.

Diagnostic/intermediate information:

(7) Number of clear sky pixels in the FOR.
(8) Number of iteration for each retrieval.
(9) Residuals of average BT between observation and calculation after retrieval.
(10) Land/Ocean flag. Please see Table A3 for details.

Metadata:

(1) Min, Max, Mean, Std of retrievals from first guess for TPW, LI, TT, CAPE, and SI.
(2) Number of IR channels.
(3) Mean difference between calculated BT (from first guess) and observed BT for each IR channel.
(4) Number of QA flag values.
(5) Percent of retrievals with each QA flag value.
(6) Definition of each QA flag.
(7) Total number of attempted retrievals.

# 3 Test Data Sets and Outputs

This section describes the inputs and coefficients files needed to process the LAP and derived products. These files are needed by the LAP software.

Note: All of the ancillary files and external functions/subroutines applied in the LAP sounding algorithm are shown in a sketch map in Fig. A1.

The list of inputs and files needed is the following:

- **Inputs**
  - i) ABI IR BT
  - ii) ABI CM
  - iii) GFS GRIB files from range [6 - 18] hour forecasted
- **ABI geographical data**
  - a. Longitude
  - b. Latitude
  - c. LZA
- **Coefficients**
  1. Bias correction coefficients
  2. Regression coefficient file. This coefficient file contains 81 regression coefficients; each coefficient dataset corresponds to one LZA ranging from 0 to 80 degrees
  3. Error covariance matrix of background and first guess (B)
  4. Error covariance of observation matrix (E)
  5. Look-up-table for sea surface emissivity
  6. EOF (Empirical Orthogonal Function) coefficients: Temperature profile EOF file derived from training dataset and Water vapor profile (in terms

of the logarithm of the mixing ratio) EOF file derived from the training dataset.

7. RTM coefficients for the GOES-R satellites are also needed

- **Geographical static data files**
    1. IR surface emissivity for ABI IR bands from University of Wisconsin (UW) baseline fit database.
    2. Land-sea mask and topographic data
- **Configuration File of LAP**

## 3.1 Input Data Sets

### 3.1.1 ABI IR BT

The ABI IR channels are the main input to LAP process. See Table 2 for the ABI BT values needed at full IR spatial resolution.

The LAP process checks the availability of mandatory ABI IR channels for each pixel; no results are produced for pixels where one or more channels are missing. The use of IR8.7 BT over ocean should be studied (the 8.7-μm has good boundary layer moisture information but might be affected by dust aerosol).

### 3.1.2 ABI Cloud Mask

LAP and derived products are only generated in clear sky pixels. As cloud mask is a mandatory input to LAP, ABI CM must be executed before LAP process.

### 3.1.3 NWP data

NWP profiles from 6 – 18 hour forecast are needed. These NWP data needs to be spatial, temporal and vertically interpolated to get NWP data collocated with ABI data. The following parameters are needed:

(1) Surface pressure (SP)

(2) Surface pressure level index

(3) Surface Skin Temperature or Sea Surface Temperature

(4) Vertical temperature (K) profile at NWP pressure levels

(5) Vertical water vapor mixing ratio (g/kg) profile at NWP pressure levels

(6) Sea surface wind speed

### 3.1.4 ABI geographical data

Longitude, Latitude and LZA associated to ABI coverage are computed on real time by functions available on the mainframe.

### 3.1.5 Coefficient files and other files

#### 3.1.5.1 Bias correction coefficients

The original satellite measurements must be bias-adjusted to account for the bias between the satellite observation and the used RTM. Such biases must be assessed in an independent step, e.g. by comparing the clear sky BTs with the calculated BTs using the same RTM and collocated forecast/analysis atmospheric profiles. In order to calculate the estimation of the bias correction coefficients, the software and datasets for bias radiance estimation will be developed after GOES-R is launched. The collocated ABI IR radiances, radiosondes and model analysis will be used for radiance bias estimate.

#### 3.1.5.2 Regression coefficients

A global radiosonde dataset with surface skin temperature and surface IR emissivities physically assigned (Seemann et al. 2003; 2008) is used to generate the regression coefficient. Since forecast temperature and moisture profiles are used as predictors to help the retrievals. Since there are no forecast data in the database, the forecast error profiles have to be constructed to simulate the forecast data. A separate match-up database is used to derive the forecast error profile; it contains RAOBs, the GOES-12 Sounder BT measurements and the NCEP GFS model forecast profiles (the RAOB/GOES/GFS match-up database) from June 2003 to September 2004 over the CONUS. One difficulty in constructing a forecast error profile is that temperature/moisture at one level is highly correlated with those from nearby levels. In order to characterize the correlation in the error profiles, the principle components analysis (PCA) is applied.

From the RAOB/GOES/GFS match-up database, a set of forecast error profiles U are obtained. Then the PCA is performed on U

$$U = E \times \Lambda \tag{16}$$

Where $E = [E_1, E_2, ....., E_m]$ is the Eigenvector and *m* is the number of Eigen vector. $\Lambda$ is the matrix set of Eigen values. For each error profile $U_i$ (i=1, n, and n is the number of profiles), we have $U_i = E \times \Lambda_i$ **w**here $\Lambda_i = [\Lambda_{i1} \quad \Lambda_{i2} \quad .... \quad \Lambda_{im}]^T$ is the Eigen values for the i$^{th}$ error profile. The j$^{th}$ Eigenvalues $\Lambda_{ij}$ corresponds to the j$^{th}$ Eigen vector $E_j$. Both the Eigen vectors and the Eigen values are arranged in the order of relative importance with the most important Eigen value/vector as the first one. Statistical analysis is performed on all the Eigen values to get the mean and the standard deviation (STD), which are used to generate random numbers as Eigen values, which in turn are used to simulate the forecast error profiles. Due to the correlation between nearby levels, it is not necessary to have all the Eigen values and vectors to reconstruct each profile. Using 90 % of the dataset as training and other 10 % for validation, it shows that 15 temperature and 9 moisture Eigenvectors are sufficient to construct 95 % of the variance of the forecast error profiles. Figure 10 shows the original (orgn) and constructed (cnst) bias and root mean square (RMS) of forecast error. The temperature is in K, and the moisture in logarithm of mixing ratio (g/kg). The thin dotted line is the constructed bias profile; the thin solid line is the original bias profile; the thick dotted line is the constructed RMS profile; and the thick solid line is the original RMS profile. Except around 200 hPa, where the temperature is highly variable near the tropopause, the constructed error profiles have very close bias and RMS as original ones.

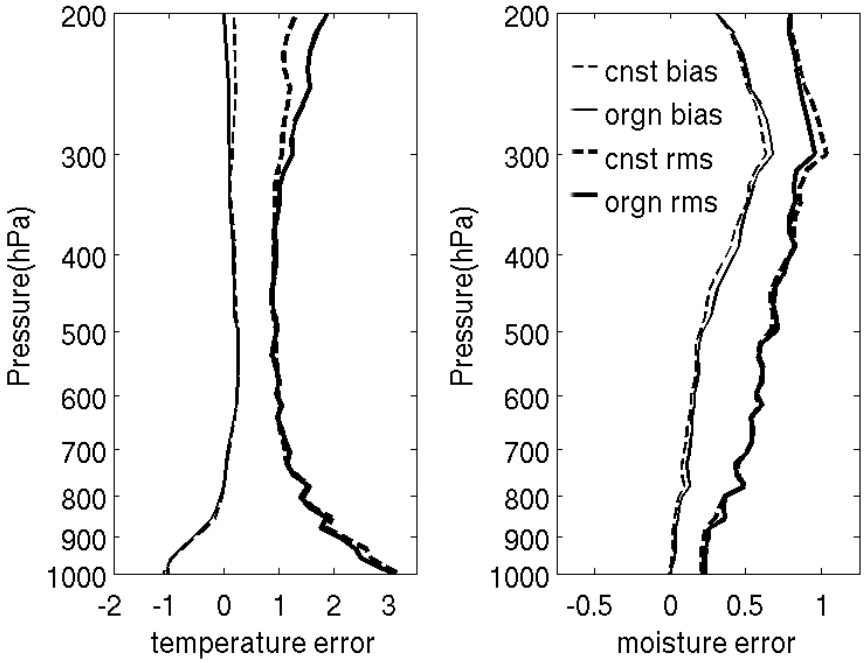


Figure 10. The original (orgn) and constructed (cnst) bias and RMS of forecast error. The temperature is in K, and the moisture in logarithm of mixing ratio (g/Kg). The thin dotted line is the constructed bias profile; the thin solid line is the original bias profile; the thick dotted line is the constructed RMS profile; and the thick solid line is the original RMS profile.

The regression derived profile is used as the first guess for physical retrieval iterations. Since forecast profile is used together with ABI IR BTs as predictors, the regression should be not be worse than the forecast.

### 3.1.5.3 The error covariance matrix of background and first guess (B)

The statistical error of the background is represented by the matrix **B** (see Figure 11). This (2*L*+1) by (2*L*+1) element matrix represents the correlation of the background error of one parameter to the same parameter in another level. The pairs of errors for temperature, humidity and skin temperature are assumed to be uncorrelated. The levels correspond to the RTM pressure levels. Schematically, the matrix has thus the above form, where the value of 6.5 in the lower right corner is the error correlation of the skin temperature to itself (by assuming that the skin temperature background has an error of 2.5 K). The matrix will be supplied by CIMSS at the University of Wisconsin-Madison (UW-Madison) and can be calculated from radiosondes and NCEP GFS forecast matchup file. The temperature error correlation values are available for every 5° latitude belt and are the same for the northern and the southern hemispheres. The humidity error matrix is available only on a global scale.

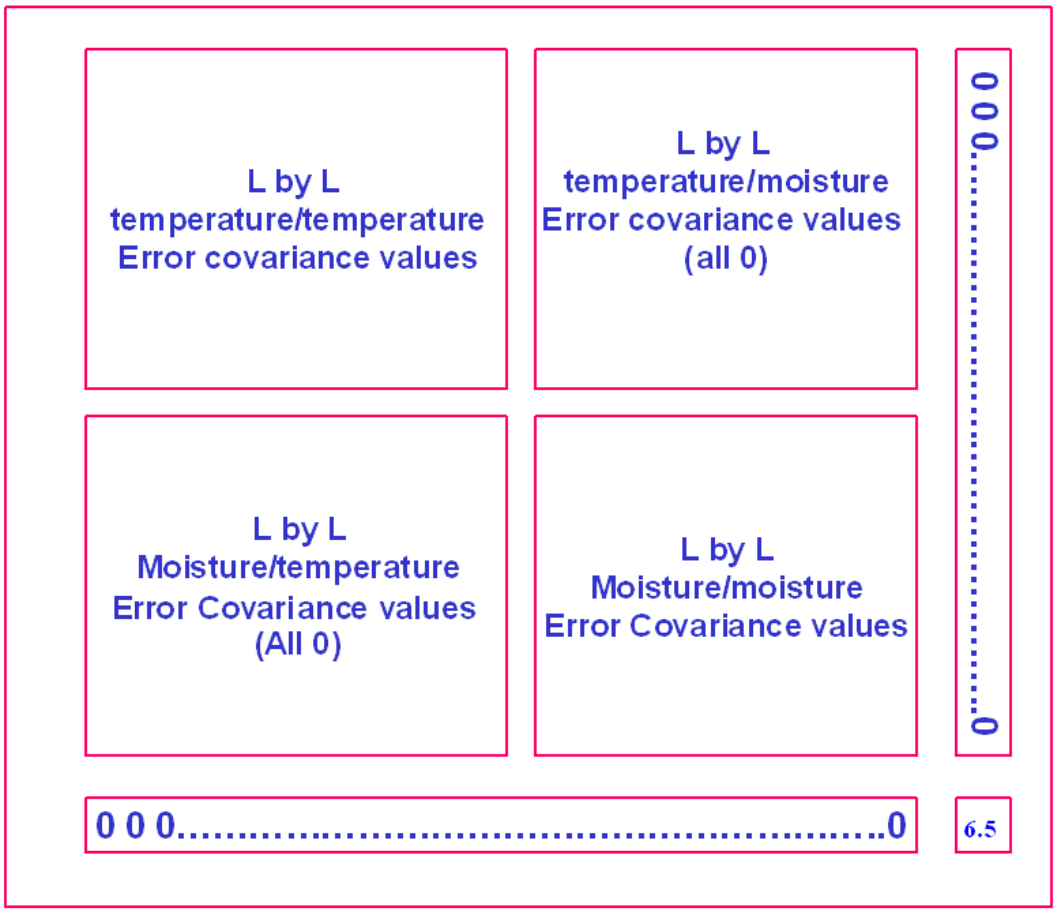

Figure 11. The background error covariance matrix.

### 3.1.5.4 The observation error covariance matrix

The errors of the observed BTs and the errors of the RTM are represented by the matrix **E**. The elements describe the covariance of the BT error of the instrument, and an assumed uncertainty of the RTM is added to that value. As the covariance of any two different spectral bands is not known, this matrix has only diagonal elements. The (assumed) error of the radiation model was merely added to these diagonal elements. The observation error covariance matrix is defined as diagonal matrix; the diagonal element is the square of observation error defined by Eq. (22).

$$E = \begin{pmatrix} e_1^2 & 0 & 0 & 0.....0 \\ 0 & e_2^2 & 0 & 0.....0 \\ ..... & & & \\ 0 & 0 & .....e_N^2 & \end{pmatrix}$$

The instrument noise is from ABI specification (0.1 K at 300 K for ABI bands 7–15 and 0.3 K at 300 K for ABI band 16); 0.15 K is assumed for forward model error for each ABI spectral IR band.

### 3.1.5.5 EOFs for temperature and moisture profiles

Since there are correlations among atmospheric variables, only a limited number of variables are needed to explain the vertical structure variations of an atmospheric profile (Smith, 1976). The number of independent structure functions (i.e., EOFs, the Empirical Orthogonal Functions) can be obtained from a set of global atmospheric profile samples. See Eq. (16) for the EOF representation of a profile. Using EOF representation is necessary because of the limited number of ABI IR spectral bands available. The advantages of using EOF representation for a profile are: (1) reducing the number unknowns in solution, which makes solution more stable, and (2) significantly reduce the time of computation in the retrieval process. We have found that using the EOF representation will not degrade the retrieval accuracy in ABI profile retrieval.

Figure 12 shows the first 5 temperature EOFs (left panel) and first 5 water vapor mixing ratio (logarithm) EOFs calculated from a global training data set.

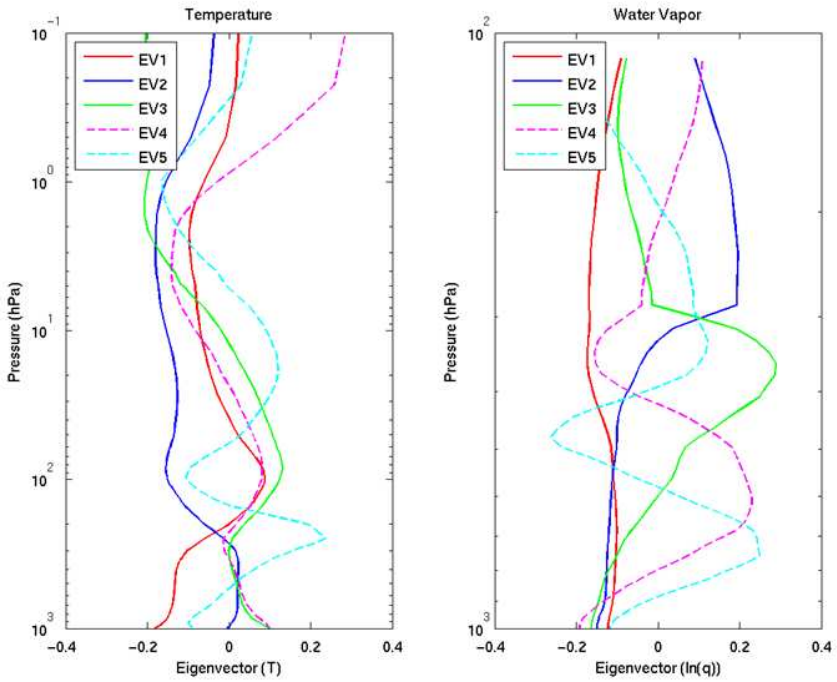


Figure 12. The first 5 temperature EOFs (left panel) and first 5 water vapor mixing ratio EOFs derived from a global training data set. The water vapor is expressed as the logarithm of mixing ratio in EOF calculations.

Table 4. The cumulative variances for T, ln(Q) and ln($O_3$) for the first 5 EOFs.

| EV | Cumulative Var for T (%) | Cumulative Var for Ln(Q) (%) | Cumulative Var for Ln(O3) (%) |
|---|---|---|---|
| 1 | 68.0 | 39.3 | 80.0 |
| 2 | 81.5 | 76.7 | 87.6 |
| 3 | 87.4 | 85.7 | 92.1 |
| 4 | 90.5 | 90.6 | 94.4 |
| 5 | 92.8 | 93.2 | 96.1 |

Table 4 lists the cumulative variances for the first 5 EOFs for temperature profile (T), water vapor mixing ratio profile (lnQ) and ozone mixing ratio profile (lnO3). Profiles from a hemispheric training dataset are used for EOF calculations. In the ABI physical retrieval process, 1 temperature profile EOF is recommended since there is only one $CO_2$ absorption band, and 3 water vapor mixing ratio EOFs are recommended since there are three water vapor absorption bands plus 12.3-µm and 13.3-µm weak water vapour absorption bands that provide boundary layer moisture information.

### 3.1.5.6 RTM coefficients

In addition, a clear sky fast and accurate RTM is needed in the retrieval process. In the current LAP version delivered to Algorithm Integration Team (AIT), the cRTM is used.

### 3.1.5.7 IR SE database

Handling IR SE is very important since an emissivity error of 0.01 in IR window region could result in approximately 0.5 K BT changes. There are three methods to handle IR SE in physical retrieval:

(1) Use emissivities from database;
    a. Advantage: monthly global coverage
    b. Disadvantage: currently only available at MODIS spectral bands
(2) Use look-up-table to calculate SE over ocean as a function of LZA and surface wind speed;
(3) Use regression based emissivities;
    a. Advantage: dynamic emissivities, at ABI bands
    b. Disadvantage: rely on emissivities in training data, might create false diurnal variation in ABI emissivity retrievals

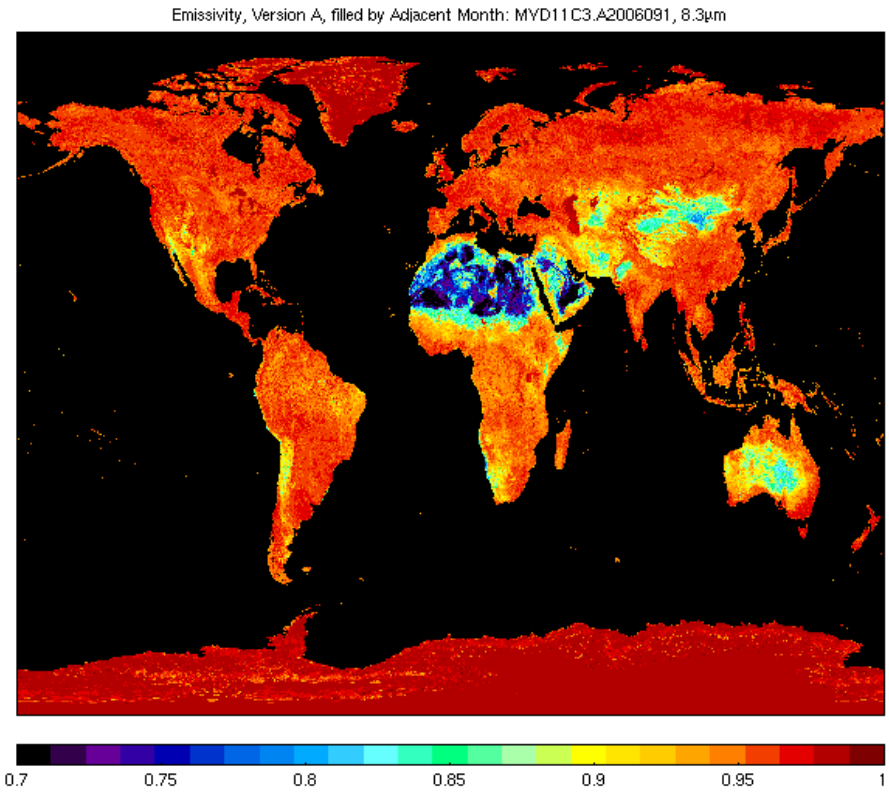


Figure 13. IR surface emissivity at 8.3 µm from operational MODIS product.

The regression for emissivity is simple but usually causes a false diurnal change of emissivities, which results in additional error in water vapor retrieval. Another option is

to use an IR emissivity model. While emissivity models have been proved quite reliable over ocean, they are much less accurate over land. An emissivity database is being developed at CIMSS by combining MODIS emissivity measurements and laboratory measured hyperspectral emissivity spectra. The ABI physical retrieval can use emissivities interpolated spectrally, temporally and spatially from this database. Some information about the emissivity database can be obtained from the following link: http://cimss.ssec.wisc.edu/iremis/ . Figure 13 shows a global emissivity image of 8.3 µm, using the operational MODIS emissivity product.

In the current version, the monthly updated emissivities from the MODIS-derived baseline fit database are used as the default setting for land pixels and the look-up-table approach is the default setting for ocean pixels. The look-up-table for ocean emissivity is based on the Wu-Smith emissivity model (Wu and Smith 1997). The regressed emissivities are discarded.

**Note:** For the oceanic cases, the default wind speed is 5 m/s if the value from forecast product is not available. The maximal wind speed and the maximal LZA for the LUT are 20 m/s and 75º respectively. For cases with larger wind speed and/or LZA values, these thresholds are applied.

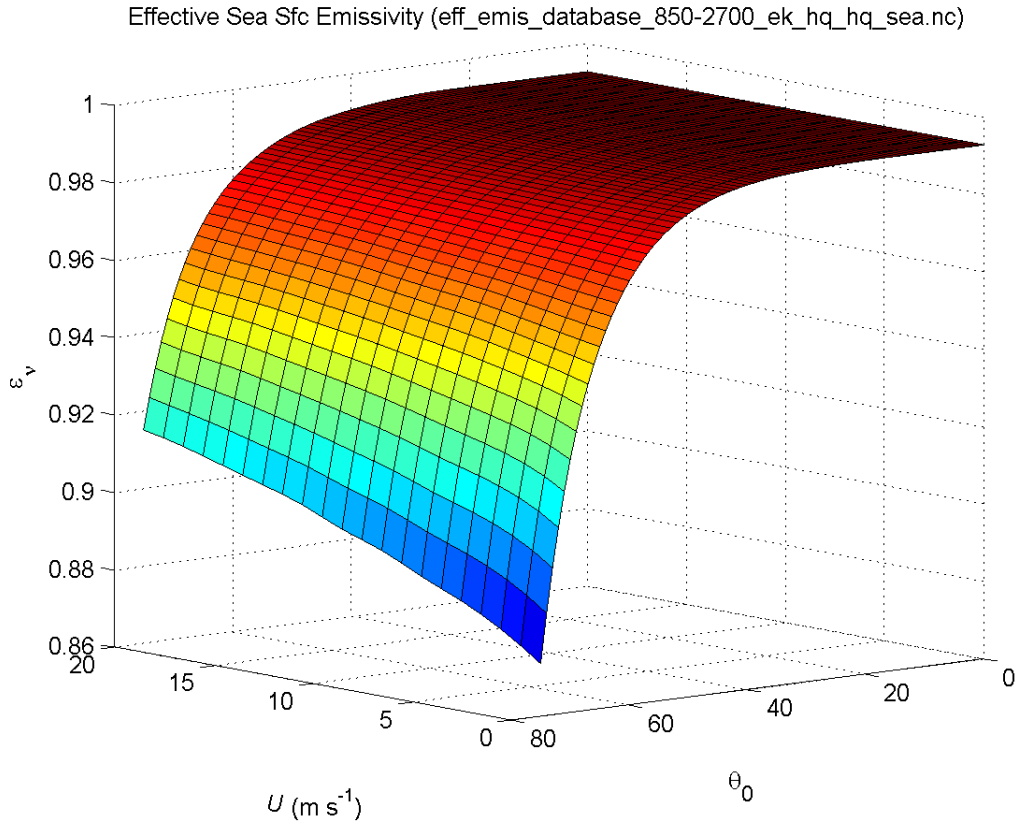


Figure 14: Sea surface emissivity ($\varepsilon_v$) against LZA ($\theta_0$) and wind speed (U).

### 3.1.6 Ancillary data sets

The following ancillary data, remapped onto satellite images, are mandatory:

- Land/sea mask

Atlas and sea/land mask datasets covering the whole GOES-R disk in the default satellite projection at full ABI IR horizontal resolution are available within mainframe package. These ancillary data are available in the mainframe software package on ABI full disk in the default satellite projection at full IR resolution.

### 3.1.7 Configuration File

Here is a list of all parameters that are included in the Configuration file for LAP:

- Block size (5), the size of the FOR;
- Minimal clear sky fraction (0.2) in FOR required for a retrieval;
- Flag of the availability of surface air temperature and moisture data;
- The default value (273.0 K) of surface air temperature if real observation is not available;
- The default value (7.0 g/kg) of surface air moisture if real observation is not available;
- Flag of printing some results during the physical retrieval iteration
- Method for BTs calculations of FOR MEAN or WARMEST at IR 10.8 channel

### 3.1.8 List of proxy data sets

Here is a list of all proxy data sets used for validation purposes:

For ABI:

- Simulated ABI BTs for all IR channels over CONUS with spatial resolution of 2 km and temporal resolution of 5 minutes for one day, i.e. between 12:00 June 04 and 12:00 June 05, 2005;

For SEVIRI:

- Real observations of full-disk MSG-1/SEVIRI IR BTs with spatial resolution of 3 km and temporal resolution of 15 minutes for August 2006;
- Real observations of regional MSG-1/SEVIRI BTs with spatial resolution of 25 km over European, North Africa and adjacent oceanic areas; this data set covers a long temporal span between April 2007 and September 2008 with two files for each data: one for the midnight and one for the noon.

Since the SEVIRI's channel configuration is slightly different with ABI, a table is presented in the following to help readers understand the application of these channels in LAP sounding retrieval.

Table 5 . Channel numbers and approximate central wavelengths for the SEVIRI.

| *Channel Number* | *Wavelength (μm)* | *Used in LAP Sounding* | |
|---|---|---|---|
| | | *Regression* | *Physical* |
| 1 | 0.635 | | |
| 2 | 0.81 | | |
| 3 | 1.64 | | |
| 4 | 3.92 | | |
| 5 | 6.3 | ✓ | ✓ |
| 6 | 7.3 | ✓ | ✓ |
| 7 | 8.7 | | (✓)* |
| 8 | 9.7 | ✓ | |
| 9 | 10.8 | ✓ | ✓ |
| 10 | 12.0 | ✓ | ✓ |
| 11 | 13.4 | ✓ | ✓ |

*: This channel is selectable in physical retrieval. It is safe to use over ocean only and must be avoided over desert.

### 3.2 Output from Input Date Sets

The primary outputs of this algorithm are legacy atmospheric profiles. They are listed in Table 6below. Note the levels of output need to be determined based on the pressure levels of a chosen RTM. For example, the current pressure levels from 100 hPa to surface from cRTM are: 96.1138, 103.0172, 110.2366, 117.7775, 125.6456, 133.8462, 142.3848, 151.2664, 160.4959, 170.0784, 180.0183, 190.3203, 200.9887, 212.0277, 223.4415, 235.2338, 247.4085, 259.9691, 272.9191, 286.2617, 300.0000, 314.1369, 328.6753, 343.6176, 358.9665, 374.7241, 390.8926, 407.4738, 424.4698, 441.8819, 459.7118, 477.9607, 496.6298, 515.7200, 535.2322, 555.1669, 575.5248, 596.3062, 617.5112, 639.1398, 661.1920, 683.6673, 706.5654, 729.8857, 753.6275, 777.7897, 802.3714, 827.3713, 852.7880, 878.6201, 904.8659, 931.5236, 958.5911, 986.0666, 1013.9476, 1042.2319, 1070.9170, and 1100.0000.

Table 6. Output LAP primary values.

| **LAP Value** | **Description** |
|---|---|
| Temperature profile (K) | Temperature values at pressure levels from 0.005 hPa to surface, but only those below 100 hPa are useful |
| Water vapor mixing ratio profile (g/kg) | Moisture mixing ratio values at pressure levels from 0.005 hPa to surface, but only those below 300 hPa are useful |
| Surface skin temperature (K) | Surface skin temperature, retrieved over land only, interpolated from NWP SST over water |

In addition, the output also includes the derived products from temperature and moisture profiles, which are listed in Table 6 below.

Table 7. Output LAP derived product values.

| **LAP derived product** | **Description** |
|---|---|
| TPW (cm) | Derived product from moisture profile |
| PW_Low (cm) | Derived product from moisture profile |
| PW_Mid (cm) | Derived product from moisture profile |
| PW_High (cm) | Derived product from moisture profile |
| LI (K) | Derived product from temperature and moisture profiles |
| CAPE (J/kg) | Derived product from temperature and moisture profiles |
| TT (K) | Derived product from temperature and moisture profiles |
| SI (K) | Derived product from temperature and moisture profiles |
| KI (K) | Derived product from temperature and moisture profiles |

Moreover, the output also includes some variables for quality control, which are listed in Tables A2 and A3.

Note that all geographical and geometric information for the output should be that of the centroid of clear FOVs within the FOR.

The following figures Fig. 15-23 are the results of output variables based on the simulated ABI observations and GFS-6 hour forecast for the moment of 22:00, June 4th, 2005 over CONUS.

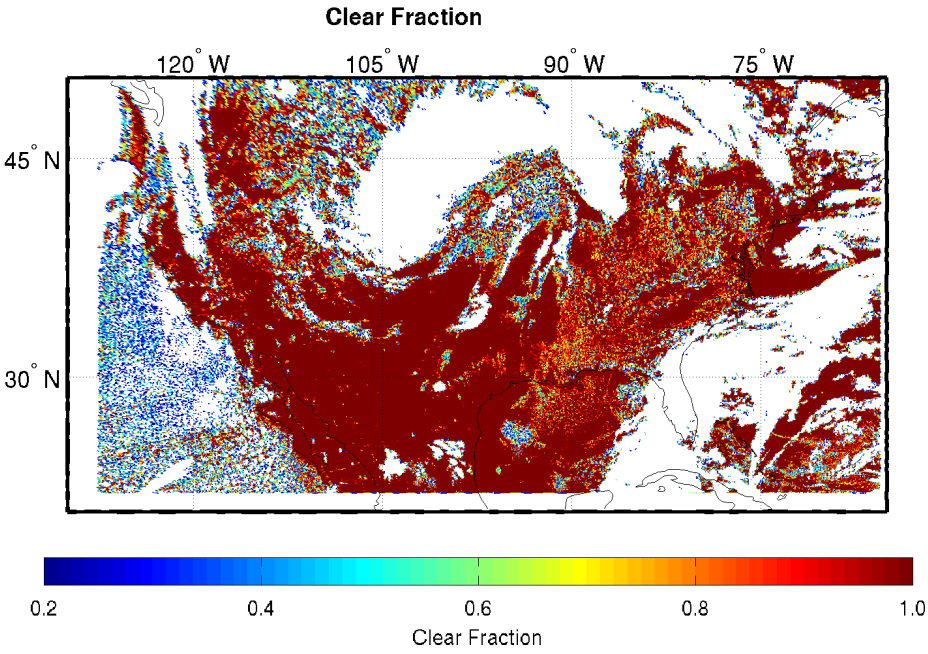

Figure 15: Clear sky fraction ( = Num_Clr_Pix / Block_Size**2) using a simulated ABI case; FORs with fraction lower than 0.2 are not retrieved.

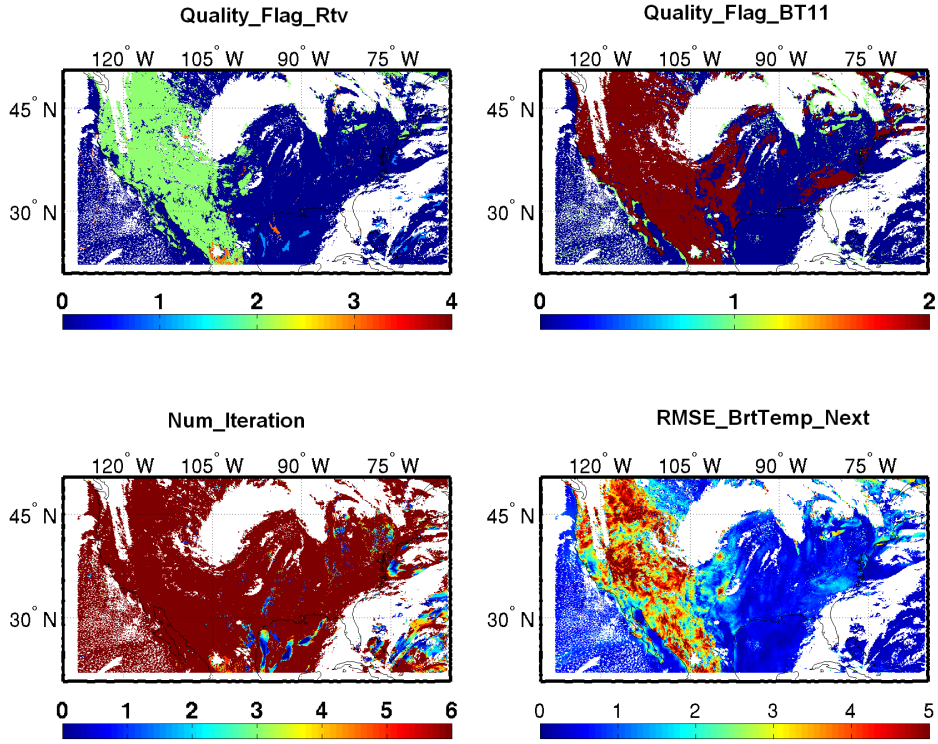


Figure 16: Output quality control variables using a simulated ABI case.

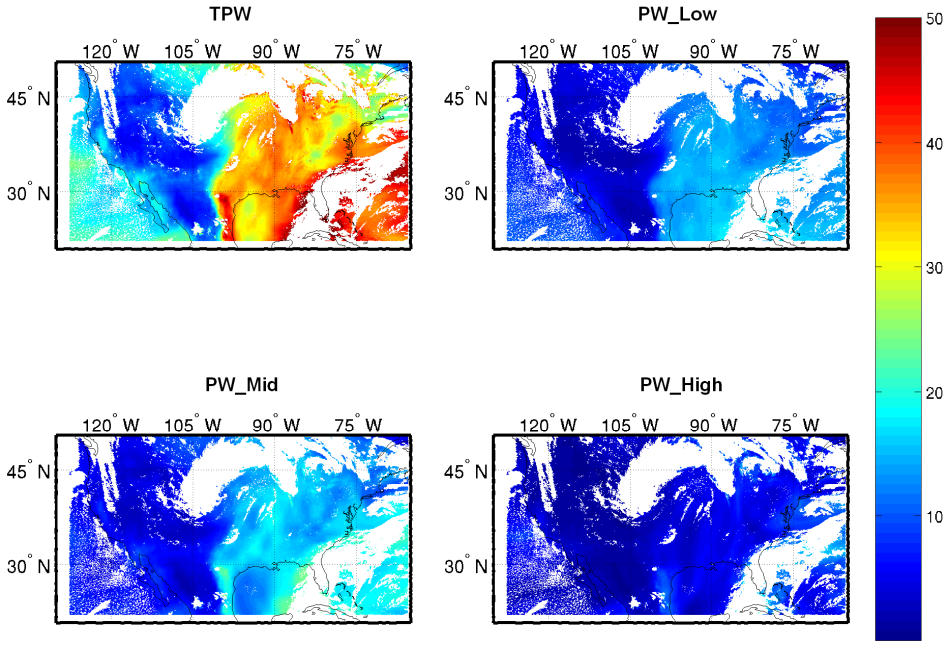


Figure 17: Same as Fig. 15 but for TPW (mm) and its three components.

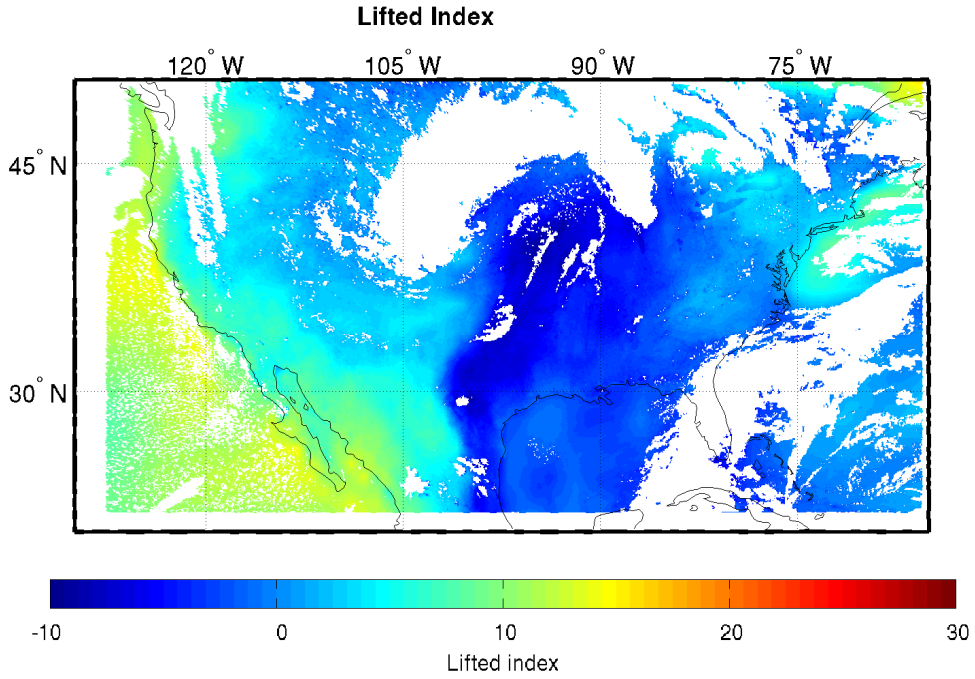


Figure 18: Same as Fig. 15 but for LI.

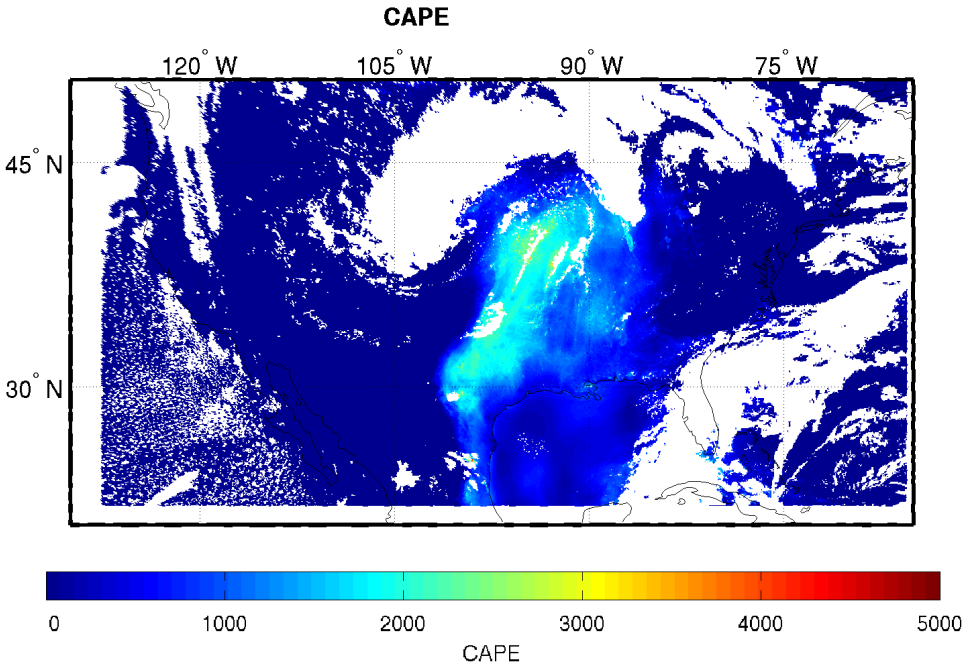


Figure 19: Same as Fig. 15 but for CAPE.

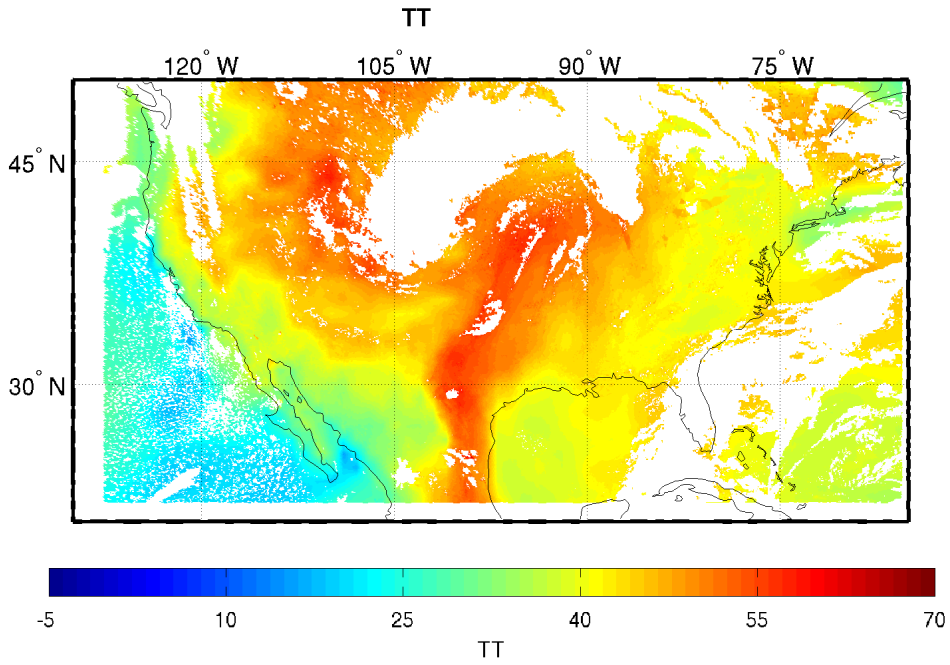


Figure 20: Same as Fig. 15 but for TT.

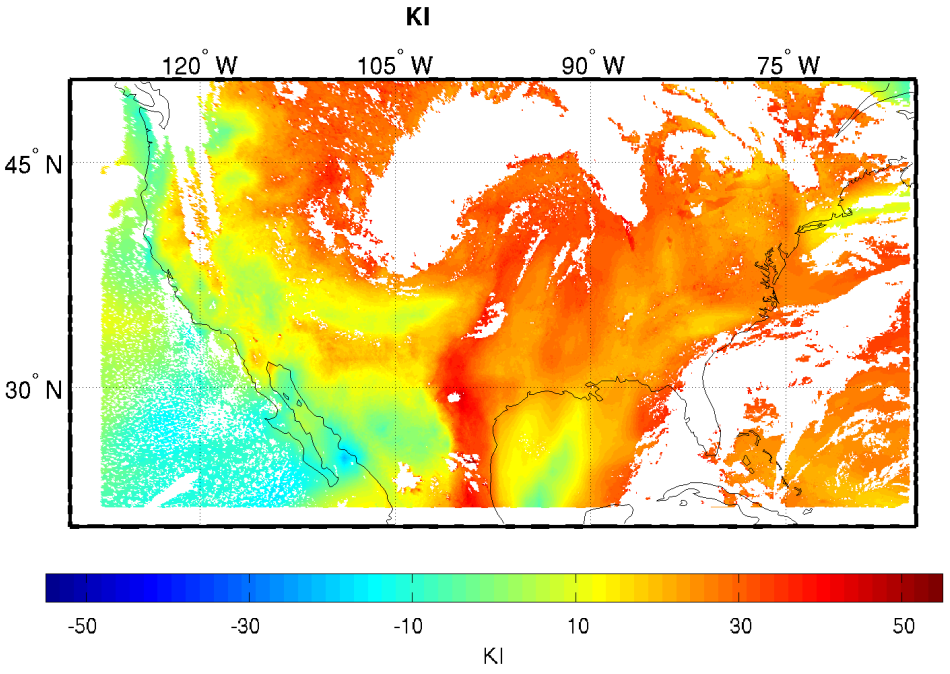


Figure 21: Same as Fig. 15 but for KI.

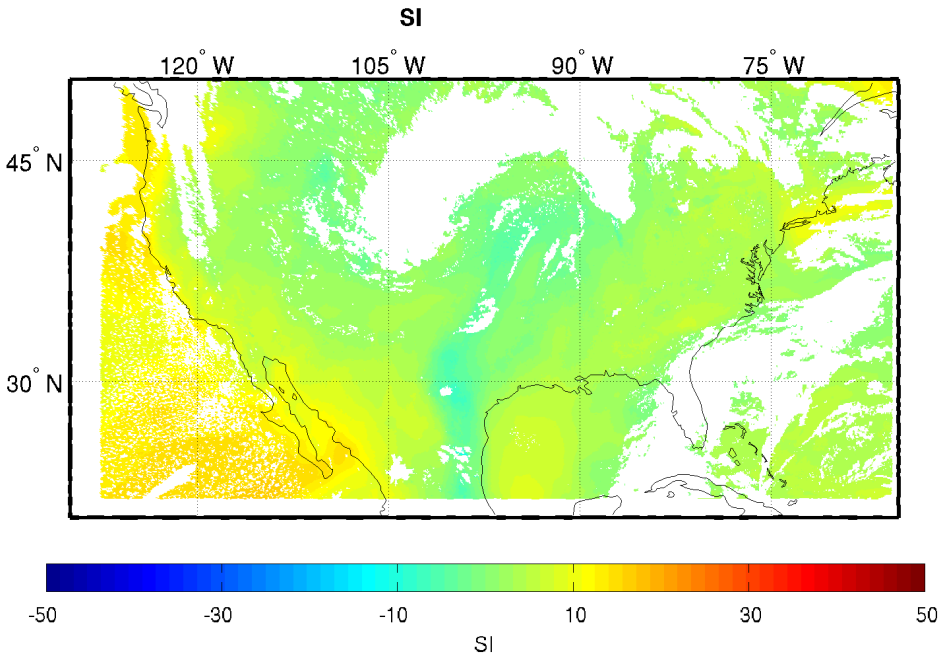


Figure 22: Same as Fig. 15 but for SI.

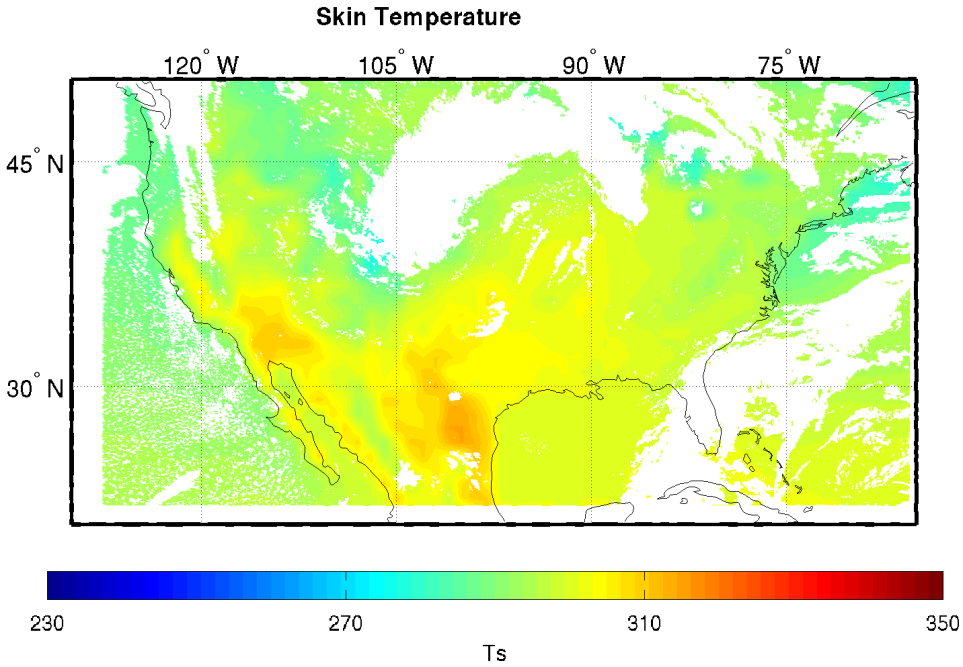


Figure 23: Same as Fig. 15 but for skin temperature.

### 3.2.1 Precision and Accuracy Estimate

The following procedures are recommended for diagnosing the performance of the LAP.

- Fraction of clear sky pixels within FOR
- Counts of total iterations.
- 11-micron BT difference between observation and calculation with first guess surface skin temperature.
- BT residuals between calculation and observation after final iteration.
- Processing time should be monitored.

### 3.2.2 Error Budget

(1) Results from SEVIRI using the LAP algorithm show that SEVIRI/ABI improves moisture forecasts between 300 – 700 hPa when compared with one month's radiosondes; SEVIRI-derived water vapor RH from the LAP algorithm meets the requirement (18%).
(2) TPW can reach an accuracy of approximately 9.5% over ocean when compared with collocated one month's AMSR-E data.
(3) TPW can reach the accuracy of approximately 11.5% over land when compared with radiosondes.
(4) Overall TPW can reach an accuracy of approximately 10% when compared with ECMWF analysis.
(5) LI has error of 2 K when compared with radiosondes over land.

Validation for other products will be carried out. ABI accuracy is expected to be better than SEVIRI because of improved water vapor spectral information, among other things. We will conduct further analyses with more validation datasets under development. For example,

- Simulated ABI datasets
- Inter-comparison with Metop IASI and NPOESS hyperspectral IR sounding data as well as other satellite measurements
- Compare with RAOBs from dedicated field campaigns, including over oceans
- Compare with ECMWF analysis
- Enhance cloud detection
- Improve handling of SE
- Algorithm improvement, including better RTM and associated Jacobian schemes
- Time continuity incorporation

Complete validation statistics are shown in Table 8.

Table 8: LAP sounding product validation vs. requirements using MSG-1/SEVIRI as proxy; data set includes 457 radiosonde-SEVIRI matchup cases of August 2006 over land.

| Product | Accuracy (Req.) | Precision (Req.) | Accuracy (SEVIRI) | Precision (SEVIRI) |
|---|---|---|---|---|
| **Temperature profile (K)** | **1K below 400 hPa and above boundary** | **2K below 400 hPa and above boundary** | **0.5K below 400 hPa and above boundary** | **<1.9K below 400 hPa and above boundary** |
| **Moisture profile (RH)** | **Sfc-500 mb: 18%<br>500-300 mb: 18%<br>300-100 mb: 20%** | **Sfc-500 mb: 18%<br>500-300 mb: 18%<br>300-100 mb: 20%** | **5%** | **Sfc-900 hPa: 12%<br>900-600 hPa: 18%<br>600-300 hPa: 15%** |
| **Derived stability indices** | **LI: 2 K<br>CAPE: 1000 J/ kg<br>SI: 2 K<br>TT: 1<br>KI: 2** | **LI: 6.5 K<br>CAPE: 2500 J/ kg<br>SI: 6.5 K<br>TO: 4<br>KI: 5** | **LI: 0.7 K<br>CAPE: 50 J/KG<br>SI: 0.5 K<br>TT: 0.5 K<br>KI: 1.5 K** | **LI: 2 K<br>CAPE: 200 J/ kg<br>SI: 2 K<br>TT: 3.5 K<br>KI: 6 K** |
| **TPW** | **1 mm** | **3 mm** | **0.3 mm** | **< 3 mm** |

As can be seen from table 8, all requirements are met using this one-month (August) of SEVIRI data compared to radiosondes, with the exception of the precision of the K-index. It is expected that this will fall within the requirements when: a larger dataset is used and/or when the additional bands of the ABI are used (that are not on the SEVIRI) and/or when the improved noise performance of the ABI is used. An improved NWP model with higher spatial/temporal resolution, such as regional meso-scale forecast models (RUC, NAM, and etc) will also be helpful. It will definitely improve the quality of first guess, therefore all stability indice, including the k_index, will be improved to meet the requirements.

## 3.3 Algorithm Validation

### 3.3.1 Input Data Sets

#### 3.3.1.1 Fast RTM in testing

The physical retrieval algorithm has been tested using SEVIRI data and PFAAST (Hannon et al. 1996). The PFAAST model has 101 pressure level vertical coordinates from 0.05 to 1100 hPa, and uses line-by-line RTM (LBLRTM) calculations and the high-resolution transmission molecular absorption spectroscopic database HITRAN 2000. The calculations take into account the LZA, absorption by well-mixed gases (including nitrogen, oxygen, and carbon dioxide), water vapor (including the water vapor continuum), and ozone. Forecast ozone is used in the radiance calculation (regression ozone can also be used), the SEVIRI spectral bands 5 (6.2 µm), 6 (7.3 µm), 9 (10.8 µm), 10 (12 µm), 11 (13.4 µm) are used in physical retrieval. For retrievals over ocean, band 7 (8.7 µm) can also be included in physical retrieval, although the radiance in this band

may be influenced by dust over the ocean from the Saharan region (e.g., Nalli et al., 2004).

### 3.3.1.2 Proxy input data sets

As described below, the data used to test the LAP includes full disk SEVIRI observations collocated with radiosondes, ECMWF 6-hour analyses, and operational AMSR-E TPW product. The time period chosen was August 2006. Our analysis spans the entire SEVIRI domain and should therefore encompass a full range of weather conditions. While SEVIRI obviously does not operate over the GOES domains, we have preferred the use of empirical SEVIRI data over simulated ABI data up to this point. The rest of this section describes the proxy and validation data-sets used in assessing the performance of the LAP.

Another proxy validation dataset is also available, including 18-month SEVIRI clear sky BTs, ECMWF 12-hour forecast and 6-hour analysis collocated at 00 and 12 UTC from April 2007 to September 2008 over Europe, North Africa and ocean areas nearby. The spatial coverage of this dataset is shown below.

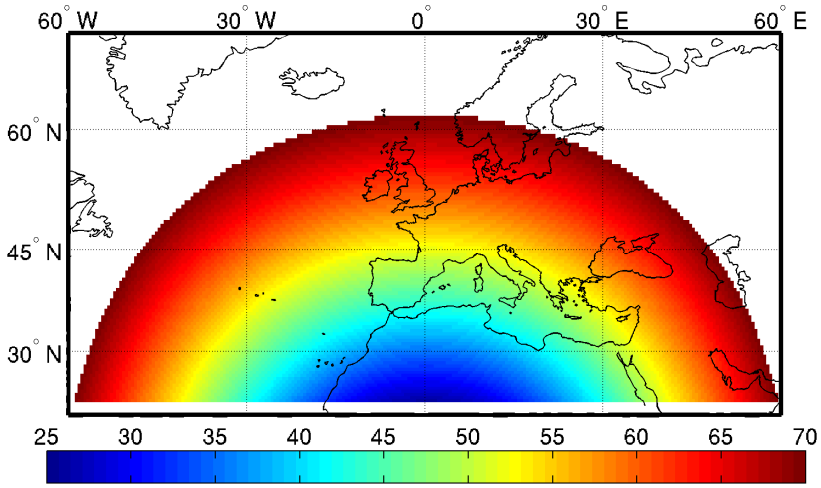


Figure 24: The spatial coverage and local zenith angle of the regional validation dataset.

#### *4.3.1.2.1 SEVIRI Data*

SEVIRI provides 11 spectral channels with a spatial resolution of approximately 3 km and a temporal resolution of 15 minutes. More information on the SEVIRI can be found in Schmid et al. (2000), Schumann et al. (2002), Aminou et al. (2003), and Schmetz et al. (2002). SEVIRI provides the best source of data currently for testing and developing the ALS. Except for the 6.95 μm and 10.35 μm IR spectral bands, SEVIRI provides an

adequate source of proxy data for the testing and development of the LAP. The SEVIRI data was provided by the SSEC Data Center.

#### *4.3.1.2.2 Radiosonde Data*

One month of radiosonde data at 00 UTC and 12 UTC in August 2006 have been collected. A matchup file has been developed for that month containing collocated radiosondes, ECMWF 12 hour forecast, and SEVIRI clear sky BT measurements. A total of 457 matches are contained. The spatial distribution of these samples is presented in the following figure.

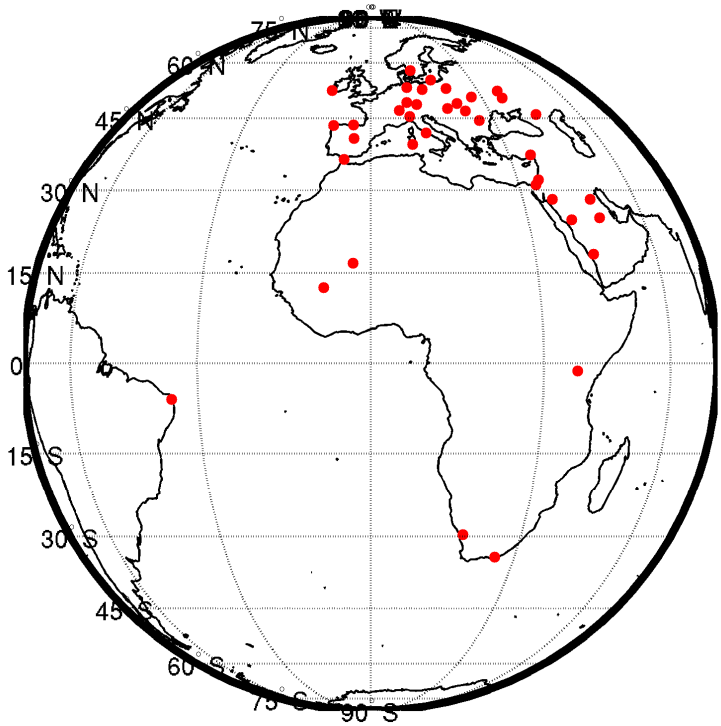


Figure 25: The spatial distribution of radiosonde sites for the full disk validation dataset.

#### *4.3.1.2.3 AMSR-E Data*

Since radiosondes are usually limited to over land, it is also very important to validate legacy sounding derived products over the ocean. LEO satellite data and products can be used for this purpose. We have used operational TPW product from AMSR-E onboard Aqua platform for validation over ocean. The collocated AMSR-E TPW and SEVIRI TPW product in August 2006 are used.

#### *4.3.1.2.4 ECMWF Analysis Data*

In order to validate LAP products over land and ocean, the ECMWF 6-hour analysis data are also used for validation, collocated ECMWF 12-hour forecast, analysis and SEVIRI BT measurements in August 2006 of the full disk coverage and April 2007 – September 2008 of the regional coverage are used.

### 3.3.2 Output from Inputs Data Sets

The LAP products were generated using the SEVIRI data from the entire month of August 2006. Figure 26 below shows the SEVIRI TPW overlaying on the 11 µm BT image (back/white). Operational SEVIRI CM applied for clear detection. This image is for 00 UTC on 18 August 2006. Figure 27 is the same as Figure 26 but for the LI.

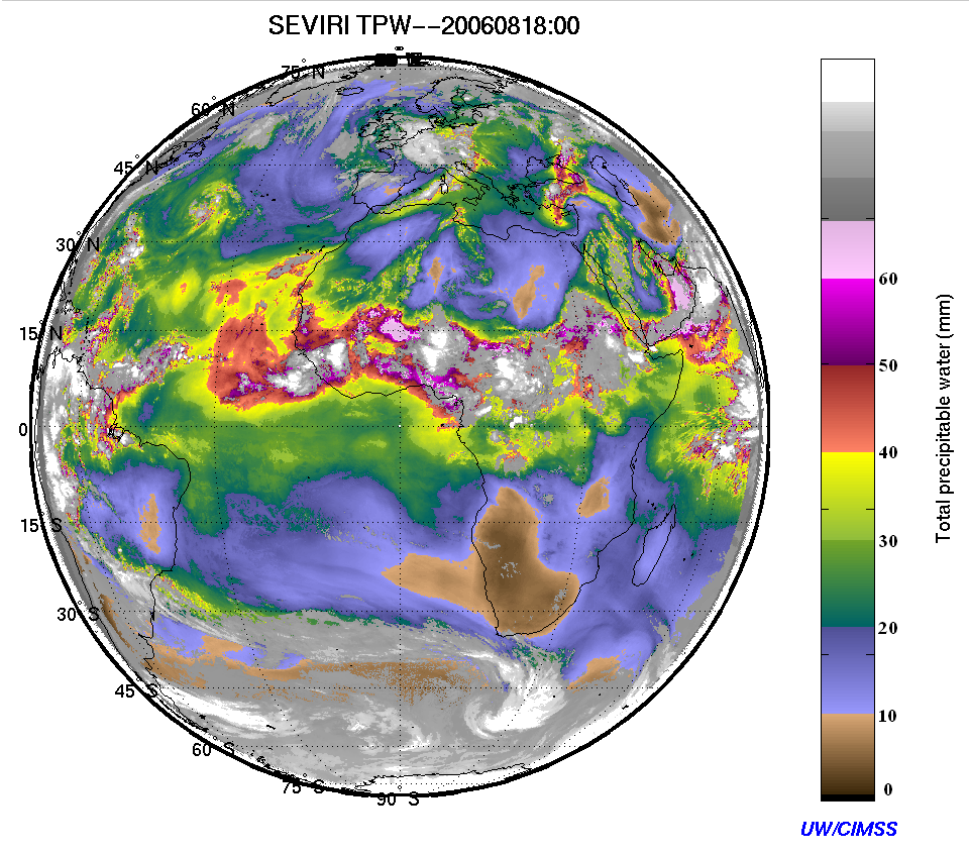


Figure 26. Example of LAP TPW from 00 UTC August 18, 2006 produced from SEVIRI on MET-8.

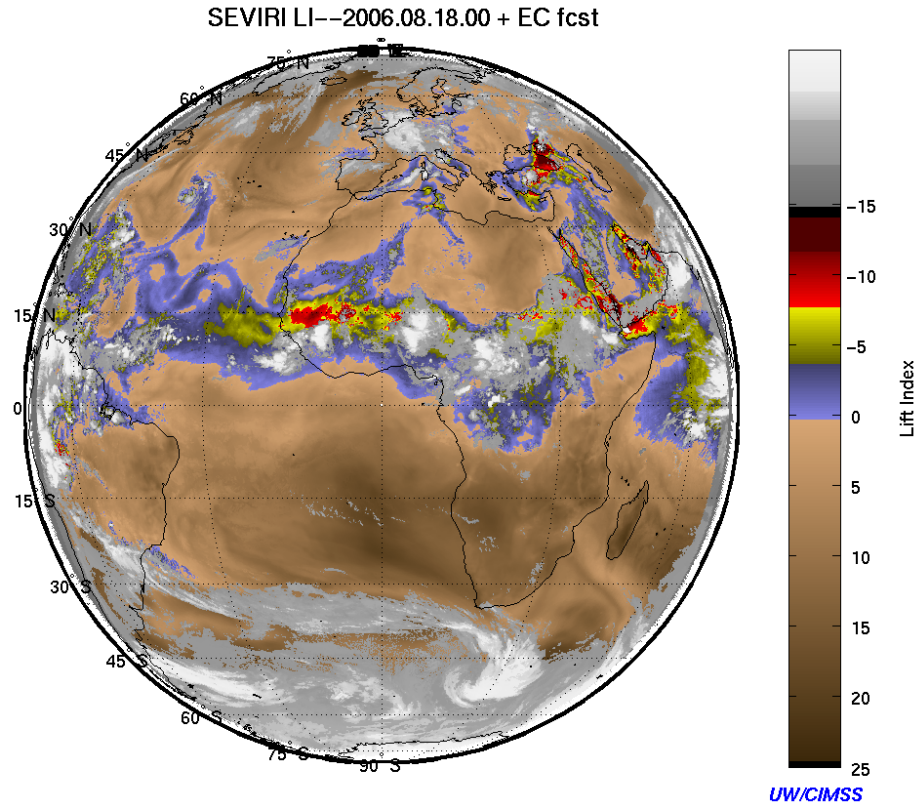


Figure 27. Example of LAP LI from 00 UTC August 18, 2006 produced from SEVIRI on MET-8.

### 3.3.2.1 Precisions and Accuracy Estimates

To estimate the performance and accuracy of the LAP, we have used radiosondes, AMSR-E, and ECMWF analysis data as described above. This section will present our analysis methodology for estimating the precision and accuracy. The next section will provide the quantitative results in terms of the F&PS specifications. Results from both summer and winter month are presented. Since the atmosphere is stable in winter over Europe for most situations, analysis on instability indices are focused on summer month only.

#### *4.3.2.1.1 TPW analysis with radiosondes*

The SEVIRI IR derived TPW values were computed and compared with RAOBs, AMSR-E and ECMWF analysis. The differences between the SEVIRI TPW and other measurements are then calculated for each pixel in the SEVIRI domain. The error for clear sky pixels is estimated as follows:

$$\text{Error (\%)} = [(A-B)/A]*100$$

The averaged percentage error can be calculated by

Average Error (%) = (1/NS) * sum(Error)

where NS is the total number of samples, A is the true value and B is the retrieved value. Figure 28 shows the scatterplot between SEVIRI TPW and radiosonde TPW for August 2006 over land for summer valdation. An average percentage error of 11.5% is obtained from SEVIRI using the LAP algorithm.

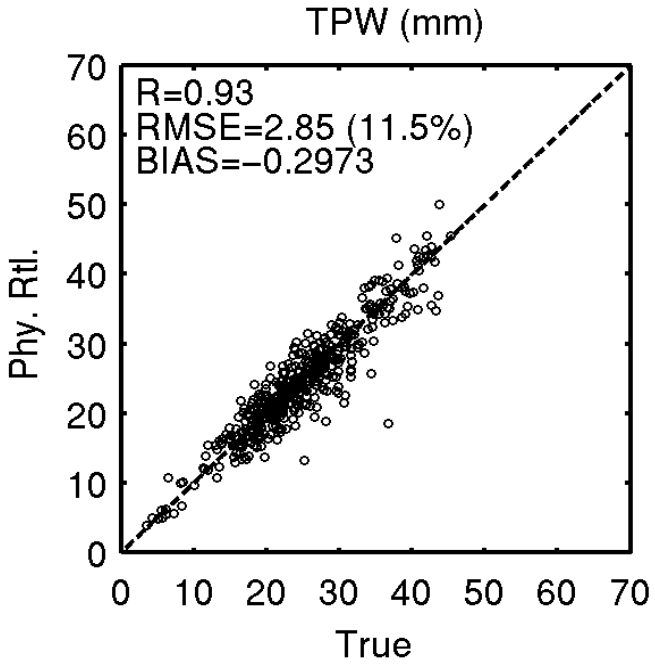


Figure 28. Scatterplot of SEVIRI TPW using the LAP algorithm versus RAOB over land, one month (August 2006) matchup (SEVIRI/RAOB) data is used for summer validation.

Figure 29 shows the scatterplots of SEVIRI TPW using LAP algorithm versus ECMWF analysis over ocean (upper right panel) and land (lower right panel), one month (January 2008) matchup (SEVIRI/ECMWF analysis) data is used for winter validation. The SEVIRI improves the forecast (upper left panel) over ocean by 0.7 mm, while it improves the forecast (lower left panel) by 0.4 mm over land.

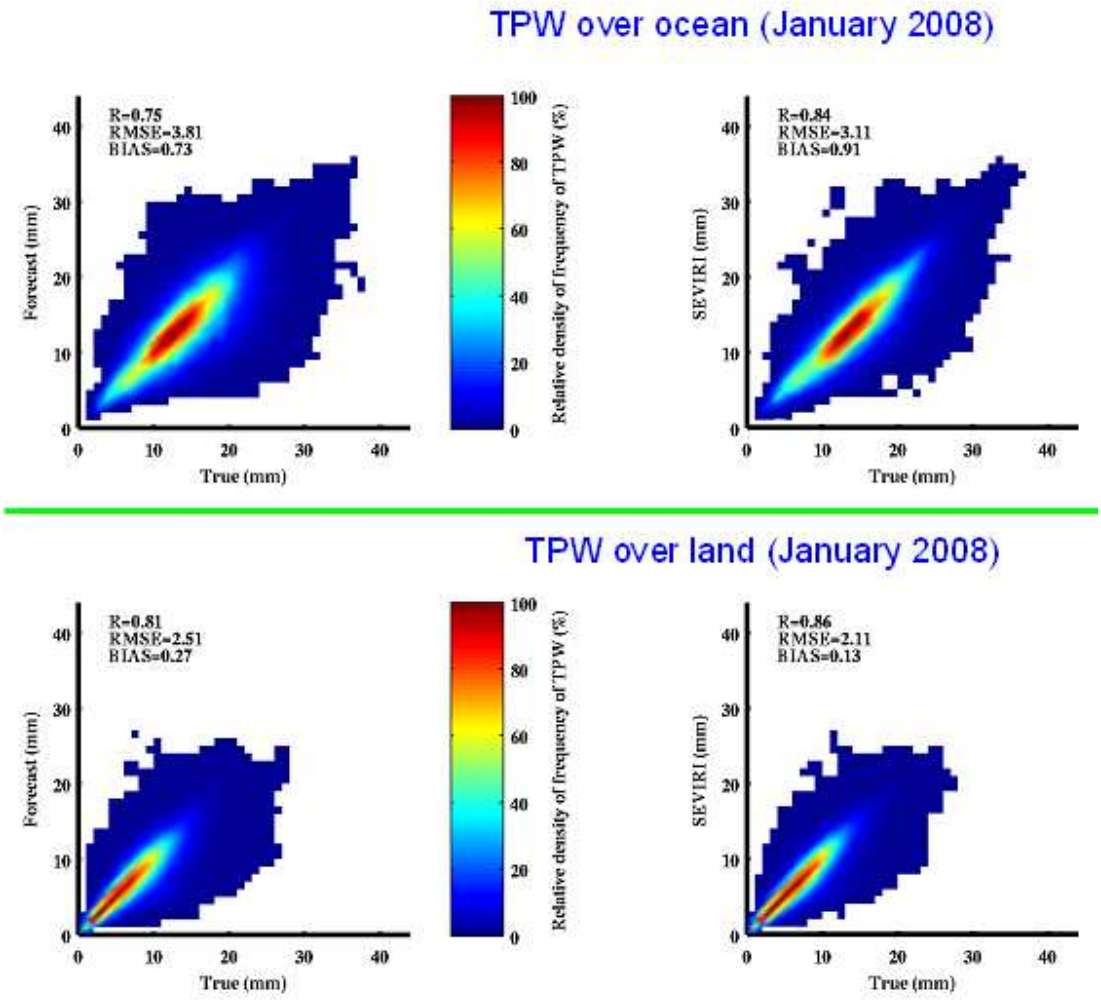


Figure 29. The scatterplots of SEVIRI TPW using LAP algorithm versus ECMWF analysis over ocean (upper right) and land (lower right), one month (January 2008) matchup (SEVIRI/ECMWF analysis) data is used for winter validation.

#### *4.3.2.1.2 TPW Analysis with AMSR-E*

The SEVIRI TPW retrievals are also compared with operational AMSR-E TPW product over ocean for August 2006. The temporal separation between SEVIRI and AMSR-E is less than 15 minutes, while the spatial distance between the two is less than 10 km. Figure 30 shows the TPW scatterplot between AMSR-E and SEVIRI, a total of 2822939 samples are used. The retrieval TPW agrees very well with AMSR-E observations with the correlation of 0.96. When SEVIRI TPW is less than 25 mm, SEVIRI has slight wet bias, while when SEVIRI TPW is greater than 25 mm; SEVIRI has slight dry bias, which is consistent with the MODIS results (Seemann et al. 2003).

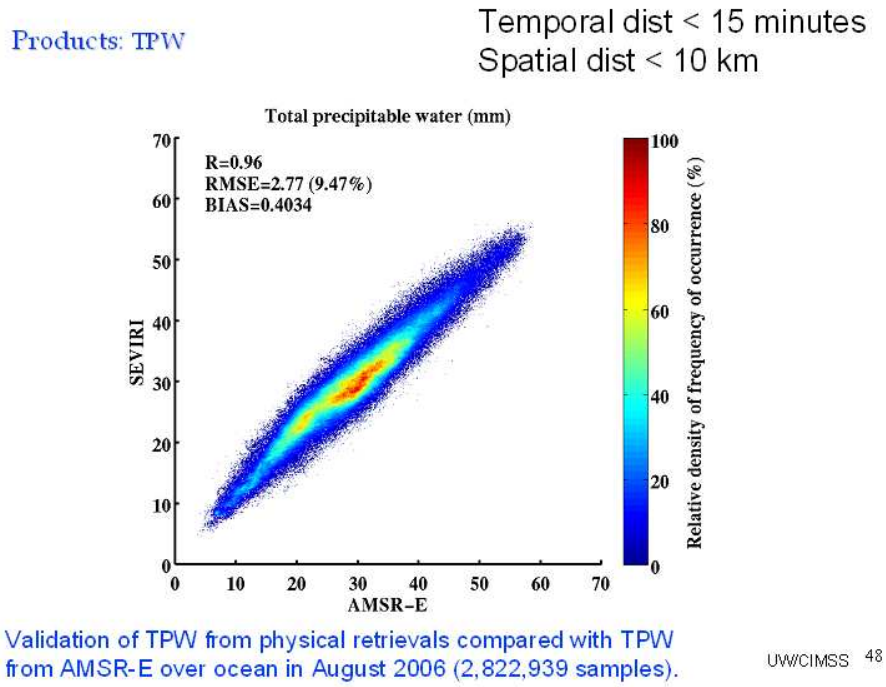


Figure 30. The TPW scatterplot between AMSR-E and SEVIRI for August 2006.

#### *4.3.2.1.3 TPW Comparisons with ECMWF Analysis*

Figure 31 shows SEVIRI TPW and LPW validation with ECMWF analysis for August 2006 (31044 samples which is 1% of all samples). As above, the LAP algorithm is used for deriving the water vapor products from SEVIRI. TPW reaches approximate accuracy of 9% over both land and ocean, as shown in the upper left panel of Figure 31.

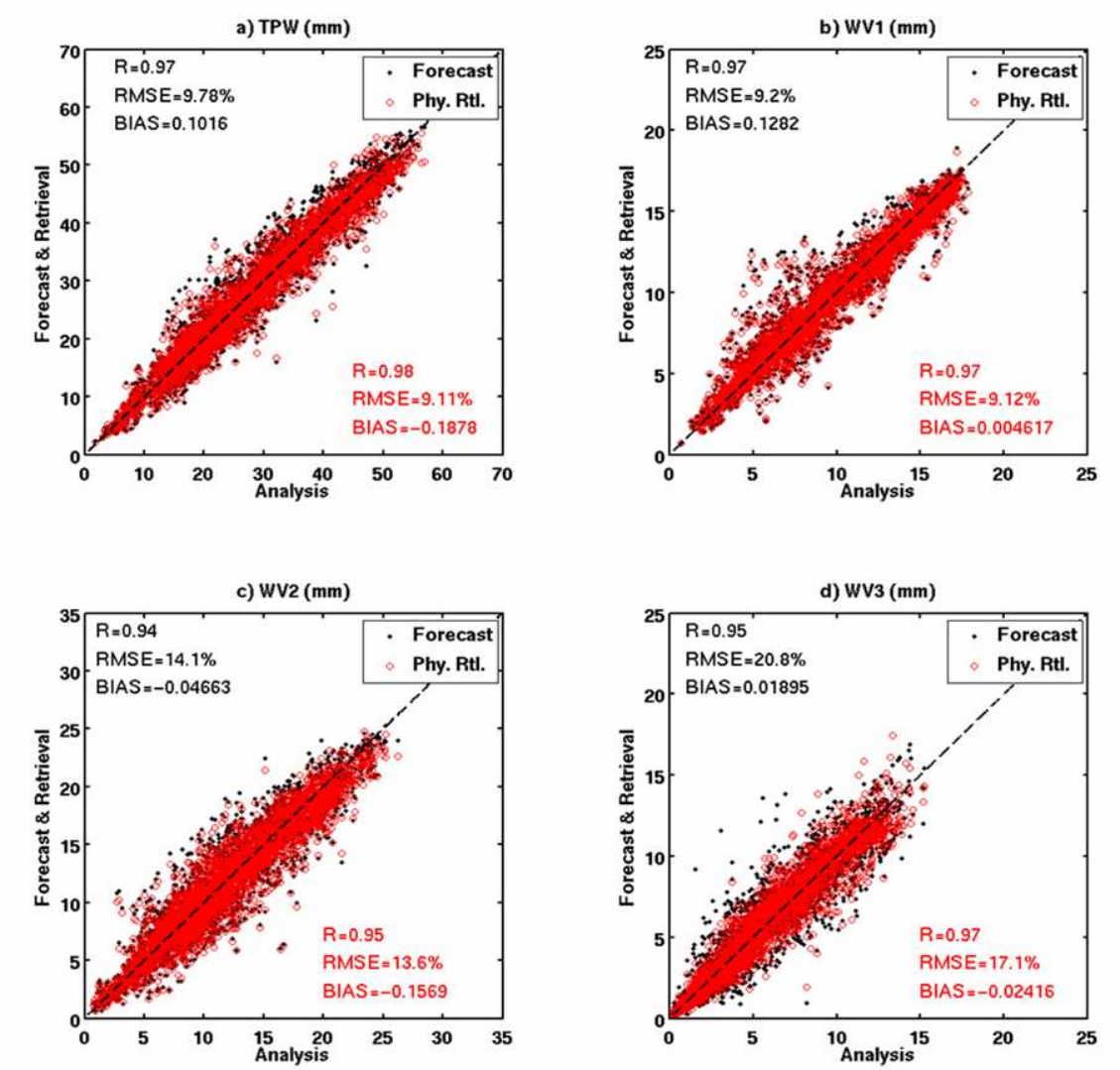


Figure 31. Scatterplot between ECMWF analysis and SEVIRI water vapor products (TPW, WV1, WV2, and WV3) for 00 UTC, August 18th, 2006; only 1% of matchup samples are included.

A monthly-averaged time series of TPW and LPW components (WV1/WV2/WV3) correlation coefficient (R) between forecast/retrieval and ECMWF analysis is presented using the 18-month regional validation dataset. For TPW, the improvement of R by LAP is about 0.5 when compared with the forecast. By retrieval, The R value can go higher than 0.9 in winter and shows less seasonal variation than the forecast. Considering there is one more moisture band in ABI than SEVIRI, the result could be even better if real ABI data is applied. The performance of LAP algorithm is quite different at different heights and best result is for the high level moisture component.

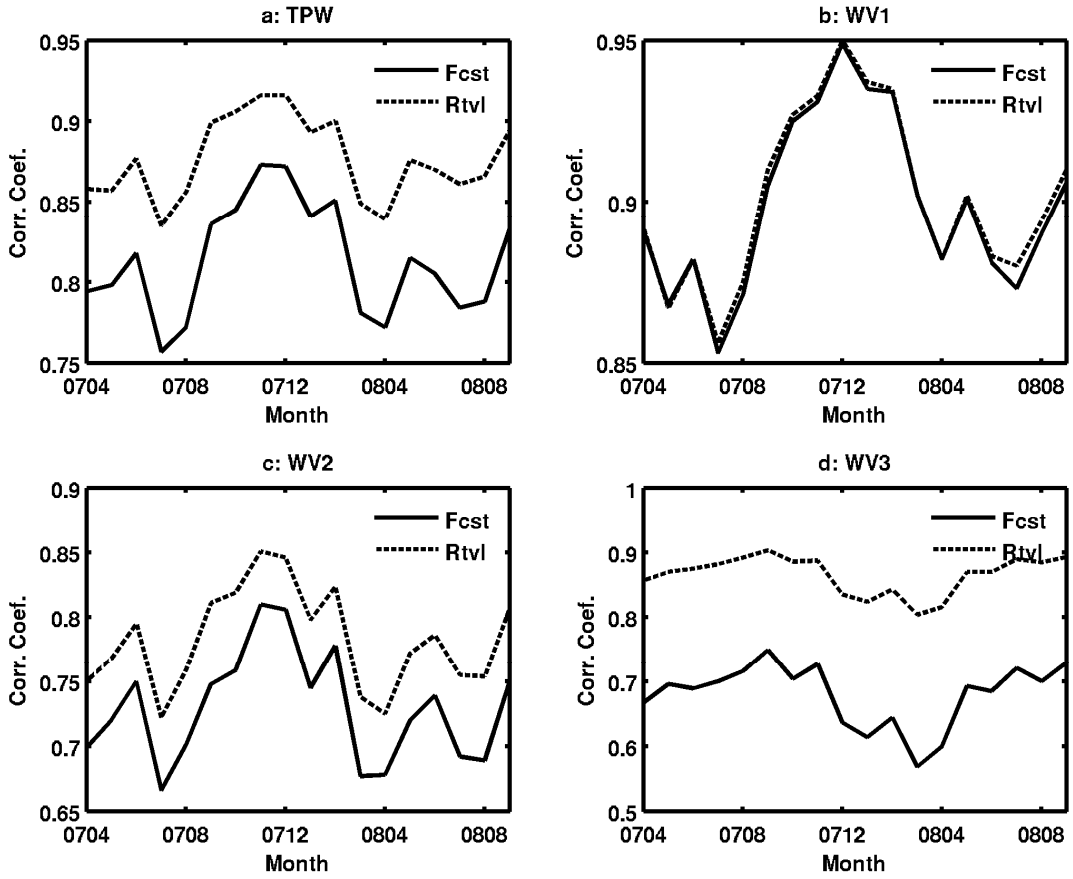


Figure 32: The time series of TPW and LPW (including WV1/WV2/WV3) correlation coefficient between forecast/retrieval and the ECMWF analysis from April 2007 to September 2008.

#### *4.3.2.1.4 LI analysis with radiosondes and ECMWF analysis*

The SEVIRI derived LI values were also computed and compared with RAOBs for August 2006. The LI RMS difference between the SEVIRI measurements and radiosondes is 2.05 K as indicated in the scatterplot given in Figure 33.

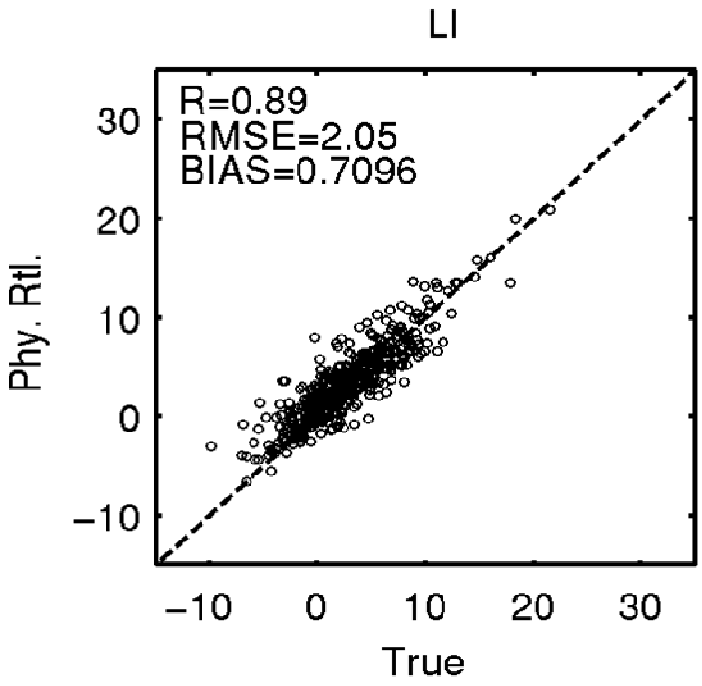


Figure 33. Same as Figure 28 but for Lifted Index. Radiosondes are used as truth.

The monthly averaged time series of LI between April 2007 and September 2008 over Europe and North Africa is plotted in the following. The difference between forecast and retrieval is trivial because temperature profile and low-level moisture profile have very little improvement.

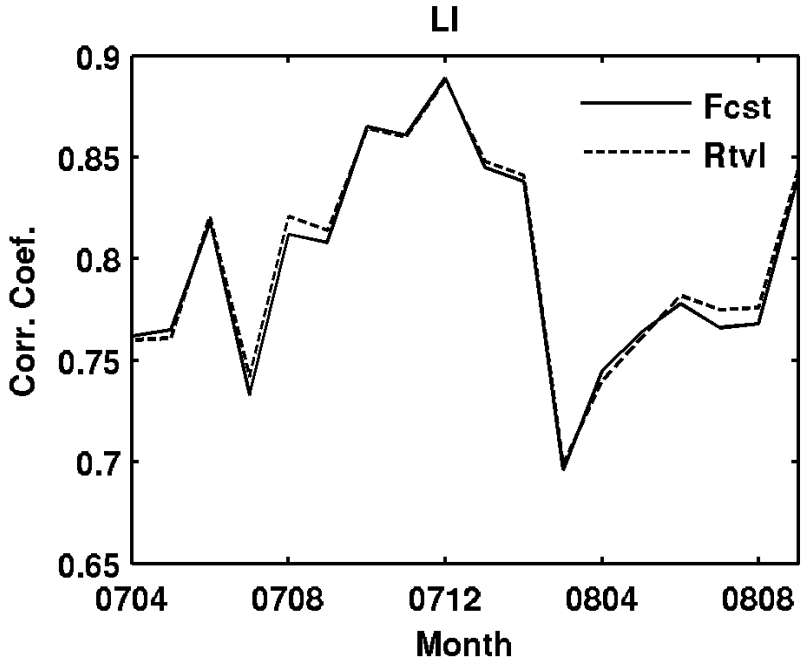


Figure 34: Same as Figure 32 but for LI.

#### *4.3.2.1.5 Profile analysis with radiosondes and ECMWF* analysis

One month (August 2006) spatially and temporally collocated SEVIRI and RAOB are used for full disk validation of the algorithm, and 18-month (April 2007-September 2008) spatially and temporally collocated SEVIRI and ECMWF analysis are used for a regional validation of algorithm. The operational SEVIRI CM product from EUMETSAT is used for clear pixel identification. Test results show that physical retrieval does improve the regression (used as the first guess), while the regression improves the forecast for both summer and winter. Since the regression algorithm uses forecast and SEVIRI radiances as predictors, an improvement from regression over forecast is expected. The physical retrieval improves the regression since it accounts better for the nonlinearity of moisture to IR radiances.

Figure 35 shows the RMSE for RH between SEVIRI retrievals and radiosondes for August 2006, a total number of 457 comparisons are included. SEVIRI provides significant improvement on the forecast. Due to the limited spectral information, it is difficult for SEVIRI to improve the boundary layer moisture forecast.

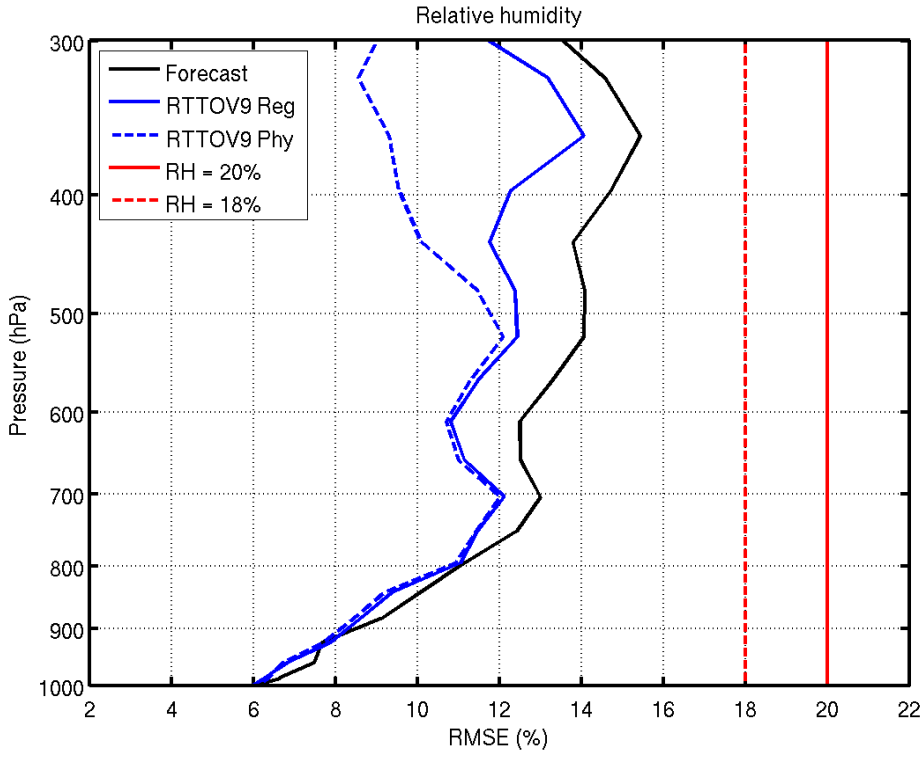


Figure 35. The RH RMSE between SEVIRI retrievals and radiosondes for August 2006.

Figure 36 shows the RMSE for temperature (left) and RH (right) between SEVIRI retrievals and ECMWF analysis for January 2008 over land, a total of 203491 matchups are included in the land statistics. Figure 37 is same as figure 36 but for mean bias. Figure 38 is the same as Figure 36 but over ocean, a total of 149724 matchups are

included in the ocean statistics. Figure 39 is same as figure 37 but for mean bias. SEVIRI slight improves the temperature forecast, while it improves the moisture significantly above 700 hPa. Compared with summer results (Figure 35), the water vapor forecast is worse and the satellite data provide can help.

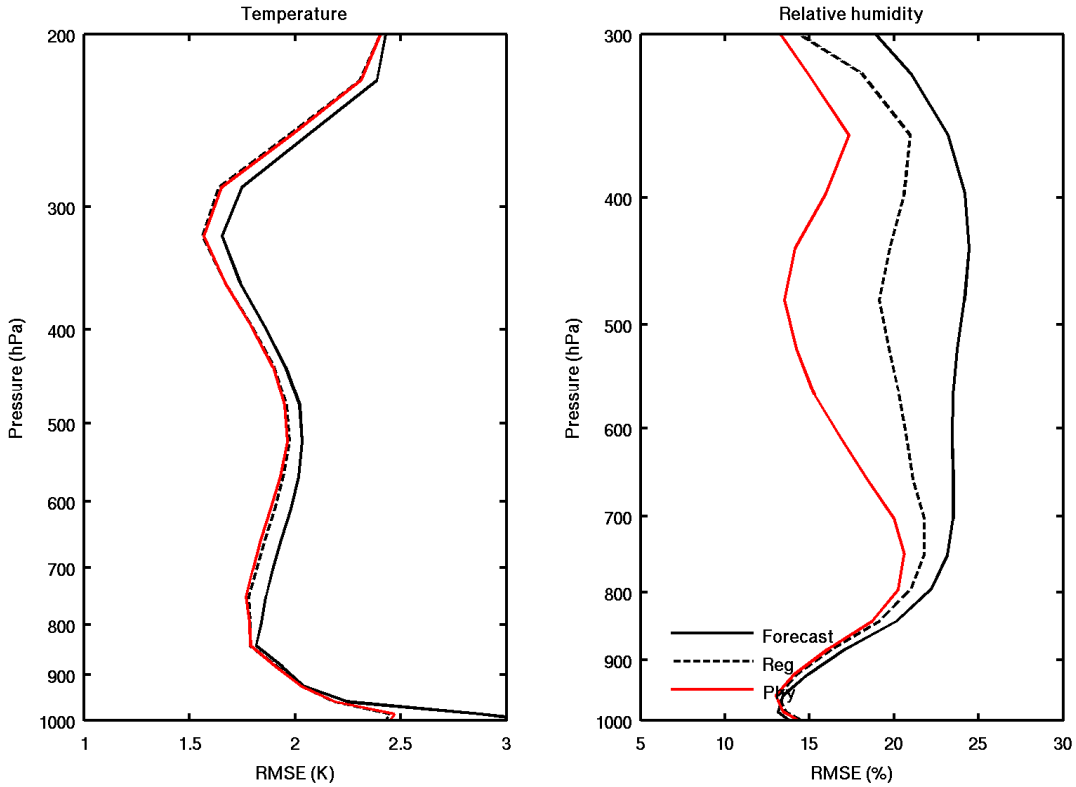


Figure 36. The RMSE for temperature (left) and RH (right) between SEVIRI retrievals and ECMWF analysis for January 2008 over land, a total of 203491 matchups is included in the land statistics.

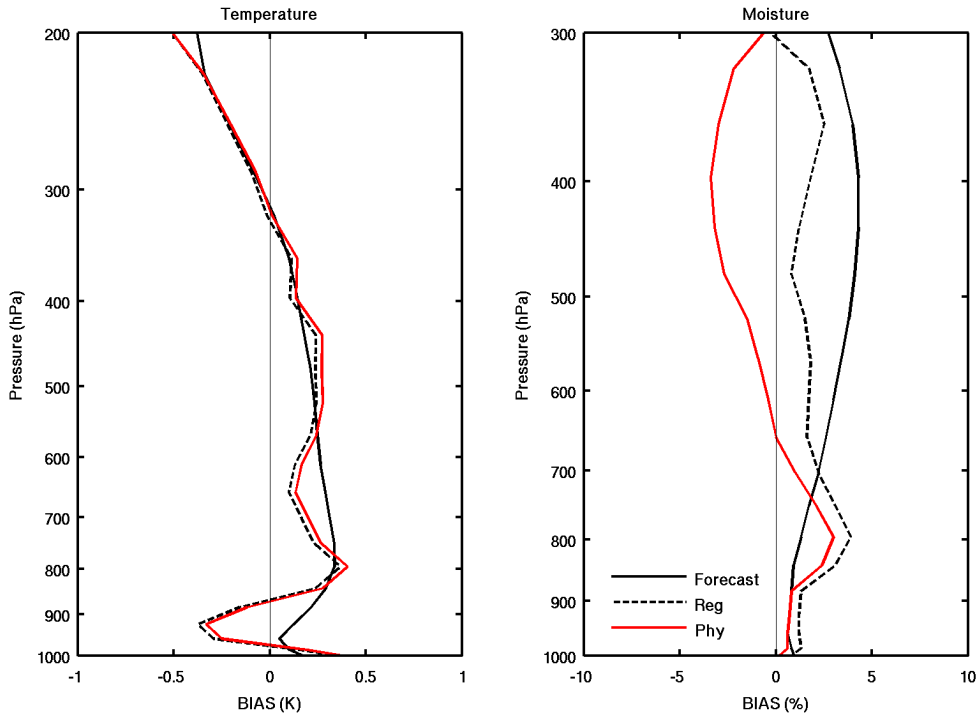


Figure 37. The mean bias for temperature (left) and RH (right) between SEVIRI retrievals and ECMWF analysis for January 2008 over land, 203491 matchups are included in the land statistics.

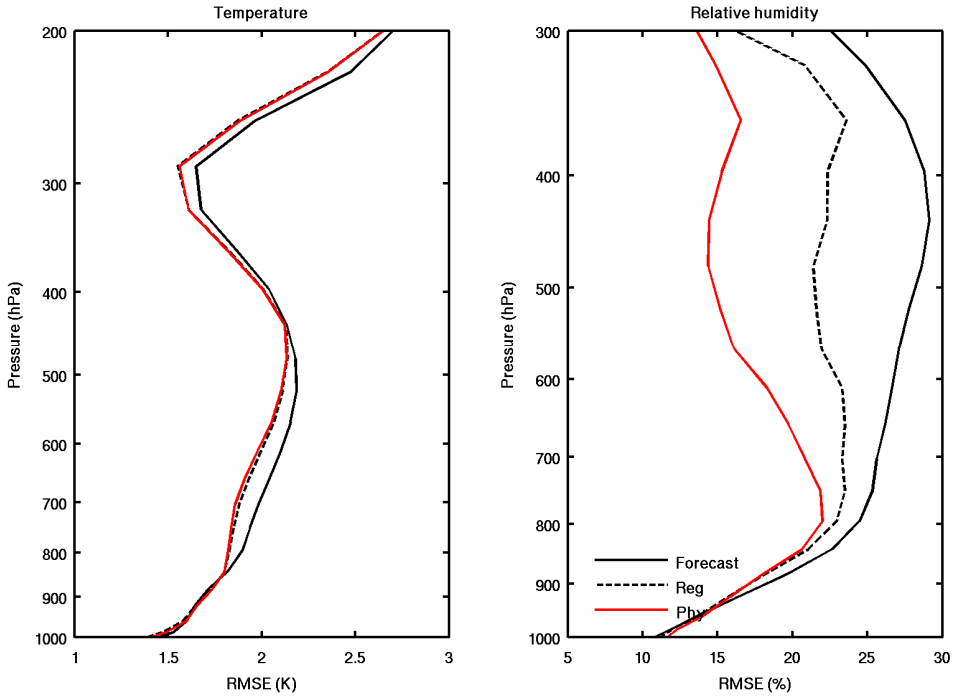


Figure 38. The RMSE for temperature (left) and RH (right) between SEVIRI retrievals and ECMWF analysis for January 2008 over ocean, a total of 149724 matchups is included in the land statistics.

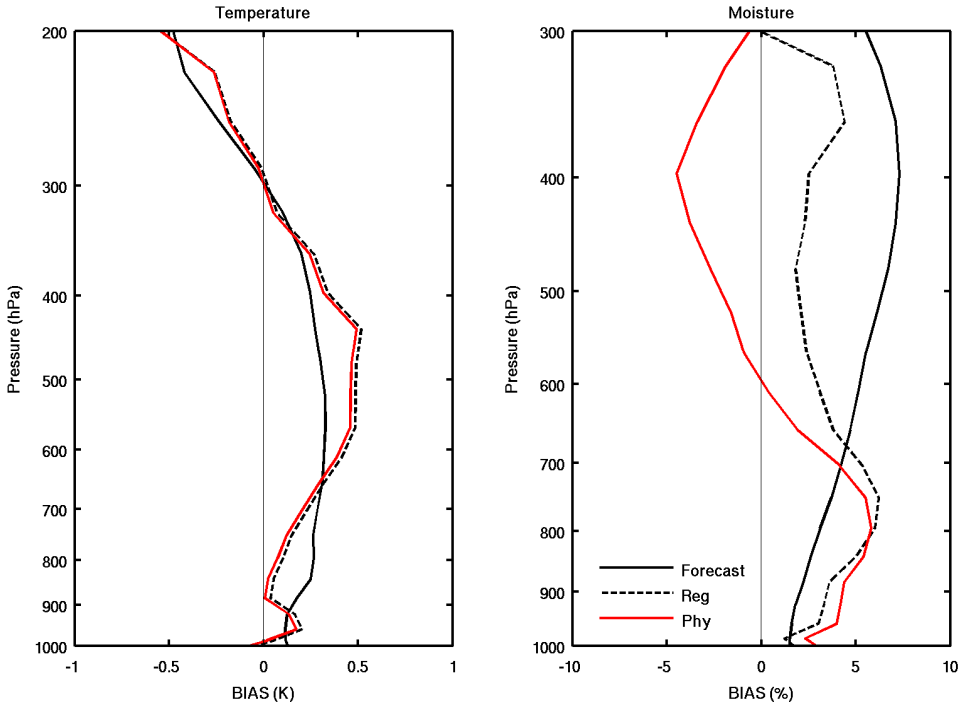


Figure 39. The mean bias for temperature (left) and RH (right) between SEVIRI retrievals and ECMWF analysis for January 2008 over ocean, a total of 149724 matchups is included in the land statistics.

The temporal evolution of the retrieved atmospheric profiles versus the forecast is carried out by processing the 18-month dataset and plotted in the following two figures. It is found that the improvement of temperature profile is limited and the major improvement occurs at the near surface levels (below 900 hPa). In winter the reduction of RMSE at low levels is about 0.3 K and in other seasons the value can go up to 0.5 K. Similar results can be expected by ABI since SEVIRI and ABI has only one CO2-absorbing band at 13.4-um.

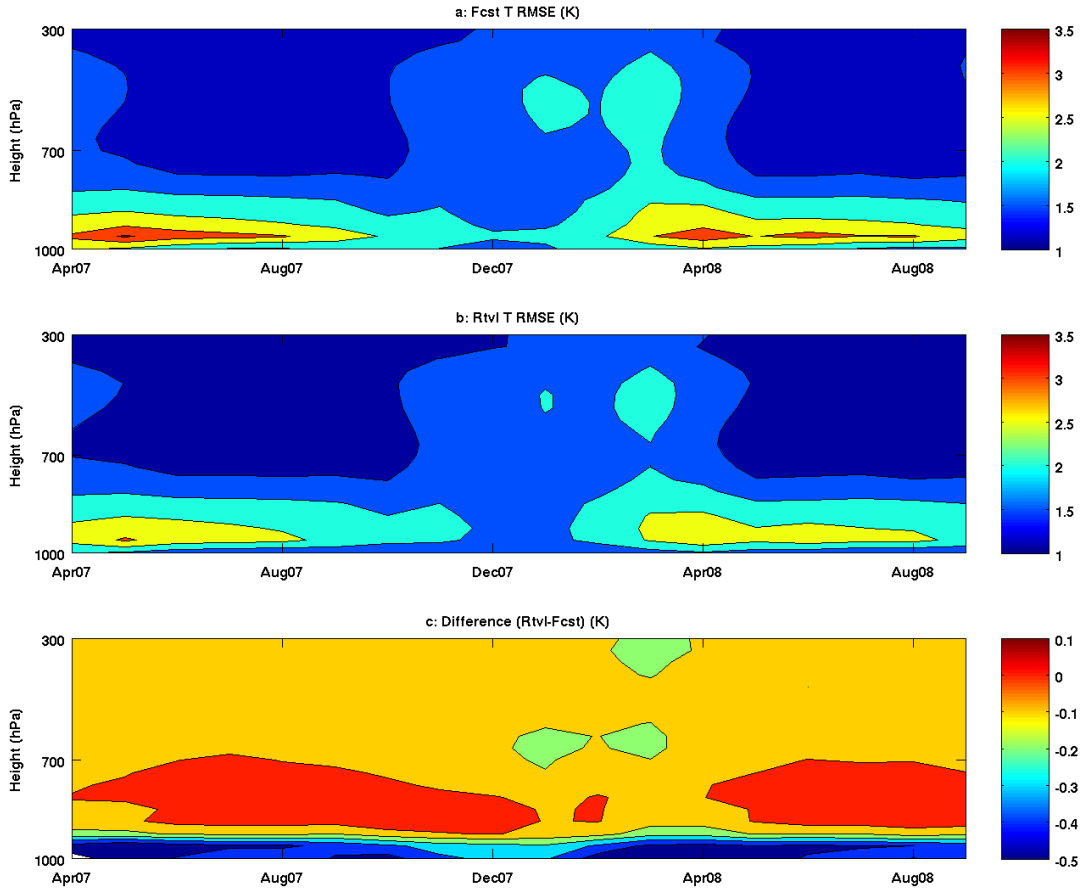


Figure 40. The evolution of forecast (top) and retrieved (middle) temperature profile RMSE (K) against ECMWF analysis from April 2007 to September 2008. Also plotted is the RMSE difference between retrieval and forecast (bottom).

The improvement of moisture profile happens at the upper levels (higher than 700 hPa) and the best results are located near the 500 hPa. Meanwhile, the seasonal pattern of the improvement is obvious: more RMSE of RH is reduced in winter and spring than other seasons and the largest improvement is about 15%. Since ABI has one more water vapor band at 6.9-um, it is expectable that the improvement of RH by ABI could be slightly better than the proxy result.

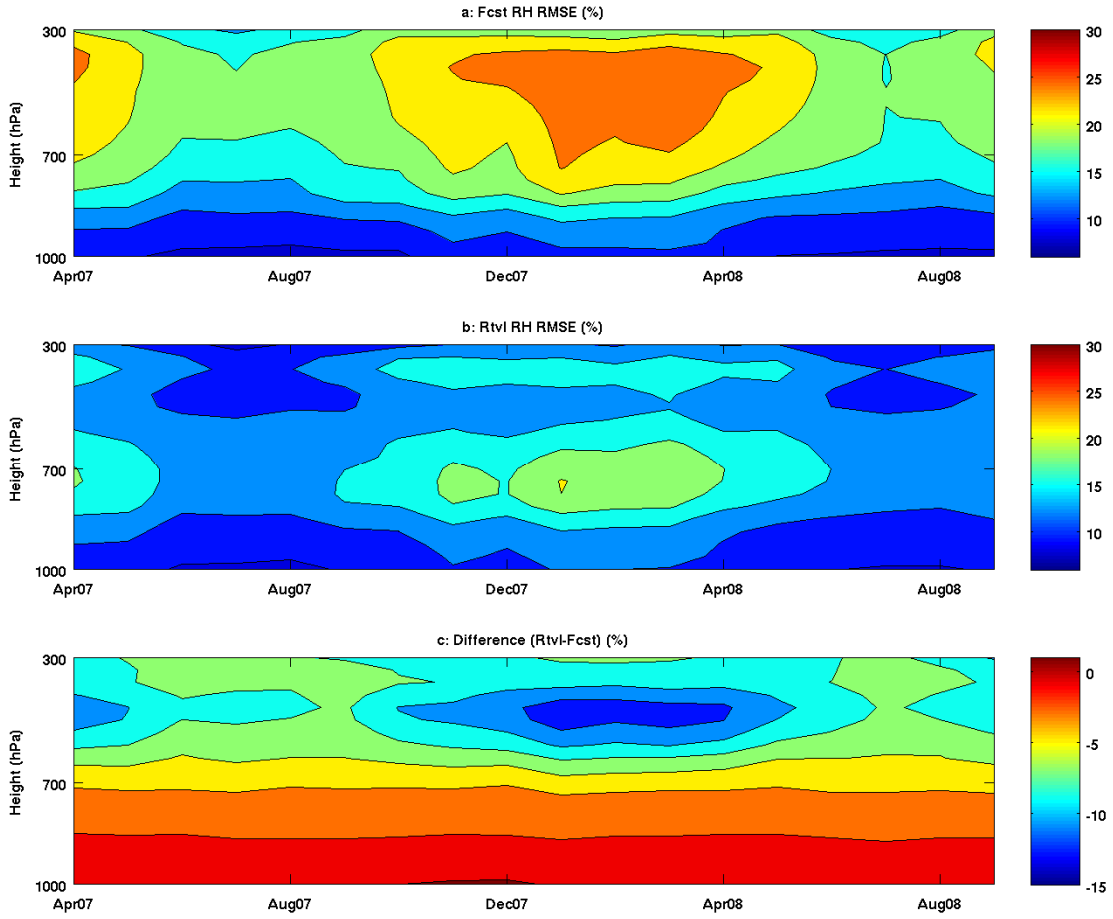


Figure 41. The evolution of forecast (top) and retrieved (middle) RH profile RMSE (%) against ECMWF analysis from April 2007 to September 2008. Also plotted is the RMSE difference between retrieval and forecast (bottom).

#### *4.3.2.1.6 CAPE analysis with radiosondes and ECMWF* analysis

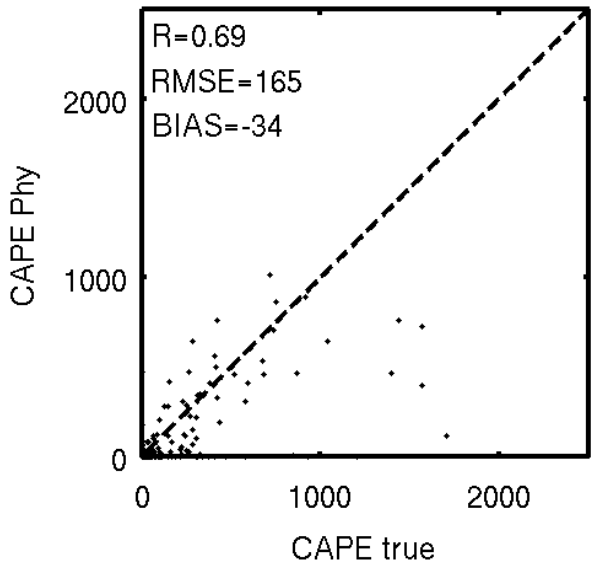

Figure 42. Same as Figure 28 but for CAPE.

Figure 42 shows the CAPE retrievals. Since CAPE has quite large variations, it is difficult to make a decent scattering plot. However, the retrieval still has good agreement with observation if filtering out some outliers.

The monthly averaged time series of CAPE between April 2007 and September 2008 over Europe and North Africa is plotted in the following. The difference between forecast and retrieval is trivial in most seasons except winter when the retrieval is much better than forecast. Such a pattern indicates that the LAP CAPE product may be helpful in predicting convective weather in winter, such as snow storms.

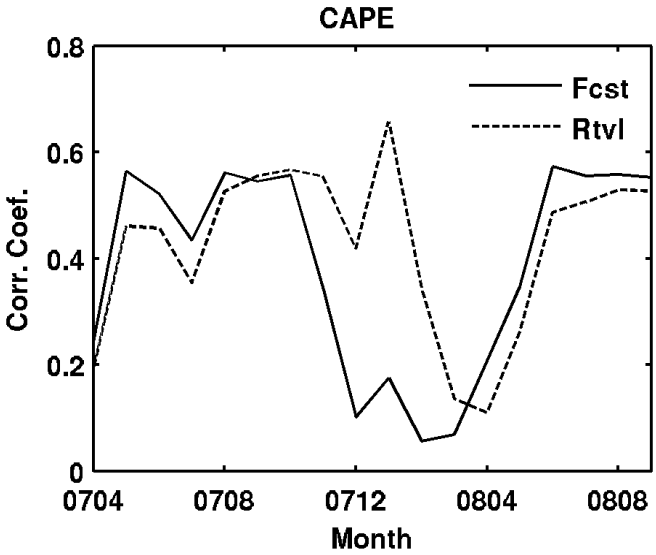

Figure 43. Same as Figure 32 but for CAPE.

***4.3.2.1.7 TT analysis with radiosondes and ECMWF analysis***

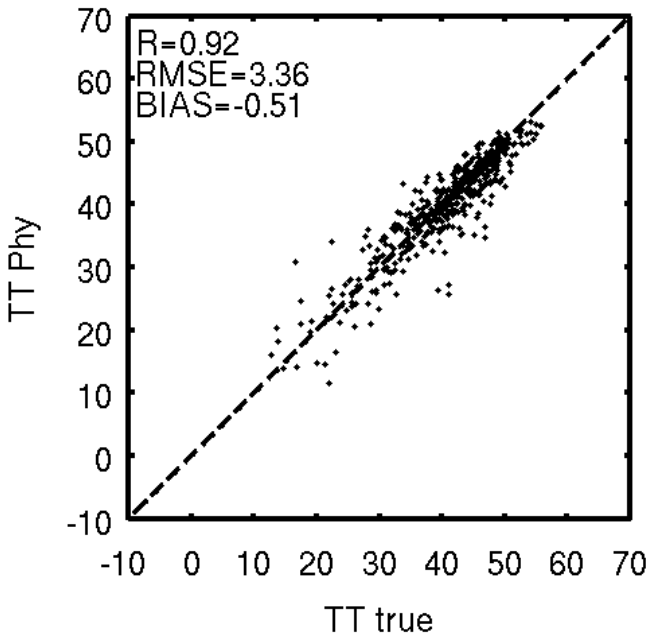

Figure 44. Same as Figure 28 but for TT.

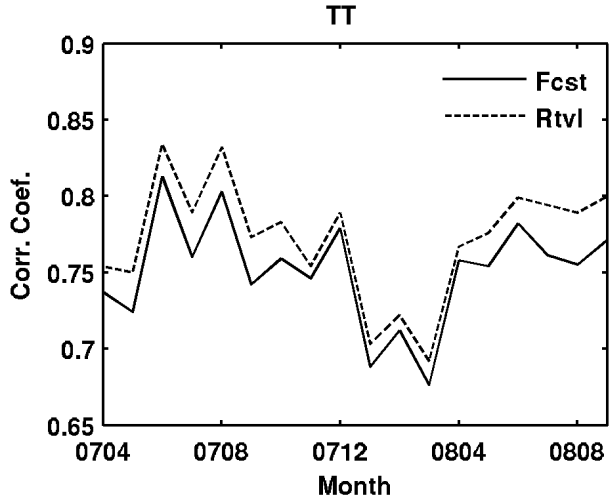

Figure 45. Same as Figure 32 but for TT.

#### *4.3.2.1.8 SI analysis with radiosondes and ECMWF analysis*

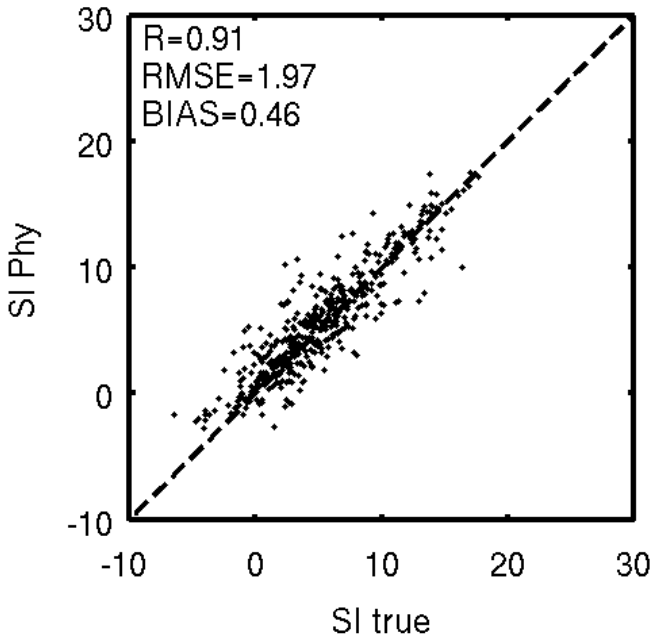


Figure 46. Same as Figure 28 but for SI.

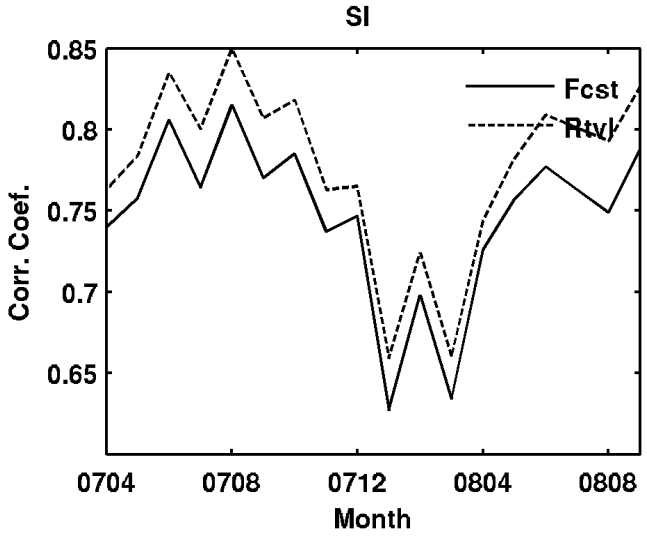


Figure 47. Same as Figure 32 but for SI.

#### *4.3.2.1.9 KI analysis with radiosondes and ECMWF analysis*

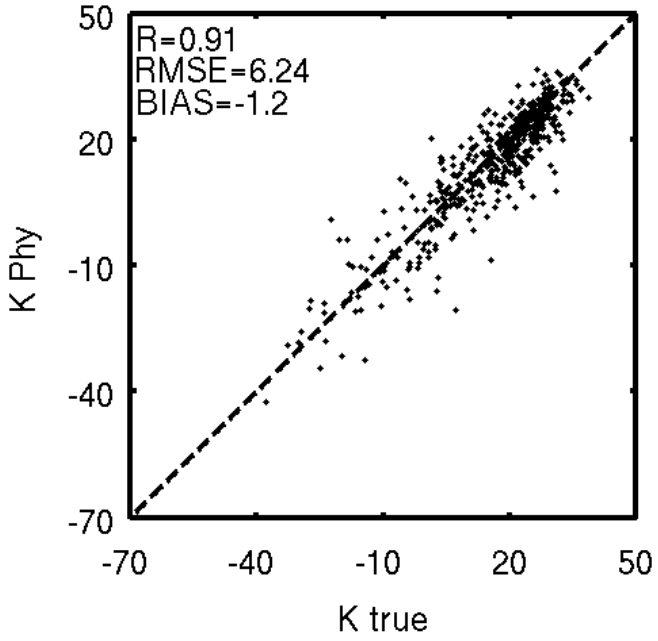

Figure 48. Same as Figure 28 but for KI.

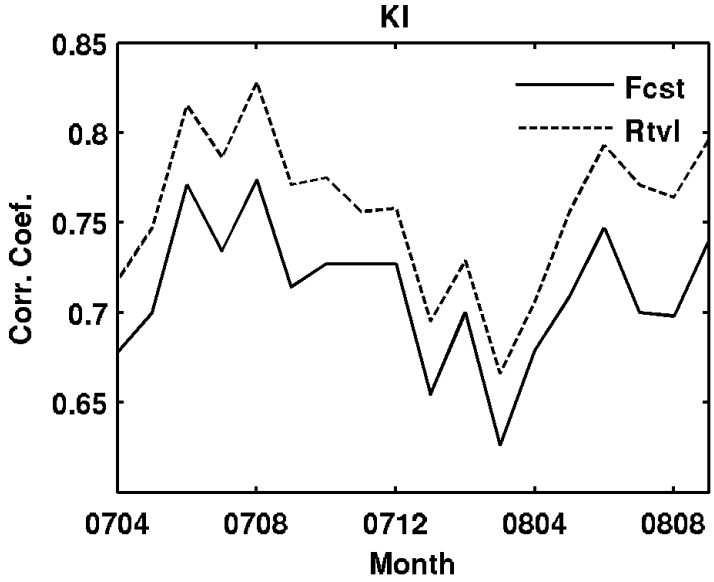

Figure 49. Same as Figure 32 but for KI.

### 3.3.3 Further Product Validation Plan

#### 3.3.3.1 Offline validation of LAP and derived products (DPs) – truth datasets

**True dataset over land**

The radiosondes (MSG spatial coverage) will be used for validating LAP and DPs over land, the ARM site radiosondes and microwave based TPW (frequent observations) over South African and Germany will also be used as truth.

**Truth dataset over ocean**

Radiosondes from AEROSE (2006 – 2008) and AMSR-E TPW observations will be used as truth over ocean.

**Truth dataset over both land and ocean**

ECMWF analysis (6-hour global ECMWF analysis for temperature and moisture profiles, 0.25 degree by 0.25 degree) will be used as truth over both land and ocean, one month's ECMWF analysis data (August 2006) will be used.

#### 3.3.3.2 Offline validation of LAP and derived products (DPs) – test datasets

**Test data over land**

(1) Collocated Radiosondes - SEVIRI radiances over MSG spatial coverage (spatial distance < 25 km, temporal difference < 0.5 hour). ECMWF or GFS forecast can be used as background. Time period is April 2007 – September 2008.
(2) Collocated radiosondes and SEVIRI radiances, collocated SEVIRI radiances and microwave TPW over ARM site in African and Germany. Spatial difference <15 km, temporal difference <15 minutes.
(3) Products to be validated: Temperature profile, moisture profile, TPW, LI, CAPE, TT, SI, K-Index.

**Test data over ocean**

(1) Collocated Radiosondes - SEVIRI radiances over ocean from AEROSE (2006 – 2008) (spatial distance < 25 km, temporal difference < 0.5 hour). ECMWF or GFS forecast can be used as background. Time period is 2006 – 2008.
(2) Collocated AMSR-E level 2 TPW product and SEVIRI radiances. Spatial difference <20 km and temporal difference <15 minutes.
(3) Products to be validated from AEROSE data: Temperature profile, moisture profile, TPW, LI, CAPE, TT, SI, K-Index.
(4) Products to be validated from AMSR-E data: TPW

**Test data over both land and ocean**

(1) Collocated ECMWF analysis and SEVIRI radiances from April 2007 – September 2008 at 00 UTC and 12 UTC (spatial distance < 25 km, temporal difference < 15 minutes). ECMWF or GFS forecast can be used as background.

(2) Products to be validated: Temperature profile, moisture profile, TPW, LI, CAPE, TT, SI, K-Index.

#### 3.3.3.3 Offline validation of LAP and derived products (DPs) – test methods

**Test methods over land**

(1) Collect spatially and temporally collocated SEVIRI radiances and radiosondes over land.
(2) Add forecast (from GFS or ECMWF) into the matchup data.
(3) Collect SEVIRI and radiosondes, SEVIRI and microwave TPW over ARM sites in Africa and Germany.
(4) Add forecast (from GFS or ECMWF) into the matchup data.
(5) Algorithm test using SEVIRI radiances,
    (a) Screen clouds using offline threshold method, or using operational SEVIRI cloud mask product;
    (b) Start with forecast, generate first guess LAP profile using regression algorithm; update LAP profile using physical retrieval algorithm.
(6) Compare LAP/DPs from SEVIRI with radisosondes over land.
(7) Compare LAP/DPs from SEVIRI with radisosondes at ARM sites in Africa and Germany.
(8) Compare TPW from SEVIRI with microwave TPW measurements at ARM sites in Africa and Germany.

**Test methods over ocean**

(1) Collocate radiosondes and SEVIRI from AEROSE over ocean.
(2) Develop dust mask for SEVIRI radiances.
(3) Add forecast (GFS or ECMWF) into the matchup data.
(4) Collect SEVIRI and AMSR-E level2 TPW product, add forecast (GFS or ECMWF) into this matchup data.
(5) Algorithm test using SEVIRI radiances,
    (a) Screen clouds using offline threshold method, or using operational SEVIRI cloud mask product;
    (b) Start with forecast, generate first guess LAP profile using regression algorithm; update LAP profile using physical retrieval algorithm.
(6) Compare LAP/DPs from SEVIRI with radisosondes over ocean.
(7) Compare TPW from SEVIRI with AMSR-E TPW product over ocean

**Test methods over both land and ocean**

(1) Collect spatially and temporally collocated SEVIRI radiances and ECMWF analysis.
(2) Add forecast (from GFS or ECMWF) into the matchup data.
(3) Algorithm test using SEVIRI radiances,

(a) Screen clouds using offline threshold method, or using operational SEVIRI cloud mask product;

(b) Start with forecast, generate first guess LAP profile using regression algorithm; update LAP profile using physical retrieval algorithm.

(4) Compare LAP/DPs from SEVIRI with ECMWF analysis

### 3.3.4 Frame work validation

(1) Take the output from the framework.
(2) Take the same test dataset of framework.
(3) Run the test dataset offline.
(4) Compare the offline results with framework output, assure the consistency.

# 4 PRACTICAL CONSIDERATIONS

## 4.1 Numerical Computation Considerations

The physical iterative procedure is less efficient than statistical approach. For computation efficiency, numerical approaches are used; see Eq. (24) and Eq. (25) for details. The interpolation of NWP field to ABI spatially, temporally and vertically can be pre-processed before the algorithm run.

## 4.2 Programming and procedural Considerations

The LAP algorithm requires knowledge of clear mask information within each FOR. The LAP is implemented sequentially (pre-process, regression followed by iterative physical approach). The LAP is purely a FOR by FOR algorithm. Then it could be parallelized in future version for processing with several CPU. The only task that is not made inside LAP code is spatial interpolation of NWP before retrieval process upon the arrival of new NWP data to avoid repeat the process every slot.

## 4.3 Quality Assessment and Diagnostics

The following procedures are recommended for diagnosing the performance of the LAP.

- Monitor the percentage of clear pixels within the FOR.
- Derive BT residuals between observations and calculations with forecast and retrieval.
- Indicate large difference of IR10.8 BT between calculation and observation.

## 4.4 Exception Handling

Algorithm cannot be run if any of the mandatory IR channels data or ABI CM is bad or missing. The LAP does check for conditions where the LAP cannot be performed. These conditions include saturated profiles or missing RTM values.

# 5 Assumptions and Limitations

## 5.1 Performance

The factors impact LAP performance include the inaccuracy of CM, uncertainty of fast RTM, desert situation, radiance and calibration bias, imperfect of background error covariance matrix. The strategies for mitigation include:

(1) For CM improvement, collaborate with cloud team and provide feedback on using their CM product, identify the problematic areas where CM algorithm needs to be improved.
(2) For desert region, develop SE database from IASI, using IASI SE for surface condition in ABI LAP retrieval.
(3) For radiance bias, develop an algorithm for bias adjustment, coefficients for radiance bias adjustment should be updated routinely. Study should be conducted on the diurnal characteristics of radiance bias.
(4) For background error covariance matrix, the radiosonde/ABI matchup database will be used to update forecast error covariance matrix, monthly update is needed.

## 5.2 Assumed Sensor Performance

Good ABI radiometric performance is required. If the signal to noise ratio is not good enough, the accuracy of LAP product will be degraded. The impact of instrument noise on LAP product will be evaluated; algorithm will be refined to mitigate this impact. For example, increase the assumed noise in training the regression coefficient for first guess estimate.

## 5.3 Pre-planned Product Improvements

Here are pre-planned product improvements based on the operational priority and feasibility.

### 6.3.1 Improvement 1: using emissivity database from polar-orbiting advanced IR sounder radiances.

The IASI provides global radiance spectra with high spectral resolution, SE spectrum can be derived from IASI radiance measurements and the emissivity can be used for ABI LAP retrieval.

### 6.3.2 Improvement 2: Radiance bias adjustment

It is very important to develop a robust algorithm for radiance bias adjustment, SEVIRI and the current GOES Sounder data can be used to test the effect of radiance bias adjustment and this algorithm can be applied to ABI once the data is available.

### 6.3.3 Improvement 3: Using time continuity in LAP product improvement

ABI has much higher temporal resolution than the current GOES Sounder; water vapor variation is small during 15 minute time step. The previous retrieval can be used as the first guess for the current time step retrieval, which will avoid the disadvantage of coarser temporal resolution of global forecast model (e.g., every 6 hours)

### 6.3.4 Improvement 4: Using regional high resolution forecast model

Ideally, forecast should be output from regional model every one hour, and spatial resolution of the regional forecast model should be 10 km or better. The next two figures are the results with different NWP model profiles as background. This is a simulated ABI case of 22:00 UTC, June 04, 2005. NAM is a typical regional model with higher spatial and temporal resolutions than the ECMWF forecast as 12-km vs. 30-km and 3-hour vs. 12-hour respectively. We found that using high-resolution regional NWP model profiles as background can significantly improve the LAP retrieval for the low level moisture profile which in turn, can improve the retrieval of TPW (Jin et al. 2008b).

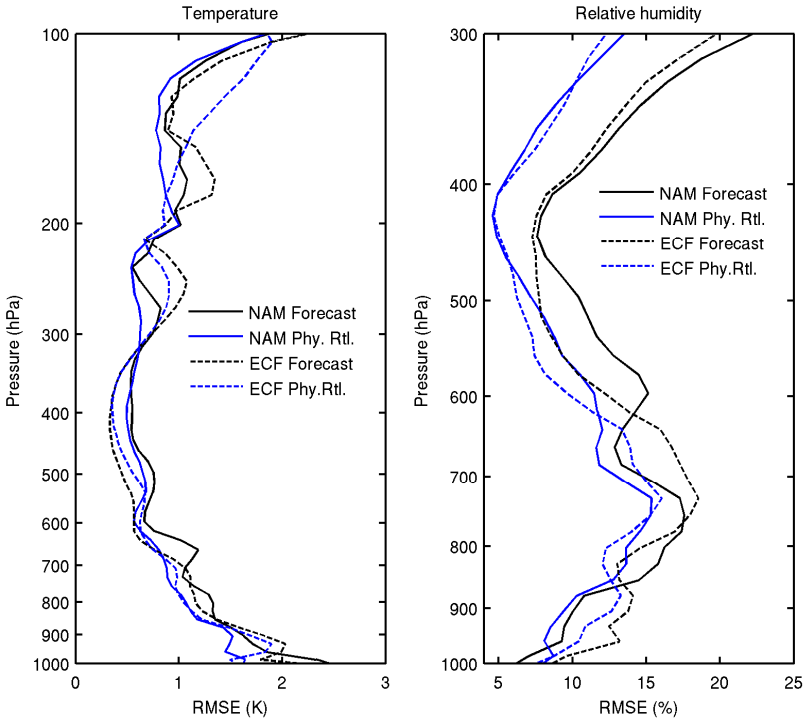


Figure 50: The (left) temperature and (right) RH profile of RMSE against the true values with WRF-simulated ABI case of 22:00 UTC June 2005. NAM 3-hour forecast and ECMWF 12-hour forecast are used as background in the LAP retrieval.

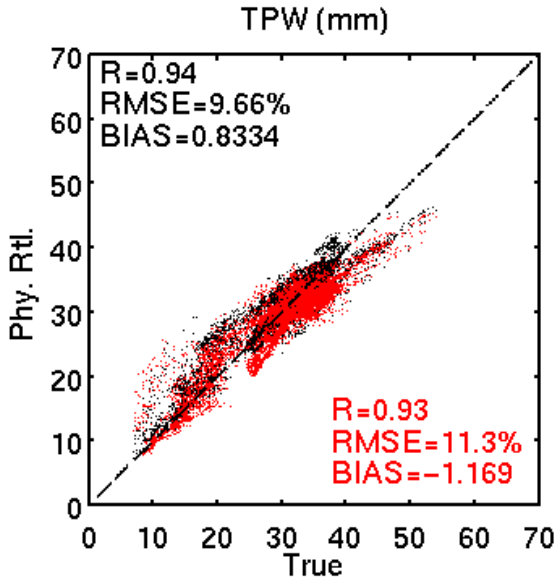


Figure 51: Retrieved TPW with NAM (black) and ECMWF (red) forecast as background against the WRF-simulated true value.

### 5.4 Assumptions

(1) The single FOV ABI CM is available before the LAP retrieval
(2) A high quality dynamic land surface IR emissivity product is available
(3) Forecast temperature, moisture profiles, as well as near surface wind speed, surface skin temperature and surface pressure are available
(4) NeDR and calibration for all ABI IR bands are known and reasonably good
(5) A fast and accurate RTM along with K-Matrix computation are available
(6) Algorithm/products will be validated with intensive ground and aircraft measurements
(7) Forecast error covariance matrix will be updated routinely from matchup file
(8) Retrieval is performed on FOR basis
(9) Spectral response knowledge is stable and known
(10) ABI satellite position is known
(11) Good quality ABI data with respect to striping, stability, cross-talk, etc.

### 5.5 Limitations

(1) LAP and derived products are available over “clear” FORs only (20% or more clear FOVs within the FOR)
(2) Effect of emissivity temporal variation is not handled. Emissivities at ABI IR bands are monthly dataset.
(3) Surface roughness and skin temperature non-homogeneousness are not handled
(4) Since it is an iterative physical retrieval, computation is relative expensive and increase the width of the FOR could be necessary in large region processing
(5) Forecast temperature is hard to improve with ABI

(6) Surface air temperature and moisture observations are hard to collect at the spatial resolution of satellite pixel size and the temporal resolution of satellite scan

Due to likely differences on accuracy on sea, non-desert and desert ABI pixels, separated validation will be provided. For desert pixels, the surface skin temperature difference between the NWP first guess and the actual skin temperature could be high. Similar behavior is expected on very hot or cold pixels over non-desert land pixels. Also the fact that the emissivity atlas is not updated in near real time may introduces some errors. Then, the quality for desert pixels may be worse.

# 7. REFERENCES


Aminou, D., and coauthors, "Meteosat Second Generation: A comparison of on-ground and on-flight imaging and radiometric performances of SEVIRI on MSG-1," *Proceedings of 'The 2003 EUMETSAT Meteorological Satellite Conference', Weimar, Germany, 29 September – 3 October 2003*, pp. 236–243.

Bayler, G. M., R. M. Aune, and W. H. Raymond, 2001: NWP cloud initialization using GOES sounder data and improved modeling of non-precipitating clouds. *Mon. Wea. Rev.*, 128, 3911-3920.

Borbas, E., S. Seemann, H.-L. Huang, J. Li, and W. P. Menzel, 2005: Global profile training database for satellite regression retrievals with estimates of skin temperature and emissivity, in *Proc. Int. ATOVS Study Conf.* 14, Bejiing, China.

Dostalek, J. F. and T. J. Schmit, 2001: Total precipitable water measurements from GOES sounder derived product imagery. *Wea. Forecasting*, 16, 573-587.

Galway, J.G., 1956: The lifted index as a predictor of latent instability. *Bull. Amer. Meteor. Soc.*, 37, 528-529.

Hayden, C. M., and T. J. Schmit, 1991: The Anticipated Sounding Capabilities of GOES-I and Beyond. *Bull. of the Amer. Meteor. Soc.*, 72, pp. 1835–1846.

Hannon, S., L. L. Strow, and W. W. McMillan, 1996: Atmospheric infrared fast transmittance models: A comparison of two approaches. *Proceedings of SPIE*, 2830, 94-105.

Jin, Xin, Jun Li, Timothy J. Schmit, Jinlong Li, Mitchell D. Goldberg, and James J. Gurka, 2008: Retrieving Clear Sky Atmospheric Parameters from SEVIRI and ABI infrared radiances. *J. Geophys. Res.*, **113**, D15310.

Jin, Xin, Jun Li, Timothy J. Schmit, Jinlong Li, Allen H. Huang, and Mitchell D. Goldberg, 2008: GOES-R/ABI legacy profile algorithm evaluation using MSG/SEVIRI and AMSR-E, *Atmospheric and Environmental Remote Sensing Data Processing and Utilization IV: Readiness for GEOSS II, edited by Mitchell D. Goldberg, Hal J. Bloom, Allen H. Huang, Philip E. Ardanuy. Proc. SPIE*, Vol. 7085, 70850F

Li, J., 1994: Temperature and water vapor weighting functions from radiative transfer equation with surface emissivity and solar reflectivity. *Adv. Atmos. Sci.*, 11, 421–426.

Li, J., W. Wolf, W. P. Menzel, W. Zhang, H.-L. Huang, and T. H. Achtor, 2000: Global

soundings of the atmosphere from ATOVS measurements: The algorithm and validation, *J. Appl. Meteorol.,* 39: 1248 – 1268.

Li, J., and H.-L. Huang, 1999: Retrieval of atmospheric profiles from satellite sounder measurements by use of the discrepancy principle, *Appl. Optics*, Vol. 38, No. 6, 916-923.

Li, J., W. P. Menzel, F. Sun, T. J. Schmit, and J. Gurka, 2004: AIRS subpixel cloud characterization using MODIS cloud products. *J. Appl. Meteorol.*, 43, 1083 - 1094.

Li, J., and co-authors, 2005: Retrieval of cloud microphysical properties from MODIS and AIRS. *J. Appl. Meteorol.*, 44, 1526 - 1543.

Li, J., Jinlong Li, Elisabeth Weize, and D. K. Zhou, 2007: Physical retrieval of surface emissivity spectrum from hyperspectral infrared radiances, *Geophysical Research Letters*, 34, L16812, doi:10.1029/2007GL030543

Li, J., W. Wolf, W. P. Menzel, W. Zhang, H.-L. Huang, and T. H. Achtor, 2000: Global soundings of the atmosphere from ATOVS measurements: The algorithm and validation, *J. Appl. Meteorol.,* 39: 1248 – 1268.

Li, Zhenglong, Jun Li, W. Paul Menzel, T. J. Schmit, J. P. Nelson, and S. A. Ackerman, 2008: GOES sounding improvement and application to severe storm nowcasting, *Geophysical Research Letters*, 35, L03806, doi:10.1029/2007GL032797.

Li, J., and Jinlong Li, 2008: Derivation of Global Hyperspectral Resolution Surface Emissivity Spectra from Advanced Infrared Sounder Radiance Measurements, *Geophysical Research Letters*, 35, L15807, doi:10.1029/2008GL034559.

Ma, X. L., Schmit, T. J. and W. L. Smith, 1999: A non-linear physical retrieval algorithm – its application to the GOES-8/9 sounder. *J. Appl. Meteor*. 38, 501-513.

Menzel, W. P., and J. F. W. Purdom, 1994: Introducing GOES-I: The first of a new generation of Geostationary Operational Environmental Satellites. *Bull. Amer. Meteor. Soc.*, 75, 757–781.

Menzel, W. P., F. C. Holt, T. J. Schmit, R. M. Aune, A. J. Schreiner, G. S. Wade, and D. G. Gray, 1998: Application of GOES-8/9 soundings to weather forecasting and nowcasting. *Bull. Amer. Met. Soc.*, 79, 2059-2077.

Nalli, N. R., P. Clemente-Colón, P. J. Minnett, M. Szczodrak, V. Morris, E. Joseph, M. D. Goldberg, C. D. Barnet, W. W. Wolf, A. Jessup, R. Branch, R. O. Knuteson, and W. F. Feltz, 2006: Ship-based measurements for infrared sensor validation during Aerosol and Ocean Science Expedition 2004, *J. Geophys. Res*, 111, D09S04, doi:10.1029/2005JD006385.

Rodgers, C.D., 1976: Retrieval of atmospheric temperature and composition from remote measurements of thermal radiation. *Rev. Geophys. Spac. Phys*., 14, 609-624.

Rodgers, C. D., 1990: Characterization and error analysis of profiles retrieved from remote sounding measurements. *J. Geophys. Res.,* **95,** 5587–5595.

Schmit T. J., W. F. Feltz, W. P. Menzel, J. Jung, A. P. Noel, J. N. Heil, J. P. Nelson III, and G. S. Wade, 2002: Validation and use of GOES sounder moisture information, *Wea. Forecasting*, 17, 139-154.

Schmit, T. J., M. M. Gunshor, W. P. Menzel, J. Li, S. Bachmeier, and J. J. Gurka, 2005: Introducing the Next-generation Advanced Baseline Imager (ABI) on GOES-R, *Bull. Amer. Meteor. Soc.,* **86**, 1079-1096.

Schmit, J. Li, J. Gurka, M. Goldberg, K. Schrab, J. Li, and W. Feltz, 2008: The GOES-R ABI (Advanced Baseline Imager) and the continuation of current sounder products, *Journal of Applied Meteorology and Climatology*, 47, 2696 – 2711.

Schmit, T. J., J. Li, S. A. Ackerman, and J. J. Gurka, 2009: High spectral and temporal resolution infrared measurements from geostationary orbit, *Journal of Atmospheric and Oceanic Technology*. (in press).

Schmetz J, Pili P, Tjemkes S, Just D, Kerkmann J, Rota S, Ratier A. 2002. An introduction to Meteosat Second Generation (MSG), *Bulletin of the American Meteorological Society*, 83, 977-992.

Schmid J, 2000. The SEVIRI Instrument. *Proceedings of the 2000 EUMETSAT Meteorological Satellite Data User's Conference, Bologna, Italy, 29 May – 2 June 2000*

Schumann W, Stark H, McMullan K, Aminou D, Luhmann H-J. 2002. The MSG System, *ESA bulletin*, 111.

Seemann, S. W., Li, J., W. Paul Menzel, and L. E. Gumley, 2003: Operational retrieval of atmospheric temperature, moisture, and ozone from MODIS infrared radiances, *J. Appl. Meteorol.*, 42, 1072 - 1091.

Seemann, S.W., E. E. Borbas, R. O. Knuteson, G. R. Stephenson, H.-L. Huang, 2008: Development of a Global Infrared Land Surface Emissivity Database for Application to Clear Sky Sounding Retrievals from Multi-spectral Satellite Radiance Measurements. *Journal of Applied Meteorology and Climatology*, 47, 108 - 123.

Seemann, S.W., E. E. Borbas, R. O. Knuteson, G. R. Stephenson, H.-L. Huang, 2008: Development of a Global Infrared Land Surface Emissivity Database for Application to Clear Sky Sounding Retrievals from Multi-spectral Satellite Radiance Measurements. *Journal of Applied Meteorology and Climatology, 47, 108 - 123.*

Smith, W. L., and H. M. Woolf, 1976: The use of eigenvectors of statistical covariance matrices for interpreting satellite sounding radiometer observations, *J. Atmos. Sci.*, *33*, 1127-1140.

Smith, W. L., G. S. Wade, and H. M. Woolf, 1985: Combined Atmospheric Sounding/Cloud Imagery—A New Forecasting Tool, *Bull. Amer. Meteor. Soc.*, 66, pp. 138–141.

Wang, F., J. Li, T. J. Schmit, and S. A. Ackerman, 2007: Trade studies of hyperspectral infrared sounder on geostationary satellite, *Applied Optics*, 46, 200 - 209.

Wu, X., and W. L. Smith, 1997: Emissivity of rough sea surface for 8-13 μm: modeling and verification, *Appl. Opt.*, 36, 2609 – 2619.

# APPENDIX 1

The following table contains the LAP sounding algorithm output variables.

Table A1: LAP sounding output variables -- products

| **Variable Name** | **Unit** | **Type** | **Size**[†] | **Description** |
|---|---|---|---|---|
| Tprof | K | Float32 | NX_NY_PROF[*] | Retrieved temperature profile |

| | | | | |
|---|---|---|---|---|
| Wprof | g/kg | Float32 | NX_NY_PROF | Retrieved moisture profile |
| Lst | K | Float32 | NX_NY | Retrieved surface skin temperature:<br>1) it is only meaningful over land<br>2) it is same as the interpolated SST from NWP over ocean and lake |
| CAPE | J/kg | Float32 | NX_NY | Convective available potential energy |
| LI | °C | Float32 | NX_NY | Lifted index |
| TT | °C | Float32 | NX_NY | Total Totals |
| KI | °C | Float32 | NX_NY | K-index |
| SI | °C | Float32 | NX_NY | Showalter index |
| TPW | cm | Float32 | NX_NY | Total precipitable water vapor |
| TPW_High | cm | Float32 | NX_NY | Layered PW from 700 to 300 hPa |
| TPW_Mid | cm | Float32 | NX_NY | Layered PW from 900 to 700 hPa |
| TPW_Low | cm | Float32 | NX_NY | Layered PW from surface to 900 hPa |
| Lon_reduced | ° | Float32 | NX_NY | Longitude |
| Lat_reduced | ° | Float32 | NX_NY | Latitude |

† NX_NY refers to the number of FORs in the x-direction by the number of FORs in the y-direction
*: Given the full disk size is X-by-Y and the stride factor is M, then NX = ceiling(X/M) and NY=ceiling(Y/M); PROF is the number of vertical levels depending on the pressure ordinate used in the RTM. PROF = 101 in cRTM version.

Table A2: LAP sounding output variables – quality flags

| **Variable Name** | **Unit** | **Type** | **Size**† | **Description** |
|---|---|---|---|---|
| Quality_Flag | none | Int8 | NX_NY | Overall quality flag :<br>=0 : good<br>=1 : space<br>=2 : latitude greater than threshold<br>=3 : local zenith angle greater than threshold<br>=4 : number of clear pixels less than threshold<br>=5 : missing NWP data<br>=6 : fatal processing error |
| Quality_Flag_Rtvl | none | Int8 | NX_NY | Retrieval quality flag:<br>=0: good retrieval<br>=1: non-convergence<br>=2: residual too large<br>=3: non-completed converge<br>=4: bad retrieval |
| Quality_Flag_BT11 | none | Int8 | NX_NY | Skin temperature first guess quality:<br>=0: ABS($Cal\_BT_{11}$- $Obs\_BT_{11}$) < 2 K, good<br>=1: ($^{\#}Cal\_BT_{11}$- $Obs\_BT_{11}$) > 2 K, bad<br>=2: ($Cal\_BT_{11}$- $Obs\_BT_{11}$) <- 2 K, bad |

† NX_NY refers to the number of FORs in the x-direction by the number of FORs in the y-direction
#: $Cal\_BT_{11}$ is the calculated BT at 11.0-um by forward RTM and first guesses of skin temperature and profiles.

Table A3: LAP sounding output variables -- quality information

| **Variable Name** | **Unit** | **Type** | **Size**† | **Description** |
|---|---|---|---|---|
| Num_Iteration | none | Int8 | NX_NY | Number of iterations |
| RMSE_BrtTemp_Next | K | Float32 | NX_NY | RMSE of average BT residual after retrieval |

| | | | | |
|---|---|---|---|---|
| Num_Clr_Pix | none | Int8 | NX_NY | Number of clear pixels in FOR[@] |
| Quality_Information | none | Int8 | NX_NY | Bit 0: QC_OCEAN_LAND_FOR<br>0 = Ocean FOR, 1 = Land FOR |

[†] NX_NY refers to the number of FORs in the x-direction by the number of FORs in the y-direction
[@]: this number changes with the FOR size.

Table A4: Coefficients used in function WLIFT5

| | |
|---|---|
| A0 | -41.536 |
| A1 | 1.36083317 |
| A2 | 1.91780552E-2 |
| A3 | 1.3333332E-4 |
| A4 | -1.66611135E-5 |
| A5 | -2.46666673E-7 |
| A6 | 8.805555540E-9 |

Table A5: Coefficients used in function WOBF

| | | | |
|---|---|---|---|
| A1 | 3.6182989E-03 | B1 | -8.8416605E-03 |
| A2 | -1.3603273E-05 | B2 | 1.4714143E-04 |
| A3 | 4.9618922E-07 | B3 | -9.6719890E-07 |
| A4 | 29.930 | B4 | 15.13 |
| A5 | 0.96 | | |
| A6 | 14.8 | | |

Table A6: Coefficients used in function TCON

| | |
|---|---|
| A1 | 1.2185 |
| A2 | 1.278E-03 |
| A3 | -2.19E-03 |
| A4 | 1.173E-05 |
| A5 | 5.2E-06 |

Table A7: Coefficients used in function TEMSAT

| | |
|---|---|
| A1 | -.225896152438D+2 |
| A2 | .261012286592D+2 |
| A3 | .30206720594D+1 |
| A4 | .370219024579D+0 |
| A5 | .72838702401D-1 |

Table A8: Coefficients used in function TVPICE

| | |
|---|---|
| A1 | -.2031888177D+2 |

| | |
|---|---|
| A2 | .2394167436D+2 |
| A3 | .2252719878D+1 |
| A4 | .1914055442D+0 |
| A5 | .9636593860D-2 |

Table A9: Coefficients used in function SVPWAT

| | |
|---|---|
| A0 | .999996876D0 |
| A1 | -.9082695004D-2 |
| A2 | .7873616869D-4 |
| A3 | -.6111795727D-6 |
| A4 | .4388418740D-8 |
| A5 | -.2988388486D-10 |
| A6 | .2187442495D-12 |
| A7 | -.1789232111D-14 |
| A8 | .1111201803D-16 |
| A9 | -.3099457145D-19 |
| B | .61078D+1 |

Table A10: Coefficients used in function SVPICE

| | |
|---|---|
| A0 | .7859063157D0 |
| A1 | .3579242320D-1 |
| A2 | -.1292820828D-3 |
| A3 | .5937519208D-6 |
| A4 | .4482949133D-9 |
| A5 | .2176664827D-10 |

Table A11: Coefficients used in function SatMix

| | |
|---|---|
| A1 | 7.90298 |
| A2 | 5.02808 |
| A3 | 1.3816E-7 |
| A4 | 11.344 |
| A5 | 8.1328E-3 |
| A6 | 3.49149 |

Table A12: LAP meta-data (legacy vertical temperature profile, legacy vertical moisture profile, total precipitable water, and stability indices)

| Name | Details/Comments |
|---|---|
| | |
| Date | swath beginning and swath end |
| Time | swath beginning and swath end |
| Bounding Box | product resolution<br>number of rows and<br>number of columns,<br>bytes per pixel<br>data type<br>byte order information<br>location of box relative to nadir (pixel space) |
| Product Name | |
| Product Units | |
| Ancillary Data to Produce Product | product precedence |
| Version Number | |
| Origin | where it was produced |
| Quality Information | |
| Name | |
| Satellite | GOES-16, etc. |
| Instrument | ABI |
| Altitude | |
| Nadir pixel in the fixed grid | |
| Attitude | |
| Latitude | |
| Longitude | |
| Grid Projection | |
| Type of Scan | |
| Product Version Number | |
| Data compression type | |
| Location of production | |
| Citations to Documents | |
| Contact Information | |
| | |
| For each Soundings product, the following information is required: | |
| Mean, Min, Max and Standard deviation of retrievals from first guess for TPW | |
| Mean, Min, Max and Standard deviation of retrievals from first guess | for Lifted Index, Total Totals, CAPE, and Showalters Index |
| Number of IR channels, channel 8 to channel 16 | |
| For each IR channel, the following information is required:<br>Mean difference between calculated BT (from first guess) and observed BT for the | |

| | |
|---|---|
| IR channel | |
| Number of QA flag values | |
| For each QA flag value, the following information is required:<br>Percent of retrievals with the QA flag value<br>Definition of QA flag | |
| Total number of attempted retrievals | |

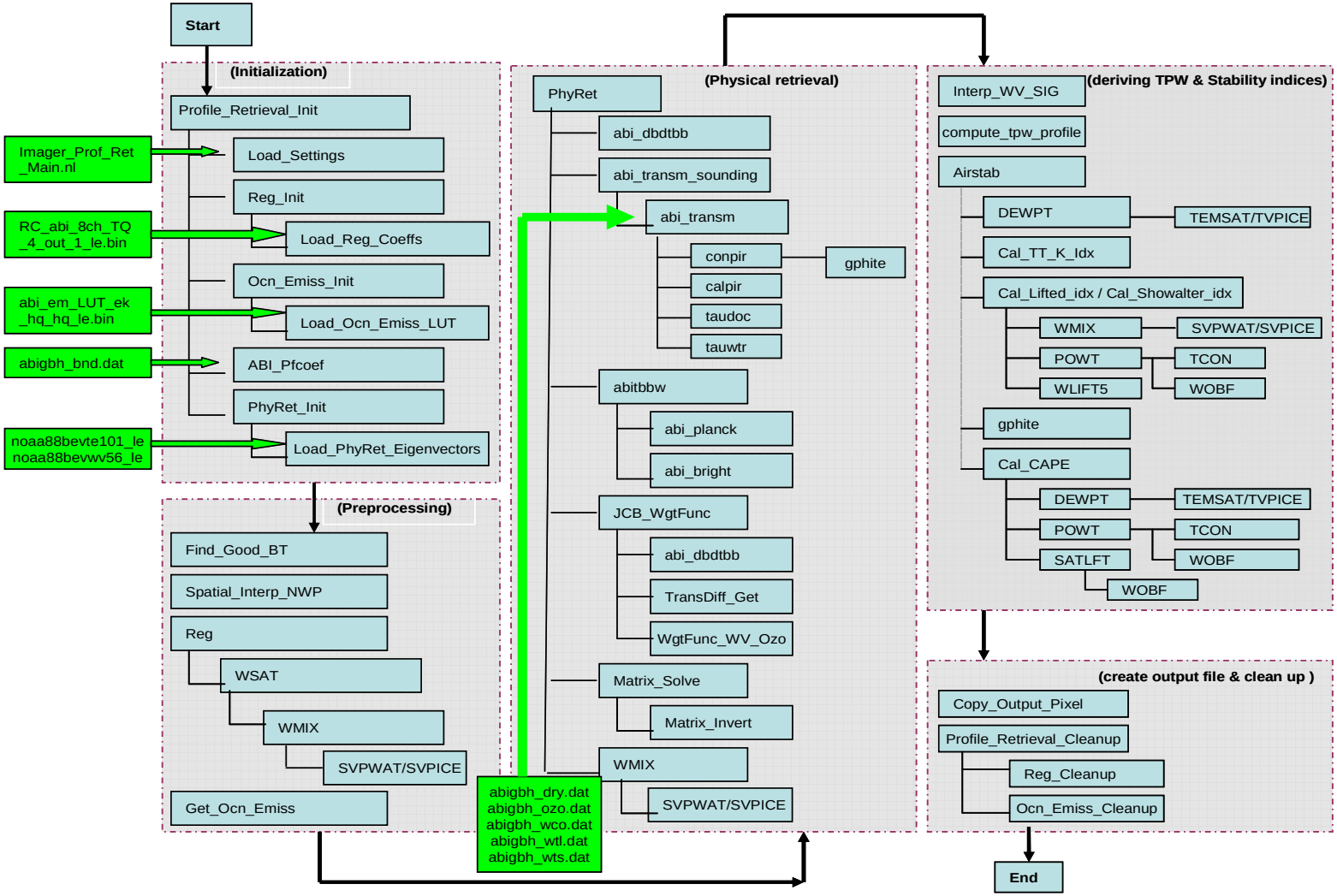


Fig A1: The sketch map of all ancillary files and external functions/subroutines applied in the LAP sounding algorithm

# Appendix 2: Common Ancillary Data Sets

## *1. LAND_MASK_NASA_1KM*

### *a. Data description*

**Description**: Global 1km land/water used for MODIS collection 5
**Filename**: lw_geo_2001001_v03m.nc
**Origin**: Created by SSEC/CIMSS based on NASA MODIS collection 5
**Size**: 890 MB.
**Static/Dynamic**: Static

### *b. Interpolation description*

The closest point is used for each satellite pixel:

1) Given ancillary grid of large size than satellite grid
2) In Latitude / Longitude space, use the ancillary data closest to the satellite pixel.

## *2. NWP_GFS*

### a. *Data description*

**Description:** NCEP GFS model data in grib format – 1 x 1 degree (360x181), 26 levels
**Filename**: gfs.tHHz.pgrbfhh
Where,
HH – Forecast time in hour: 00, 06, 12, 18
hh – Previous hours used to make forecast: 00, 03, 06, 09
**Origin**: NCEP
**Size**: 26MB
**Static/Dynamic**: Dynamic

### *b. Interpolation description*

There are three interpolations are installed:

**NWP forecast interpolation from different forecast time:**

Load two NWP grib files which are for two different forecast time and interpolate to the satellite time using linear interpolation with time difference.

Suppose:

T1, T2 are NWP forecast time, T is satellite observation time, and T1 < T < T2. Y is any NWP field. Then field Y at satellite observation time T is:

$$Y(T) = Y(T1) * W(T1) + Y(T2) * W(T2)$$

Where W is weight and

$$W(T1) = 1 – (T-T1) / (T2-T1)$$
$$W(T2) = (T-T1) / (T2-T1)$$

**NWP forecast spatial interpolation from NWP forecast grid points. This interpolation generates the NWP forecast for the satellite pixel from the NWP forecast grid dataset.**

The closest point is used for each satellite pixel:

1) Given NWP forecast grid of large size than satellite grid
2) In Latitude / Longitude space, use the ancillary data closest to the satellite pixel.

**NWP forecast profile vertical interpolation**

Interpolate NWP GFS profile from 26 pressure levels to 101 pressure levels

For vertical profile interpolation, linear interpolation with Log pressure is used:

Suppose:

y is temperature or water vapor at 26 levels, and y101 is temperature or water vapor at 101 levels. p is any pressure level between p(i) and p(i-1), with p(i-1) < p <p(i). y(i) and y(i-1) are y at pressure level p(i) and p(i-1). Then y101 at pressure p level is:

$$y101(p) = y(i-1) + \log( p[i] / p[i-1] ) * ( y[i] – y[i-1] ) / \log ( p[i] / p[i-1] )$$

## 3. CRTM

### a. Data *description*

**Description:** Community radiative transfer model
**Filename**: N/A
**Origin**: NOAA / NESDIS
**Size**: N/A
**Static/Dynamic**: N/A

### *b.* Interpolation description

A double linear interpolation is applied in the interpolation of the transmissitance and radiance profile, as well as in the surface emissivity, from four nearest neighbor NWP grid points to the satellite observation point. There is no curvature effect. The weights of the four points are defined by the Latitude / Longitude difference between neighbor NWP grid points and the satellite observation point. The weight is defined with subroutine ValueToGrid_Coord:

NWP forecast data is in a regular grid.

Suppose:
Latitude and Longitude of the four points are:
(Lat1, Lon1), (Lat1, Lon2), (Lat2, Lon1), (Lat2, Lon2)
Satellite observation point is:
(Lat, Lon)

Define
aLat = (Lat – Lat1) / (Lat2 – Lat1)
alon = (Lon – Lon1) / (Lon2 – Lon1)

Then the weights at four points are:
w11 = aLat * aLon
w12 = aLat * (1 – aLon)
w21 = (1 – aLat) * aLon
w22 = (1-aLat) * (1 – aLon)

Also define variable at the four points are:
a11, a12, a21, a22

Then the corresponding interpolated result at satellite observation point (Lat, Lon) should be:

a(Lat, Lon) = ( a11*w11 + a12*w12 + a21*w21 + a22*w22 ) / u

Where,

u = w11 + w12 + w21 + w22

**c. CRTM calling procedure in the AIT framework**

The NWP GFS pressure, temperature, moisture and ozone profiles start on 101 pressure levels.
They are converted to 100 layers in subroutine Compute_Layer_Properties. The layer temperature between two levels is simply the average of the temperature on the two levels.
layer_temperature(i) = (level_temperature(i) + level_temperature(i+1))/2
While pressure, moisture and ozone are assume to be exponential with height.
hp = (log(p1)-log(p2))/(z1-z2)
p = p1* exp(z*hp)
Where p is layer pressure, moisture or ozone. p1,p2 represent level pressure, moisture or ozone. z is the height of the layer.

CRTM needs to be initialized before calling. This is done in subroutine Initialize_OPTRAN. In this call, you tell CRTM which satellite you will run the model. The sensor name is passed through function call CRTM_Init. The sensor name is used to construct the sensor specific SpcCoeff and TauCoeff filenames containing the necessary coefficient data, i.e. seviri_m08.SpcCoeff.bin and seviri_m08.TauCoeff.bin. The sensor names have to match the coefficient file names. You will allocate the output array, which is RTSolution, for the number of channels of the satellite and the number of profiles. You also allocate memory for the CRTM Options, Atmosphere and RTSoluiton structure. Here we allocate the second RTSolution array for the second CRTM call to calculate derivatives for SST algorithm.

Before you call CRTM forward model, load the 100-layer pressure, temperature, Moisture and ozone profiles and the 101 level pressure profile into the Atmosphere Structure. Set the units for the two absorbers (H2O and O3) to be MASS_MIXING_RATIO_UNITS and VOLUME_MIXING_RATIO_UNITS respectively. Set the Water_Coverage in Surface structure to be 100% in order to get surface emissivity over water. Land surface emissivity will be using SEEBOR. Also set other variables in Surface data structure, such as wind speed/direction and surface temperature. Use NWP surface temperature for land and coastline, and OISST sea surface temperature for water. Set Sensor_Zenith_Angle and Source_Zenith_Angle in Geometry structure. Call CRTM_Forward with normal NWP profiles to fill RTSolution, then

call CRTM_Forward again with moisture profile multiplied by 1.05 to fill RTSolution_SST. The subroutine for this step is Call_OPTRAN.

After calling CRTM forward model, loop through each channel to calculate transmittance from each level to Top of Atmosphere (TOA). What you get from RTSolution is layer optical depth, to get transmittance

```
 Trans_Atm_Clr(1) = 1.0

 Do Level =  2 , TotalLevels
   Layer_OD = RTSolution(ChnCounter, 1)%Layer_Optical_Depth(Level
-1)
   Layer_OD = Layer_OD /
COS(CRTM%Grid%RTM(LonIndex,LatIndex) &
                    %d(Virtual_ZenAngle_Index)%SatZenAng * DTOR)
   Trans_Atm_Clr(Level) = EXP(-1 * Layer_OD) &
                   * Trans_Atm_Clr(Level - 1)
 ENDDO
```

DTOR is degree to radius PI/180.

Radiance and cloud profiles are calculated in Clear_Radiance_Prof

```
 SUBROUTINE Clear_Radiance_Prof(ChnIndex, TempProf, TauProf,
RadProf, &
                         CloudProf)
 B1 = Planck_Rad_Fast(ChnIndex, TempProf(1))
 RadProf(1) = 0.0_SINGLE
 CloudProf(1) = B1*TauProf(1)

 DO LevelIndex=2, NumLevels
   B2 = Planck_Rad_Fast(ChnIndex, TempProf(LevelIndex))
   dtrn = -(TauProf(LevelIndex) - TauProf(LevelIndex-1))
   RadProf(LevelIndex) = RadProf(LevelIndex-1) +
(B1+B2)/2.0_SINGLE * dtrn


   CloudProf(LevelIndex) = RadProf(LevelIndex) +
B2*TauProf(LevelIndex)
   B1 = B2
 END DO
```

Transmittance, radiance and cloud profiles are calculated for both normal CRTM structure and the 2nd CRTM structure for SST.

Call Clear_Radiance_TOA to get TOA clear-sky radiance and brightness temperature.

```
SUBROUTINE Clear_Radiance_TOA(Option, ChnIndex, RadAtm,
TauAtm, SfcTemp, &
                          SfcEmiss, RadClr, BrTemp_Clr, Rad_Down)
IF(Option == 1) THEN
```

```
  IF(PRESENT(Rad_Down))THEN
    RadClr = RadAtm + (SfcEmiss * Planck_Rad_Fast(ChnIndex,
SfcTemp) &
          + (1. - SfcEmiss) * Rad_Down) * TauAtm
  ELSE
    RadClr = RadAtm + SfcEmiss * Planck_Rad_Fast(ChnIndex,
SfcTemp) &
               * TauAtm
  ENDIF

  CALL Planck_Temp(ChnIndex, RadClr, BrTemp_Clr)

 ELSE
   RadClr = 0.0
   BrTemp_Clr = 0.0
ENDIF
```

In this subroutine, Rad_Down is optional, depending on if you want to have a reflection part from downward radiance when you calculate the clear-sky radiance. Notice that clear-sky radiance and brightness temperature on NWP grid only calculated for normal CRTM structure not the SST CRTM structure.

Also save the downward radiances from RTSolution and RTSolution_SST to CRTM_RadDown and CRTM_RadDown_SST. Save CRTM calculated surface emissivity to CRTM_SfcEmiss. The above steps are done in subroutine CRTM_OPTRAN